1986-12

The effects of an embedded vortex on a film cooled turbulent boundary layer.

Joseph, Stephen Leo

NAVAL POSTGRADUATE SCHOOL
Monterey, California

THESIS

THE EFFECTS OF AN EMBEDDED VORTEX
ON A
FILM COOLED TURBULENT BOUNDARY LAYER

by

Stephen Leo Joseph

December 1986

Thesis Advisor: P. M. Ligrani

REPORT DOCUMENTATION PAGE

1a REPORT SECURITY CLASSIFICATION UNCLASSIFIED	1b. RESTRICTIVE MARKINGS
2a SECURITY CLASSIFICATION AUTHORITY	3 DISTRIBUTION / AVAILABILITY OF REPORT Approved for public release; distribution is unlimited
2b DECLASSIFICATION / DOWNGRADING SCHEDULE	
4 PERFORMING ORGANIZATION REPORT NUMBER(S)	5 MONITORING ORGANIZATION REPORT NUMBER(S)
6a NAME OF PERFORMING ORGANIZATION Naval Postgraduate School 6b OFFICE SYMBOL (If applicable) Code 69	7a NAME OF MONITORING ORGANIZATION Wright Aeronautical Laboratories
6c ADDRESS (City, State, and ZIP Code) Monterey, California 93943-5000	7b ADDRESS (City, State, and ZIP Code) Wright-Patterson Air Force Base Ohio 45433
8a NAME OF FUNDING / SPONSORING ORGANIZATION Wright Aeronautical Lab. 8b OFFICE SYMBOL (If applicable)	9 PROCUREMENT INSTRUMENT IDENTIFICATION NUMBER Mipr No. FY 1455-86-NO616
8c ADDRESS (City, State, and ZIP Code) Wright-Patterson Air Force Base Ohio 45433	10 SOURCE OF FUNDING NUMBERS PROGRAM ELEMENT NO / PROJECT NO / TASK NO / WORK UNIT ACCESSION NO

11 TITLE (Include Security Classification)

THE EFFECTS OF AN EMBEDDED VORTEX ON A FILM COOLED TURBULENT BOUNARY LAYER

12 PERSONAL AUTHOR(S) Joseph, Stephen L.

13a TYPE OF REPORT	13b TIME COVERED	14 DATE OF REPORT (Year, Month, Day)	15 PAGE COUNT
Master's Thesis	FROM _____ TO _____	1986 December	222

16 SUPPLEMENTARY NOTATION

17 COSATI CODES			18 SUBJECT TERMS (Continue on reverse if necessary and identify by block number)
FIELD	GROUP	SUB-GROUP	Embedded vortex, film cooling, heat transfer, endwall secondary flows

19 ABSTRACT (Continue on reverse if necessary and identify by block number)

This study was designed to model some of the secondary flow effets on endwalls, blades, and combustion chambers of gas turbine engines. Measurements were made in a turbulent boundary layer developing over a flat plate, using a single row of injection holes spaced three diameters apart inclined at 30 degrees with respect to horizontal. The hole diameter to boundary layer thickness ratio, non-dimensional injection temperatures, and blowing rates were the same as exist in turbine first tages. The injection system was designed to provide uniform injection temperatures for various blowing rates with discharge coefficients ranging from 0.58 to 0.73. The heat transfer surface was designed to provide constant heat flux with adjustable temperature range.

Experimental heat transfer results were obtained with a turbulent boundary layer only, with boundary layer and injection of film cooling,

20 DISTRIBUTION / AVAILABILITY OF ABSTRACT ☒ UNCLASSIFIED/UNLIMITED ☐ SAME AS RPT ☐ DTIC USERS	21 ABSTRACT SECURITY CLASSIFICATION UNCLASSIFIED
22a NAME OF RESPONSIBLE INDIVIDUAL Phillip M. Ligrani	22b TELEPHONE (Include Area Code) (408) 646-3382 22c OFFICE SYMBOL Code 69Li

Block 19 (cont.)

with boundary layer and embedded vortex, and finally with boundary layer, film cooling, and embedded vortex. Results with a turbulent boundary layer only show excellent agreement with correlations accounting for unheated starting length. Results with film cooling only show expected trends, and results with embedded vortex only show excellent agreement with data from the literature. The effects of the vortex on heat transfer in the film cooled boundary layer are significant and important: (]) On the downwash side of the vortex, heat transfer is augmented, effects of the film cooling are negated and local "hot-spots" will exist in engines. (2) Near the upwash side of the vortex coolant is pushed to the side of the vortex, appearing to augment the protection provided by film cooling.

The Effects of An Embedded Vortex on a Film Cooled Turbulent Boundary Layer

by

Stephen Leo Joseph
Lieutenant, United States Navy
B.S., The University of Connecticut, 1977

Submitted in partial fulfillment of the
requirements for the degrees of

MASTER OF SCIENCE IN MECHANICAL ENGINEERING
and
MECHANICAL ENGINEER

from the

NAVAL POSTGRADUATE SCHOOL
December 1986

ABSTRACT

The study was designed to model some of the secondary flow effects on endwalls, blades, and combustion chambers of gas turbine engines. Measurements were made in a turbulent boundary layer developing over a flat plate, using a single row of injection holes spaced three diameters apart inclined at 30 degrees with respect to horizontal. The hole diameter to boundary layer thickness ratio, non-dimensional injection temperatures, and blowing rates were the same as exist in turbine first stages. The injection system was designed to provide uniform injection temperatures for various blowing rates with discharge coefficients ranging from 0.58 to 0.73. The heat transfer surface was designed to provide constant heat flux with adjustable temperature range.

Experimental heat transfer results were obtained with a turbulent boundary layer only, with boundary layer and injection of film cooling, with boundary layer and embedded vortex, and finally with boundary layer, film cooling, and embedded vortex. Results with a turbulent boundary layer only show excellent agreement with correlations accounting for unheated starting length. Results with film cooling only show expected trends, and results with embedded vortex only show excellent agreement with data from the literature. The effects of the vortex on heat transfer in the film cooled

boundary layer are significant and important: (1) On the downwash side of the vortex, heat transfer is augmented, effects of the film cooling are negated and local "hot-spots" will exist in engines. (2) Near the upwash side of the vortex coolant is pushed to the side of the vortex, appearing to augment the protection provided by film cooling.

TABLE OF CONTENTS

LIST OF TABLES

LIST OF FIGURES

TABLE OF SYMBOLS

A - area, m^2

C_d - discharge coefficient

Cp - specific heat at constant pressure, J/kg*K

d - injection hole diameter, m

F_{ij} - radiation view factor

g_c - Newton's Second Law proportionality constant

h - heat transfer coefficient with film cooling (spanwise averaged), $q''/(T_{r\infty} - T_w)$

h_f - heat transfer coefficient with film cooling (spanwise averaged), $q''/(T_{aw} - T_w)$

h_o - heat transfer coefficient without film cooling (spanwise averaged), $q''/(T_{r\infty} - T_w)$

k - thermal conductivity, W/m*K

m - blowing ratio

$\dot{m}_c$ - injection mass flow rate, kg/s

P - static pressure, kg/m^2

R - gas constant

Re_d - freestream Reynolds number based on diameter of injection holes

Re_x - freestream Reynolds number based on downstream distance measured from effective origin of turbulent boundry layer

St, St_x - Stanton number

St_o - baseline Stanton number

St_f - baseline Stanton number with film cooling

T - static temperature, K, °C

U - mean velocity, m /s

$\dot{V}$ - volumetric flow rate, m^3/s

ξ - unheated starting length (1.10 m)

ϵ - emmisivity of test surface (0.95)

ϵ - emmisivity of lexan walls (0.70)

η - effectiveness

ρ - density, kg/m^3

θ - nondimensional coolant temperature, $(T_{rc} - T_{r\infty})/(T_w - T_{r\infty})$

δ - boundary layer displacement thickness, m

σ - Stefan-Boltzan constant

SUBSCRIPTS

aw - adiabatic wall

c - coolant at exits of injection nozzles

i - isentropic

o - total or stagnation condition

p - coolant in plenum chamber

r - recovery condition

rad - radiation

w - wall

∞ - freestream

ACKNOWLEDGEMENT

This work was supported by the Wright Aeronautical Laboratories, Wright-Patterson Air Force Base, MIPR number FY 1455-86-N0616. Dr. Charles MacArthur was program monitor. The Shear Layer Research Facility and other experimental apparatus were purchased using funds from the NPS Research Foundation. Technical contributions were made by Professor T. W. Simon, Professor T. Wang, Dr. R. V. Westphal, and Professor A. D. Kraus.

I wish to express my thanks to Professor Phil Ligrani for his understanding, infinite patience, and good humor. I would also like to thank the staff of the NPS Department of Mechanical Engineering, especially James T. Scholfield and William Dames, Jr. who spent many hours in the design and construction of the experimental apparatus. Last, but by no means least, I would like to extend my deep appreciation to my wife, Mary Ann, who gave me her total support throughout the entire project.

I. INTRODUCTION

In gas turbines the need to increase thermal efficiency and specific power is a major concern. One way is to increase turbine inlet temperatures. At present, increasing such temperatures is limited by thermal fatigue strengths, creep strengths, and melting points of the alloys used in turbine components. While the development of improved alloys is part of the solution, the development of efficient cooling systems of blade and endwall surfaces is just as important [Ref. 1]. In order to design an efficient cooling configuration, the heat transfer distributions for the gas turbine components are needed. Because of the complex geometries and flows involved near blades and endwalls, accurate convective heat transfer rates are difficult to obtain.

A. FLOW IN TURBINE CASCADE

Flows through turbine passages are highly complex, containing numerous vortices, and secondary flows, as well as three-dimensional seperations. In recent studies, large portions of these complex flows have been identified and mapped out. The sketch in Figure 1, taken from [Ref. 2], shows the flows which are thought to exist. As the inlet boundary layer approaches the blade, one portion forms cross flow A, and the other approaches the blade. Just in front of

the blade a horseshoe vortex forms. At the saddle point, it splits into a vortex on the suction side and a vortex on the pressure side. The pressure side vortex becomes the passage vortex, moving from the leading edge of one blade towards the low pressure side of the adjacent blade. The number of rotations of the passage vortex have been exaggerated in Figure 1 for clarity. Ordinarily it rotates only once or twice through the passage. As the suction side vortex convects along the blade, it is eventually pushed away from the endwall by the passage vortex from an adjacent blade. [Ref. 2] A smaller, corner vortex, rotates in an opposite direction to the passage vortex as verfied by Sieverding (1983) [Ref. 3].

B. FILM COOLING

Film cooling is used to provide cool fluid between a surface and high temperature free stream gases to which it is exposed. Film cooling not only insulates the surface but acts as a heat sink for the hot free stream gases. The overall effect of film cooling is to reduce the temperature of the developing boundary layer, which in turn reduces heat transfer to the surface.

In our studies, knowing heat flux, q'', h is found using

$$q'' = h(T_w - T_{r\infty}) \qquad (1.1)$$

The effect of film cooling will be indicated by the h

distribution for constant q'' and $T_{r\infty}$ while varying T_w. When $T_w = T_{r\infty}$, equation 1.2 indicates $q'' = 0$, which may not be physically correct with film cooling.

Another approach is one used by Goldstein, [Ref. 1]:

$$q'' = h_f(T_w - T_{aw}) \qquad (1.2)$$

Here $q'' = 0$ when $T_w = T_{aw}$ with film cooling, by defintion. Without film cooling $T_{r\infty} = T_{aw}$ and the two equations are the same. Effectiveness of film cooling may then be defined using

$$\eta = \frac{T_{aw} - T_r}{T_{oc} - T_r} \qquad (1.3)$$

The [Ref. 1] method is not used for this study because of the difficulty in finding T_{aw} for the test surface.

The effectiveness of a film coolant in protecting a surface is dependent on numerous factors. The most important of these are: the blowing rate, size and number of injection holes, the location of the injection system in relation to the affected surface, and the curvature of the turbine blade or surface from which the injectant issues. The curvature of the blade in relation to the blowing rate is very important in the effectiveness of the cooling system. At low blowing rates, film cooling is more effective near convex surfaces than near flat surfaces or concave surfaces. If the blowing rate is increased, this behavior is reversed such that concave surfaces exhibit the best performance.

The approaches given by equations 1.1 and 1.2 can be compared for constant property conditions by showing linear dependence of h/h_o on θ, where θ is the nondimensional temperature of the film coolant. Equating equations 1.2 and 1.3 gives

$$h=h_f(1-\eta\theta) \qquad (1.4)$$

Dividing by h_o then yields. [Ref. 4]

$$\frac{h}{h_o}=\frac{h_f}{h_o}(1-\eta\theta) \qquad (1.5)$$

C. OTHER STUDIES

Numerous studies have been conducted on the effects of film cooling on heat transfer, effects of secondary flows on heat transfer, and more recently, on the effects of film cooling and secondary flows on heat transfer in a turbulent boundary layer.

Studing the effects of secondary flows on heat transfer, Gaugler and Russell (1984) compared visualized secondary flow patterns over six vanes with heat transfer distributions. The authors found that the horseshoe vortex causes a local peak in the heat transfer rate near the vane leading edge. Large peaks in Stanton number were found downstream of the vanes but the authors concluded that this effect was related more to vane wake rather than the induced horseshoe vortex. [Ref. 5]

Studing the effects of film cooling and secondary flows on heat transfer, Goldstein and Chen (1985) performed an experimental study on the influence of the endwall on film cooling of gas turbine blades using a single row of injection holes. The authors concluded that the convex side of the blade was highly effected by the flow originating from near endwall.Here film coolant was swept away by the passage vortex, whereas the concave side was not significantly effected by flows originating near the endwall. [Ref. 1] Other work on the effects of film cooling is given in [Ref. 6], [Ref. 7], and [Ref. 8].

Studing the effects of secondary flows on heat transfer, Eibeck and Eaton (1986) conducted a study of a single vortex embedded in a turbulent boundry layer over a constant heat flux flat plate. The authors found significant increases and decreases in local Stanton numbers, due to thinning of the boundry layer on the downwash side of the vortex and thickening on the upwash side of the vortex. Spanwise heat transfer was larger as the circulation of the embedded vortices increased. [Ref. 9] Other work on the effects of embedded vortices is given in [Ref. 10] and [Ref. 11]

Öngören (1981) performed a study on the effects of film cooling on the heat transfer on the endwall of a turbine cascade, where the effects of secondary flows and cooling injection rates were observed. The author found that measurements showed a good match with predications in the

case of no injection. Heat transfer measured on the center streamline of the endwall showed qualitative agreement with that of the flat plate. Secondary flows, which were believed to cause non-uniform distributions of film coolant, resulted in variations in heat transfer across the width of the endwall. [Ref. 2]

D. PRESENT STUDY

The object of the present study is to increase the understanding of the effects of a longitudinal vortex on heat transfer in a film cooled boundary layer. These effects are important regarding turbine blade endwall heat transfer. The experimental model was constructed in a series of steps. The first was the design and construction of the injection system, including qualification testing to verify uniformity and controllability, as well as the calculation of discharge coefficients for the various flow conditions. The next step was the design and construction of the heat transfer test surface followed by qualification tests to verify uniform heat flux and an energy balance to identify and quantify the sources of heat loss. After completion of the experimental apparatus four types of tests were conducted: heat transfer data with developing boundary layer only, with boundary layer and injected film cooling, with boundary layer and embedded vortex and finally with boundary layer, film cooling, and embedded longitudinal vortex.

II. EXPERIMENTAL APPARATUS

A. INJECTION SYSTEM

The injection system was designed and developed to provide film coolant at temperatures above ambient. The coolant is ejected from a single row of injection holes into the boundary layer developing along the bottom wall of the wind tunnel. The diameters of the injection holes were scaled relative to boundary layer thickness to be similar to a turbine blade, with a δ/d ratio ranging from 0.37 to 0.40. The free stream air is at ambient temperature and thus the direction of heat transfer is opposite that of a gas turbine. The temperature range for this study has been kept small (25 - 35 °C) to minimize the effects of variable properties.

The injection parameters m and θ were scaled to resemble parameters near gas turbine blades where m ranges from 0.5 to 1.0 and θ ranges from 1.2 to 1.8. Due to the reversed direction of heat flow for our experimental apparatus the $T_{rc} : T_{r\infty} : T_w$ ratio is 1.04 - 1.07:0.94 - 0.95:1.0 as compared to 0.67 - 0.83:1.5:1.0 for actual gas turbines.

1. Description

Air for the injection system originates in an Ingersoll-Rand air compressor, (two stage, 150 psi, 10 Hp, model number 71TD), where it is then sent to three large

storage tanks. As shown in Figure 2, the air then flows through an adjustable pressure regulator, a cut off valve, reinforced flexible tubing (2.54 cm, 1 in, inside diameter), moisture seperator, flow regulator, a Fisher and Portor rotometer (full scale 9.345E-3 m^3/sec, 19.8 SCFM, model number 10A3565A), a diffuser, and finally into the injection heat exchanger and plenum chamber. The rotometer monitors the volumetric flow rate for film cooling. A schematic of the diffuser is shown in Figure 3.

A photograph of the chamber is shown in Figure 4. The chamber is constructed of 1.27 cm (1/2 in) plexiglass, with outside dimensions of 0.305 x 0.508 x 0.457 m (12 x 20 x 18 in). As shown in Figure 5, the internal structure consists of three thin metal plates 0.381 x 0.508 m (15 x 20 in) starting 5.08 cm (2 in) from the bottom and proceeding up at 5.08 cm intervals. Two silcon rubber heaters, 0.381 x 0.483 m (15 x 19 in), 120 volt, are seperately placed over the bottom two plates. The heaters are controlled through a Powerstat variable autotransformer (type 136). The top surface contains 13 plexiglass injection tubes each 8 cm long with an inside diameter of 0.95 cm (3/8 in) with a l/d ratio of 8.42. The 13 injection holes are inclined at an angle of 30 deg., with 3 diameter spanwise spacing between centerlines where the middle tube is set on the centerline of the test surface.

Air enters the chamber through the diffuser section and is then directed over the two heating surfaces where the air can be heated from ambient temperature up to 80 °C by controlling the input voltage to the heaters through a variable autotransformer.

Three pressure taps, positioned at the center of the front and two side faces, are used to measure $P_{oc} - P_{\infty}$. Three 0.254 mm (0.010 in) diameter copper-constantan wire thermocouples with welded junctions are place at different locations inside the chamber to measure the uniformity of T_{op} in the plenum.

2. Qualification and Performance

The uniformity of the plenum chamber pressure, P_{oc}, was found to be satisfactory over the range of injection conditions with typical differences of approximatly 1% in the spanwise direction and a maximum of 4% occurring for only one case at a low flow rate of 0.327E-4 m^3/sec.

The plenum produces a reservoir of air at an elevated temperature and pressure, which is near stagnation conditions. The temperature at the nozzle exit, T_{rc}, is not equal to the temperature in the plenum chamber, T_{op}, due to conduction heat loss through the nozzle surfaces to the surrounding ambient air. It is necessary to know the relation between T_{rc} and T_{op} because injection parameters are estimated at exits of the jets and plenum chamber temperature is more convenient to measure. A test was

conducted to determine the relationship between these two temperatures over the flow rates ranging from 0.327E-4 to 0.701E-2 m^3/sec. Results are shown in Figure 6. The data trend shown in the figure was the same regardless of flow rate, and an average of exit and plenum temperatures were used to determine each data point. Exit temperature shows a near linear dependence on plenum chamber temperature. A curve of the form $T_{oc} = C*T_{op}^{B}$, where C = 1.455 and B = 0.868, was fitted to this data so that T_{rc} could be estimated from plenum chamber temperatures in subsequent tests.

The recovery temperature at the nozzle exit, T_{rc}, is given by

$$T_{rc} = T_c + \alpha \frac{U_c^2}{2g_c C_p} \qquad (2.1)$$

where α is the recovery factor, having typical values of 0.6 to 0.9. α represents the percent of dynamic temperature which is not lost to viscous dissipation, where α is defined by

$$\alpha = \frac{T_r - T}{T_o - T} \qquad (2.2)$$

The total nozzle exit temperature, T_{oc}, may be expressed using

$$T_{oc} = T_c + \frac{U_c^2}{2g_c C_p} \qquad (2.3)$$

Because of the low velocities employed, (and neglible viscous disipation), $T_{oc} \simeq T_{rc}$ within a fraction of a degree.

Measuring parameters $P_\infty, T_\infty, \dot{V}_c, P_{oc}$, and T_{oc} and knowing the area, A, normal to the flow, of the injection holes, designed to be 9.2633E-4 m^2, the coolant velocity U_c is given by

$$U_c = \frac{\dot{V}_c}{A} \tag{2.4}$$

The static density is estimated using

$$\rho_c = \frac{P_\infty}{RT_c} \tag{2.5}$$

Mass flux, m_c, is now the product of U_c and ρ_c. To calculate the isentropic mass flow, ρ_{ci} and U_{ci} are found using

$$\rho_{ci} = \frac{P_\infty}{RT_{op}} \tag{2.6}$$

and

$$U_{ci} = \sqrt{\frac{2(P_{oc} - P_\infty)}{\rho_{ci}}} \tag{2.7}$$

These two equations are derived from the equation for compressible flows:

$$(\rho_c U_c)_i = P_\infty \left(\frac{P_{oc}}{P_\infty}\right)^{2/7} \left[\frac{7}{RT_{oc}}\left(1 - \left(\frac{P_{oc}}{P_\infty}\right)^{-2/7}\right)\right]^{1/2} \tag{2.8}$$

Discharge coefficients, C_d, are then estimated using

$$C_d = \frac{\rho_c U_c}{(\rho_c U_c)_i} \tag{2.9}$$

The variation of discharge coefficients with volumetric flow rate is shown in Figure 7. The dependence is near linear, where C_d decreases slightly with T_c at a given flow rate. Discharge coefficients range from 0.581 to 0.730, which is consistent with other workers' results [Ref. 12]. When plotted verses the Reynolds number as shown in Figure 8, the discharge coefficients at different temperatures collapse more closely together than in Figure 7. Such behavior indicates satisfactory injection system performance [Ref. 4]. Numerical tabulations of the data are found in Tables 1, 2, 3, and 4.

During qualifications tests small hysteresis was indicated by the plenum chamber pressure as the flow increased and decreased. With increasing flow rate plenum chamber pressures relative to ambient pressures, were 2 to 10% lower than when flow rates decreased. These data were taken over time intervals long enough to ensure steady state conditions were obtained. This result was probably due to fluid circuit effects of the air supply system and plenum chamber, specifically, behavior similar to that produced by inductances and capacitances in electric circuits. This hysteris was probably the result of a velocity dependent separation occuring in the diffuser of the injection system. However, in spite of the hysteresis, data are self

consistent (even though obtained as the flow rate both decreased and increased) with minimal scatter: C_d varations from hysteresis are no greater than 1 or 2%.

B. HEAT TRANSFER SURFACE

The heat transfer surface was designed and developed to provide a constant heat flux over its area. The average surface temperature may be adjusted and maintained from ambient up to 60 °C. The device was constructed so that the upward facing part is exposed to the wind tunnel airstream, with minimal heat loss by conduction from the sides and beneath the test surface. The surface itself has been instrumented to measure surface temperatures with thermocouples place just beneath the surface, and a film of liquid crystals sprayed on the top surface.

1. Description

A photograph of the heat transfer surface is shown in Figure 9. The design is based on a similar surface used by the University of Minnesota [Ref. 13] and [Ref. 14]. It consists of a thin stainless steel foil (AISI 302 full hard), 0.127 mm x 1.194 m x 0.467 m, painted flat black with approximately 5 layers of liquid crystals. Attached to the underside of the foil are 88 copper-constantan, 0.254 mm diameter, thermocouples integrated into grooves cut into a single sheet of 0.25 mm (10 mil) thick double-sided tape (manufactored by the 3M Company). The grooves are then

filled with RTV. A silicon rubber heater, 1.0 mm x 1.143m x 0.457 m, 120V/100W, is attached to the tape with Electobound epoxy which was applied to both the tape and heater surfaces. The heater is then backed by a 12.7 mm (1/2 in.) thick lexan sheet, followed by 25.4 mm of foam insulation, 82.55 mm thick styrofoam and one sheet of 9.53 mm thick balsa wood, as shown in Figure 10.

Around the edges of the foil grease was inserted between the foil and plexiglass frame to allow for thermal expansion of the top surface. Two thin metal wires are also attached to the back corners of the foil and guided down through the floor of the wind tunnel with 3 lb weights attached to each wire to add tension to the foil and help maintain a flat surface during thermal expansion. Additional vertical movement of the foil surface above the bottom wall of the wind tunnel occurs due to thermal expansion during heating. The surface is maintained level by adjusting screws in the plexiglass frame supporting the heat transfer surface from below. During heat transfer tests, the top surface of the foil remained remarkably flat and smooth with minimal surface irregularities.

Thermocouples are placed on the surface as shown in Figure 11. In each row, thermocouples are 2.54 cm apart. The surface temperature is controlled by adjusting input voltage to the heater using a Standard Electrical Product Co. variac, type 3000B. With this type of heat transfer surface,

addition of more thermocouples for improved spatial resolution of surface temperature is difficult because of cold spots and paths for leakage caused by large numbers of thermocouple wires between the foil and heater.

2. Qualification and Performance

Preliminary qualification tests were made using an early version of the heat transfer surface in order to understand its behavior and performance characteristics. Improvements in design and construction led to the heat transfer surface used to obtain the final results. Qualification results from the final surface, using temperature sensitive liquid crystals, showed more uniform temperatures, giving evidence of more uniform heat flux, than results from the early version.

To test the early version of the heat transfer surface, a Hughes Probeye Thermal Video System series 4000, consisting of a infrared and video camera with display screen, was used to measure the surface temperatures with heat transfer surface outside the wind tunnel. With this system temperature variations as small as 1 $^{\circ}$C can be measured. The surface was observed under four operating conditions: natural convection with a surface temperature of approximately 33 $^{\circ}$C, forced convection with an initial surface temperature of approximately 33 $^{\circ}$C, natural convection with a surface temperature of approximately 45 $^{\circ}$C, and forced convection with an initial temperature of

approximately 40 °C. Results of these tests are shown in Figures 12, 13, 14, and 15 respectivily. The test were undertaken to measure temperature differences in order to provide some verification of uniform heat flux under different operating conditions.

a. Preliminary Tests

The natural convection conditions shown in Figures 12 and 14 indicate that the surface temperature distribution is uniform within 2 - 3 °C. A low temperature region is located near the leading edge on the left side, caused by the larger number of thermocouple wires located near the forward section of the test surface. This problem was eliminated in the final heat transfer surface design.

Figures 13 and 15 show the surface isobars for the forced convection tests to be spanwise uniform midway between the two sides along most of the length of the test surface. Such behavior evidences a locally two-dimensional turbulent boundary layer with a constant heat flux at the surface. Moving air was provided by a Tahoe Products Inc. fan (model number PF-05-1) with a 22.25 cm blade diameter, which produced a free stream velocity estimated to be between 2 and 4 m/s. Away from the flow produced by the fan, near the sides of the test surface, temperature variations are highly non-uniform as would be expected. Comparing results in Figures 12 and 14 with those in Figures 13 and 15, the small cold spot present with natural convection near

the leading edge almost disapears with forced convection, probably as a result of the higher heat transfer coefficients involved.

A circular cool spot is located near the trailing edge and is present with all surface conditions as shown in Figures 12, 14, and 15. The variation is caused by a small non heated portion of the silicon heater containing a thermostat. In the final design, this heater was replaced with one without a thermostat to avoid formation of a local cold spot.

b. Energy Balance

An energy balance was performed to determine heat loss by conduction on the heat transfer surface used to obtain final results. During the energy balance, heat loss by radiation and convection were prevented since the metal foil surface, ordinarily exposed to convection in the wind tunnel, was covered three layers of, 25.4 mm thick, foam insulation. For the energy balance and for all wind tunnel testing, foam insulation was also placed around the sides of the test surface located below the wind tunnel convection surface. To estimate heat loss through the insulation placed on top of the foil surface, the one-dimensional, linear form of Fourier's conduction equation was employed

$$q = kA\frac{\Delta T}{\Delta X} \qquad (2.10)$$

where k is .04 W/m K, A is 0.4897 m^2, X is 0.0254 m, and ΔT is the temperature drop in the X direction. Heat conduction through the bottom and sides of the heat transfer device are then given by

$$q_{cond} = VI - q_w \qquad (2.11)$$

where VI is the power into the test plate, and q is the conduction loss through the top insulation. Tests to determine q_{cond} were made at five power levels 12.00, 14.20, 16.52, 20.44, and 20.45 Watts. These levels were choosen to be of the same magnitude as conduction losses experienced under normal test conditions with convective heat transfer from the top of the plate.

q_{cond} is plotted verses T_w - T amb in Figure 17. From these results an emperical equation was generated

$$q_{cond} = 0.93 + 1.45\Delta T - 0.051\Delta T^2 + 0.00068\Delta T^3 \qquad (2.12)$$

Where, here ΔT is T_w - T amb. This equation is only valid over a range of T_w - T amb from 8 to 30 °C. When exposed to convection in the wind tunnel, conduction losses are only 1.5 to 2.5% of the total power, therefore even a 25% error in the estimate of conduction losses will cause less than a 1/2% change in the estimate of heat transfer by convection.

In order to have additional verification of the conduction model given by equation (2.12), conduction losses were estimated beneath the surface, through the plexiglass

sides, as well as from the foil to the plexiglass frame. Numerous thermocouples were placed at key positions between the layers of material and the test plate to make these estimates, as shown in Figure 16. Temperatures from these thermocouples were then employed in the one-dimensional form of Fourier's conduction equation. The estimates were made for the same power levels mentioned earlier. Results are listed in Table 6. The total of these estimates showed rough agreement with equation (2.12). At low power inputs, less than 16 Watts, the model slightly under estimated losses, while at higher power levels, greater than 18 Watts, the model slightly over estimated conduction losses. The differences are probably due to the multi-dimensional effects at the corners and sides of the foil surface, which could not be accounted for using a one-dimesional conduction equation.

Radiation losses were estimated from the following relationships [Ref. 15]

$$q_{ij} = \frac{\sigma(T_w^4 - T_{amb}^4)}{\frac{1-\epsilon_i}{\epsilon_i A_i} + \frac{1}{A_i F_{ij}} + \frac{1-\epsilon_j}{\epsilon_j A_j}} \qquad (2.13)$$

and

$$q_{rad} = \sum_{j=1}^{N} q_{ij} \qquad (2.14)$$

The view factors, F_{ij} , for the top wall and each side wall

were estimated to be 0.66 and 0.17 respectivily, where

$$\sum_{j=1}^{N} F_{ij} = 1 \qquad (2.15)$$

From these equations, radiation losses for an average plate temperature of 40°C was found to be 53 Watts, approximately 8.5% of the total power into the transfer surface.

c. Contact Resistance

In the present study, thermocouples are attached to the stainless steel foil using the 0.25 mm double-sided tape and RTV silicon rubber epoxy. Welding was not used due to the thinness of the foil. Consequently, a thermal contact resistance, $1/(h_c A)$, is present between the back of the foil surface and the thermocouples. This contact resistance along with the thermal conductivity, k, of the metal foil will cause the thermocouples to measure a higher temperature than actually found on the test surface, where this difference, ΔT, is given by

$$\Delta T = q\left(\frac{1}{h_c A} + \frac{\Delta X}{kA}\right) \qquad (2.16)$$

Contact resistance is highly dependent on the contact pressure as well as the area of the surfaces in contact. Due to the method of construction of the test surface, contact pressure can only be estimated while the area of the thermocouples in contact with the surface can vary in the shape and size of each bead. These unknown properties precluded an emperical estimate of the value of the contact

resistance. Two different methods were used to determine the average contact resistance experimentally: (1) with conductive heat transfer conditions and thermocouples above and below the foil, noting that the contact resistance is twice as large due to the presence of two layers of thermocouples, and (2) by direct measurement of the drop in temperature with convective heat transfer. The second method involved comparing the surface temperatures indicated by liquid crystals to ones measured with thermocouples beneath the surface. From these two methods the contact resistance plus the conductivity resistance in the plate was estimated to be 0.016 K/Watt. The same value was used for all thermocouples. Because this is an average value over the entire plate, the actual resistance for individual thermocouples may vary from this value, causing small deviations in the spanwise heat transfer coefficients and Stanton numbers. As would be expected these variations were unaffected by flow conditions. As will be seen, small variations due to contact resistance are eliminated by presenting results as Stanton number ratios for local conditions.

3. Earlier Design

The final heat transfer surface design is the third iteration. The first one had 146 thermocouples held in place by two layers of tape. Due to the large number of thermocouples and associated wires, the surface did not

exhibit uniform heat flux. The thermal video system indicated that isobars were nonuniform in the spanwise direction with many cool spots above the locations of large numbers of thermocouple wires. The cool spots were observed under both natural and forced convection. The original foil also had some small dents, incurred in shipping. A better grade of stainless steel foil, packaged as a single sheet rather than a coil, was used in later designs to minimize surface deformities.

Of the three designs, the final one was believed to produce the most uniform surface heat flux because (1) the surface was the smoothest, (2) fewer thermocouples were used, attached with indusrial strength double backed liner instead of 2 layers of tape, (3) thermocouple wires were spread uniformly behind the foil instead of being bunched in groups, and (4) slots were carefully cut into the tape for placement of thermocouple wires to prevent and raised surfaces between the foil and heater. A plexiglass frame was also added to provide better support from the sides in addition to a lexan sheet which was added to supply a more rigid support from below. The lexan helped prevent sagging and to maintain continous contact between the foil, tape, and heater.

C. TEMPERATURE MEASUREMENT

All thermocouples used in this study were type-T (copper-constantan), 0.254 mm diameter, manufactured by Omega Engineering. Two thermocouples (freestream probe and temperature profile probe) were calibrated using a temperature regulated bath consisting of liquid nitrogen and electric heaters and a known platinum resistance reference ($\pm$ 0.01 $^{\circ}$C).The calibration was performed over the temperature range of 18 - 60 $^{\circ}$C. The millivolt reading of the thermocouples verses the reference temperature was used to generate a fourth degree polynomial equation using a least squares curve fitting technique.

$$T = 26.573E - 1.937E^2 + 0.998E^3 - 0.261E^4 \qquad (2.17)$$

where

$$E = \text{millivolts} \times 1000 \qquad (2.18)$$

The same polynomial was used for the thermocouples used on the heat transfer test plate as all thermocouples indicated very similar behavior at different temperatures.

Temperature profiles were performed using one of the calibrated thermocouples mounted on a traversing mechanism. The traversing mechanism was driven by a simple threaded shaft (18 threads per inch). This threaded shaft was used to move a traveling block attached to the mounting stem of the

thermocouple probe, such that shaft rotations could be converted to vertical probe position with respect to the wall.

D. WIND TUNNEL

The wind tunnel pictured in Figure 18, built by Aerolab, was designed to provide a flow field from the nozzle with uniform velocity and low turbulence intensity. It is designated the NPS Shear Layer Research Facility (SLRF). The tunnel has numerous pressure taps along both side walls and contains many instrument ports along the top wall to measure flow characteristics.

1. Description

The SLRF, shown in Figures 19 and 20, is a wind tunnel of the open circuit blower type with fan upstream and air entering the fan inlet from the surrounding room. The air speed through the test section can be adjusted from 5 to 40 m/s. The tunnel frame has leveling screws to adjust the centerline of the tunnel to a horizontal position. The discharge part of the fan slips into the inlet end of the wide-angle diffuser with a 1.6 mm (1/6 in) clearance all the way around to isolate vibrations from the fan to the wind tunnel body. The diffuser section contains a filter pack and a nozzle leading to the test section. The test section is a rectangular duct, 3.048 m (10 ft) long, and 0.6096 m (24 in) wide, as shown in Figure 20. The top wall is a continous

panel fabricated from 4.76 mm thick Lexan sheet with neoprene channel seals at the edges. The ceiling panel height and shape may be changed to permit adjustment of static pressure along the length of the test section. A test section height variation of 0.1524 to 0.3048 meters (6 to 12 inches) can be obtained. The floor of the test section consists of 0.6096 meters (2 ft) and 1.2192 meters (4 ft) sections which are removable and replaceable. Each floor section has "O" ring seals at their seams. Removable side windows allow good accessibility to the test section. Profile measurements may be made using probes inserted through the top and bottom walls.[Ref. 16]

A schematic of the test section components used in the present study are shown in Figure 21. An unheated starting length of 1.10 m exists upsteam of the heated test surface. The injection nozzles are located 1.08 m downstream of the boundry layer trip and 0.02 m upstream of the test surface. The leading edges of the vortex generators are placed 0.479 m downstream of the boundry layer trip. A schematic of vortex generator geometry is shown in Figure 22.

2. Qualification and Performance

Extensive qualification test of the Shear Layer Research Facility were conducted by Ligrani [Ref. 17]. Results show that the variation of total pressure at the exit plane of the nozzle is less than 0.4% at 26 m/s and 34

m/s. Mean velocity varies less than 0.7% for the same mean freestream speeds. From five-hole pressure probe measurements, the velocity angle deviation is nowhere greater than about 0.6 degrees at the nozzle exit plane.

Profile measurements of the mean velocity and longitudinal turbulence intensity in the turbulent boundary layer developing at 20 m/s indicate normal, spanwise uniform behavior. For this qualification test, and all results which follow, the boundary layer was tripped near the exit of the nozzle with a 1.5 mm high strip of tape. Total pressure measurements along the test section surface at the nozzle exit were uniform within 0.5% indicating spanwise uniform skin friction.

Freestream turbulence intensity was measured to be 0.00085 (8.5 one - hundreths of one percent) at 20 m/s increasing to 0.00095 at 30 m/s.

E. DATA ACQUISITION SYSTEM

The data acquisition system was designed to rapidly measure thermocouple voltages and convert them to temperatures in deg C. Using these temperatures, along with user supplied information on ambient conditions, freestream conditions, and power input, the system calculates free stream velocity, density, local heat transfer coefficients and Stanton numbers, and spanwise averages of heat transfer coefficients and Stanton numbers.

1. Hardware

The data acquisition system is comprised of an HP-85B computer with its associated memory module and interface cards. Mass storage is provided by an internal cassette storage drive. Voltages from the type-T (copper-constantan) thermocouples are read by an HP-3497A Data Acquisition/Control Unit with a HP-3498A Extender. The unit communicates with the computer through a HP-829737A Interface. Software, described below, converts the voltage inputs into temperatures. The HP-85B is used to calculate, store, display, and print desired information.

2. Software

Three programs, STDAT1, STDAT3, and TPROF were developed to be used under various flow conditions. The three programs are listed in Appendix D.

a. STDAT1

STDAT1, developed by Ligrani, Ortis, and Joseph, prompts the user for current (amps) and voltage to the heater to calculate the power (Watts) into the heat transfer surface. The program continues by prompting the user for stagnation pressure (in H_2O) of freestream and ambient pressure (in Hg). The computer than reads the thermocouple voltages, converting them into temperatures and storing them in a matrix. After all temperatures have been calculated the freestream density and velocity are calculated in SI units. From this point, the program accounts for conduction and

radiation losses, and contact resistance. It continues by calculating local and spanwise averaged heat transfer coefficients, and Stanton numbers. Reynolds number are also given based on the downstream distance. Upon completetion of these calculations the program prints the data on an attached printer and stores them on a disk file.

b. STDAT3

STDAT3 is a modification, by Joseph, to the original STDAT1. This program runs in the same manner as STDAT1 except for modifications to use previously stored baseline measurements to obtain ratio type relationships. The program also contains an option to calculate film cooling injection parameters including discharge coefficients, density ratios, massflux ratios, momentum flux ratios, and blowing rate.

c. TPROF

TPROF was written by Ligrani to calculate temperatures from thermocouple probe output, as the probe was traversed in the turbulent boundary layer, above the heated test surface. As the program begins, local flow, wall heat flux and wall temperatures are read in. The program then calculates a friction temperature and a friction velocity. The program then enters a loop where it acquisitions a voltage from the thermocouple, and then calculates temperatures from the volatage using probe calibration results. This loop is repeated as the probe is

moved to new locations, where probe location is read in and accounted for. After the last profile point (the probe is moved from the freestream to the wall), the program prints out relevant parameters including thermal boundary layer thickness, as well as dimensional and normalized profile tabulations.

III. EXPERIMENTAL RESULTS

The study was conducted in four parts. The first consisted of establishing baseline Stanton numbers and heat transfer coefficients for a turbulent boundary layer over a constant heat flux test surface at U_∞ =10 m/s with an unheated starting length of 1.10 meters. The second part consisted of documenting the effects of various size vortices over the same surface using the same freestream conditions. The next step involved measurements in a turbulent boundary layer with film cooling at three blowing rates. The final series of tests were conducted to study the effects of an embedded vortex on heat transfer in the film cooled turbulent boundary layer.

A. BASELINE MEASUREMENTS

Heat transfer measurements were performed and recorded for three different freestream velocities over the test surface: 10, 15 and 20 m/s. Numerical tabulation of heat transfer coefficients, Stanton numbers at different thermocouple positions in addition to spanwise averaged Stanton numbers by thermocouple row are listed in Appendix E.

The spanwise heat transfer coefficients of the test surface at 10 and 20 m/s are shown in Figures 23 and 24 respectivily. Except for row 1, the spanwise uniformity is

very good with maximum variations of 10% (from the average for a given row) at 10 m/s. These small variations are due to differences in contact resistance between different thermocouples. As shown in the two figures the qualitative form of these variations is the same at different flow conditions. Larger spanwise variations for row 1 appear to be due to multi-dimensional conduction losses near the leading edge of the test surface in addition to contact resistance.

Spanwise averaged Stanton numbers for 10, 15, and 20 m/s are plotted as functions of Reynolds number in Figures 25, 26, and 27. These data show agreement with the empirical equation for turbulent boundary layers at constant free stream velocity along a flat plate, with constant heat flux and an unheated starting length of 1.10 m. [Ref. 18]

$$St_x Pr^{0.04} = 0.030 Re_x \left[1 - \left(\frac{\xi}{X}\right)^{0.9}\right]^{-0.111} \qquad (3.1)$$

The maximum variation between the emperical equation and measured data is approximately 5%, at 15 m/s, with excellent agreement at 10 and 20 m/s. At a given Reynolds number and test plate location, Stanton numbers may be repeated within a few percent provided thermal equilibrium of the wind tunnel and heated test surface have been achieved.

Mean temperature profiles were measured at X=1.44 and 1.85 meters. These are shown in Figures 28 and 29, indicating expected behavior. At 1.85 meters, profiles show

excellent spanwise uniformity at three different span locations, which indicates that the mean flow field is two-dimensional

Figure 30 shows mean temperature data plotted in non-dimensional wall coordinates Y+ and T+. When compared to the empirical law of the wall [Ref. 18]

$$T^+ = 2.195 \ln Y^+ + 13.2 Pr - 5.66 \qquad (3.2)$$

the data show agreement for $100 < Y+ < 200$. At larger Y+, data show behavior typical of outer portions of thermal layers developing with an unheated starting length. Mean temperature profile data deviate from equation (3.2) for $Y+ < 100$ due to probe spatial resolution effects and significant heat transfer from the heated wall to the probe.

B. SINGLE VORTEX

Four different size vortex generators, Figure 22, were individually positioned 0.479 m downstream from the boundary layer trip. All results were obtained at a free stream velocity of 10 m/s. The heat transfer are given in terms of St/St_o for thermocouple position. The measured data for each test is found in Appendix G.

The St/St_o ratios, as a function of Z position, where Z=0 is the centerline, are shown for each vortex in Figures 28 - 35.

Vortex generator #1, smallest, was positioned with its tip 4.29 cm left of the wind tunnel centerline. The effects of the vortex are evident in the Stanton number ratios. The ratio increases near the downwash side of the vortex to a maximum of 1.19 and decreases over the upwash side to a minimum of 0.975. The downwash side of the vortex appears to be thinning the boundary layer, thus increasing the localized heat transfer, while the upwash side appears to be thickening the boundary layer, decreasing the localized heat transfer. The baseline Stanton number, St_o data used to non-dimensionalize results in Figures 28-35, and all subsequent figures, was obtained at conditions which were not at exact thermal equilibrium. A repeat of these data give St_o values a few percent higher, which gives slightly lower St/St_o ratios. Referring to Figures 28-35, St/St_o values at locations away from the vortex are thus closer to 1.0 than indicated in the figures.

Vortex generator #2 was positioned 4.79 cm left of the wind tunnel centerline. The effects on heat transfer are much the same as with #1 only with an increase in the variation of the St/St ratio to a high of 1.204 and a low of 0.949. The overall effect in the spanwise averaged Stanton number is nearly the same as with vortex #1: both are approximatley 5% greater than the baseline data without a vortex.

Vortex generator #3 was positione 8.08 cm left of the centerline. Again, the results are very similar to those from generator #1,with a high of 1.274 and a low of 0.951 in Stanton number ratios. The spanwise average of Stanton numbers are nearly identical to those of vortex #1 and #2. The major difference noted with vortex #3 is the smearing of Stanton number ratios on the upwash side of the vortex at positions Z=2.54 and 5.08 cm. This effect may suggest the presence of a small secondary vortex.

Vortex generator #4, positioned 9.096 cm left of centerline, produces a vortex so large that it dominates the entire measured flow field of the surface. The diameter of the vortex appears to range from 10 to 15 cm. while the spanwise averaged Stanton numbers show a marked increase from the baseline of approximately 10 -14%. The effects of a secondary vortex have become more visible and can be seen from Z=0 to 7.62 cm. Due to the large size and effects of vortex #4 it was not used in any subsequent tests.

These results, especially those found in Figures 30 and 31 compare very favorably with those of Eibeck and Eaton, Figures 36 and 37. Figure 36 shows the spanwise Stanton number ratio with a vortex generator 2 cm high and a 20 deg angle of attack. Figure 37 shows the spanwise Stanton number ratio with a vortex generator 3 cm high and a 12 deg angle of attack. [Ref. 9]

The strength of the individual vortices can be quantified by their respective circulations, where

$$\text{circulation} = 2.5HU_{\infty}0.10 \qquad (3.3)$$

For this study the circulation of vortices #1, #2, #3, and #4 were determined to be approximately 0.045, 0.075, 0.125, and 0.175 m /s respectivily. [Ref. 19]

C. FILM COOLING

Heat transfer measurements were performed and recorded at 10 m/s with film cooling at θ = 1.543, 1.485, and 1.474 with blowing ratios, 0.68, 0.55, and 0.54 respectivily. Numerical tabulations of local heat transfer coefficients, local St/St_o ratios, and spanwise averaged Stanton numbers are listed in Appendix F. The Stanton number results for each of the three blowing ratios were stored in a data file to be used for comparison with those measured under the influence of both a vortex and film cooling.

When comparing this film cooling data with results from injection system qualification, measured discharge coefficients, were a few percent lower for the same flow rates. This was due to two seperate effects: (1) no external flow existed with qualification tests whereas in later tests, jets were subject to external flow as the exited, and (2) when the injection system is connected to the wind tunnel test section floor, small steps were present at seam

locations in injection tubes. The slightly lower discharge coefficients, measured during wind tunnel testing, had no significant effect on flow behavior in the film cooled boundary layer or on the accuracy of measured injection flow parameters.

The spanwise averaged St/St_o ratios are plotted as functions of Reynolds number in Figure 38. Here a Reynolds number of 7.2E5 corresponds to an X/d ratio of 3.47 while a Reynolds number of 1.3E6 corresponds to an X/d ratio of 103.8, where X is distance from the down stream edge of injection holes, and injection hole diameter d=0.95 cm. As can be seen from the figure, the overall heat transfer rate has been substantially reduced when compared with that of the baseline. The greatest effect on the heat transfer due to the film cooling is near the leading edge of the test plate. The results show trends consistent with other heat transfer data from turbulent boundary layers cooled using a single row of injection holes [Ref. 12]

Temperature profiles were measured at 10 m/s with film cooling at a blowing ratio of 0.682 and θ=1.543. These are compared to profiles without film cooling for the same downstream position in Figure 42. The profiles with film cooling show larger differences from the freestream temperature, with smaller apparent near wall gradients and $T - T_\infty$ deficits which extend to greater Y than without

film cooling. Such behavior evidences some effects produced by film cooling: thicker thermal boundary layers and lower heat transfer from the wall to the freestream.

D. SINGLE VORTEX AND FILM COOLING

The final phase of research consisted of measuring the effects of a single vortex on heat transfer in a film-cooled turbulent boundary layer. Measurements were performed using vortex generator #2 placed at three different locations, Z=-3.52, -4.79, and -6.06 cm. All three sets of data were taken with a film cooling blowing ratio of approximately 1.5. Numerical output, found in Appendix E, were calculated in a similar manner to those of previous tests except two Stanton number ratios have been calculated: St/St_o, the Stanton number ratio in relation to the original baseline, and St/St_f, the Stanton number ratio in relation to tests with film cooling only at the same and m values.

The graphical representations of St/St_o as a function of Z, with the vortex located at Z=-4.79 cm, are shown in Figures 43 through 49. In these figures, St/St_o =1 corresponds to an undisturbed turbulent boundary layer, square symbols correspond to a boundary layer with film cooling, and circular symbols show results for a boundary layer with film cooling and an embedded vortex. As shown in the figures, except for local hot spots, overall heat transfer rates are lower than in an undisturbed turbulent

boundary. Localized heat transfer rates greater than St/St=1.0 occur near the vortex downwash side. The increase begins at approximately X=1.3 meters and continues down the length of the test surface. At X=1.457 meters the maximum where St/St =1.112. Another interesting feature is the overall drop in the Stanton number ratio, ranging from 6 - 11%, on the upwash side of the vortex. This effect persists not only in the downstream direction along the length of the surface, but also in the spanwise direction.

Figure 50 shows the effect of an embedded vortex on Stanton numbers in a film cooled turbulent boundary layer in terms of St/St_f .From this figure, it is apparent that there is a large heat transfer gradient near the upwash side of the vortex. The rise in heat transfer rates, although demonstrating localized maximums, persists along the length of the test surface at a Z value of approximately 2.54 cm.

When the vortex generator was moved to Z=-3.52 and -6.06 cm, Figures 51 through 58 indicate that the same overall qualitative data trends are present. However, drastic local quantitative changes occur because the vortex location is changed with respect to the film cooling holes. Local increases in Stanton number ratios are again present along with decreases on the upwash side of the vortex. These decreased St/St_o values persist not only in the direction of flow but also in the spanwise direction.

Decreased St/St_f ratios are seen in Figures 54 and 58. On the +Z side of the test surface St/St_f ratios are as low as 0.85. The vortex appears to push the coolant from its upwash side causing the coolant to disperse in a fairly uniform manner. In contrast, without film cooling, decreases in local heat transfer near the vortex upwash side are more localized.

Figure 59 shows the temperature distribution in the Y, Z plane of vortex #2 with film cooling. An approximate location of the thermal boundary layer is identified. The results used in this figure are only tentative.

IV. SUMMARY AND CONCLUSIONS

Baseline measurements show excellent agreement with Stanton number correlations for a flat plate with constant wall heat flux and unheated starting length. Results with film cooling show expected trends, and results with an embedded vortex show excellent agreement with data from the literature. The effects of the vortex on heat transfer in the film cooled boundary layer are significant and important: (1) on the downwash side of the vortex, heat transfer is augmented, effects of film cooling are negated and local "hot-spots" will exist in engines; (2) near the upwash side of the vortex, coolant is pushed to the side of the vortex, appearing to augment the protection provided by film cooling; and (3) as the vortex location is changed with respect to film cooling holes, significant local quantitative changes in heat transfer occur even though overall qualitative trends remain unchanged.

It is recommended that in subsequent experimentation that spatial resolution be increased, provided it can be done without compromising the integrity of the heat transfer surface. In order to more clearly visualize the interaction of the vortex with film cooling injection, it would also be desireable to employ flow visualization.

APPENDIX A

FIGURES

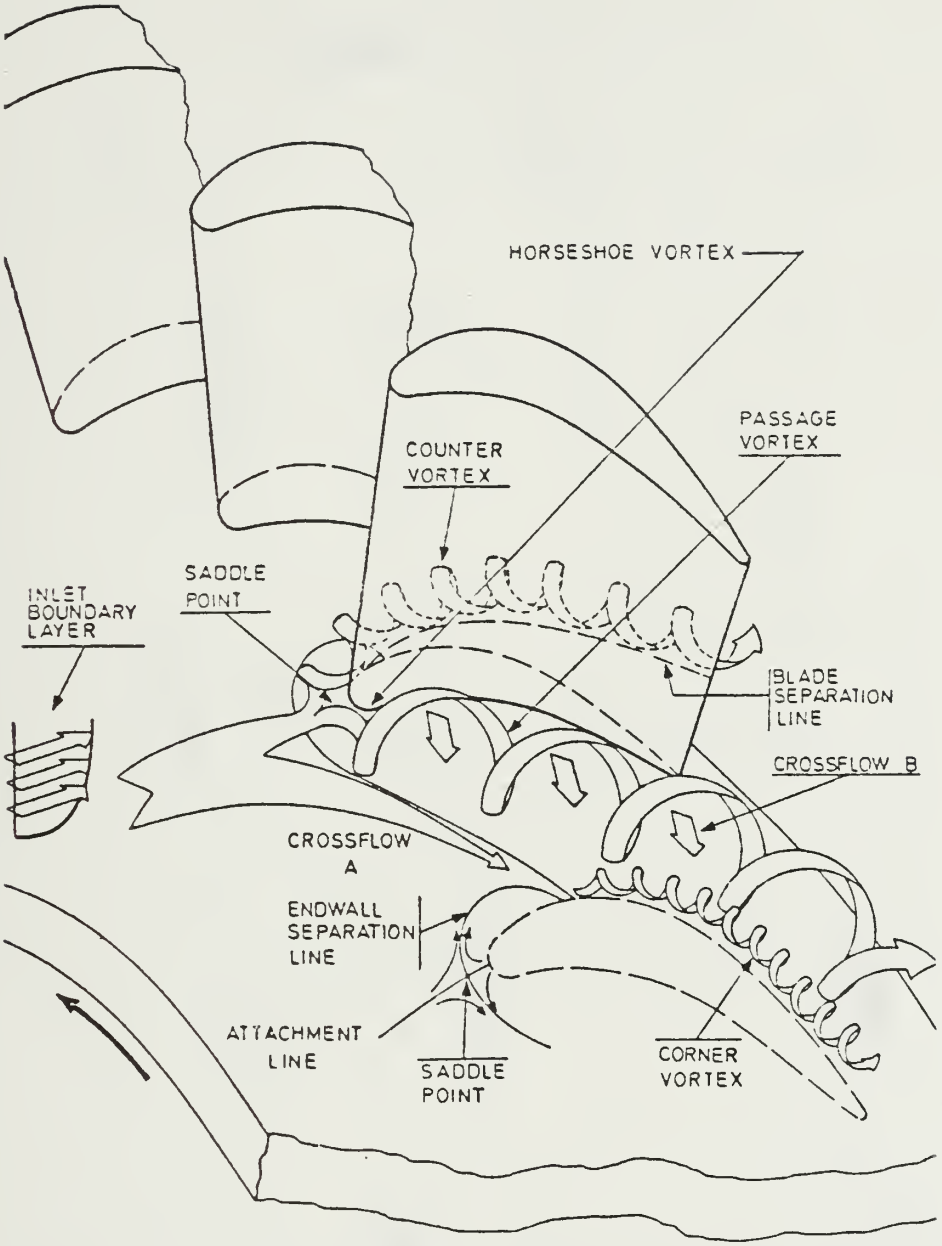

Figure 1. Endwall Secondary flows

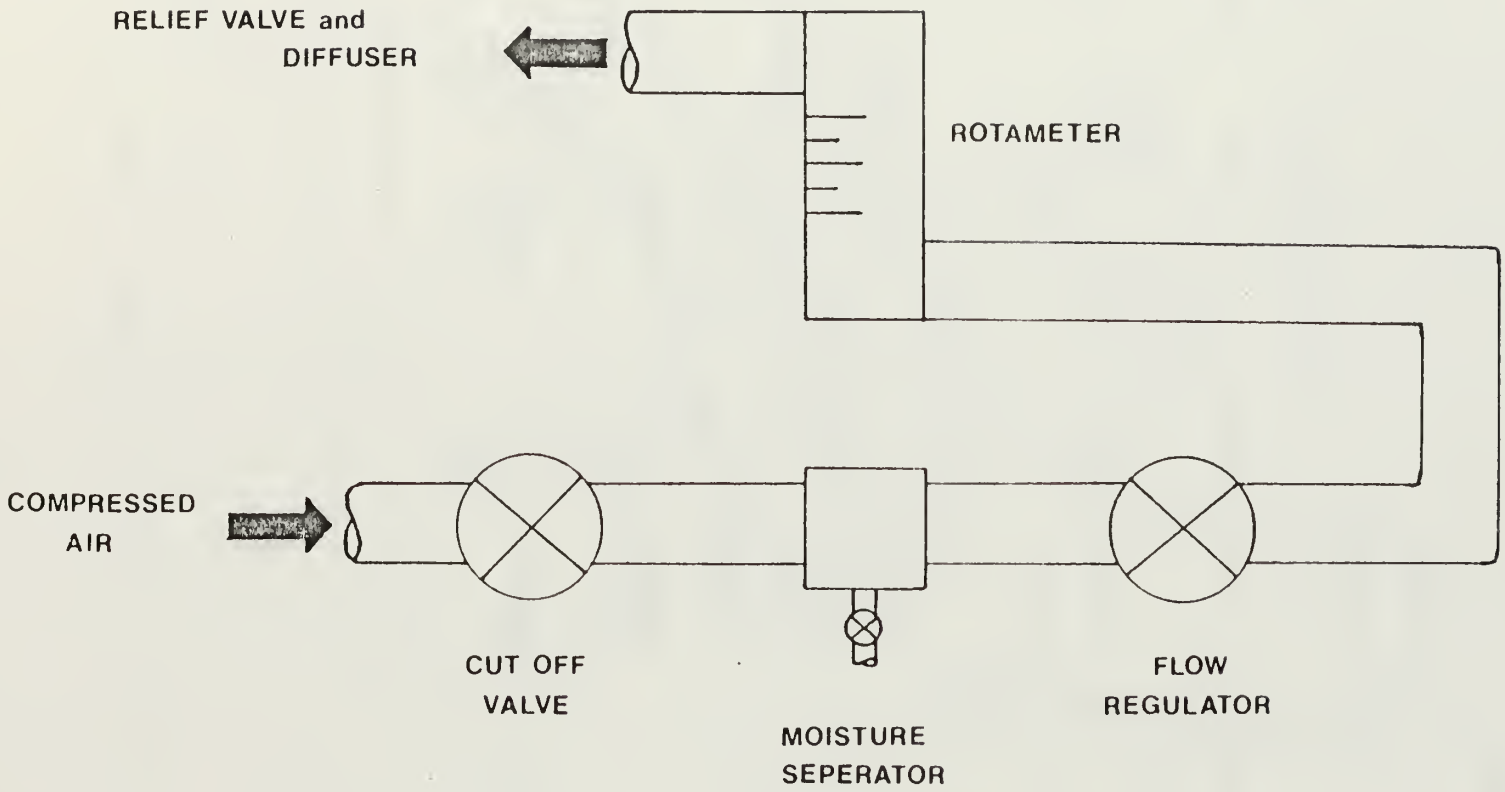

Figure 2. Schematic of Air Supply

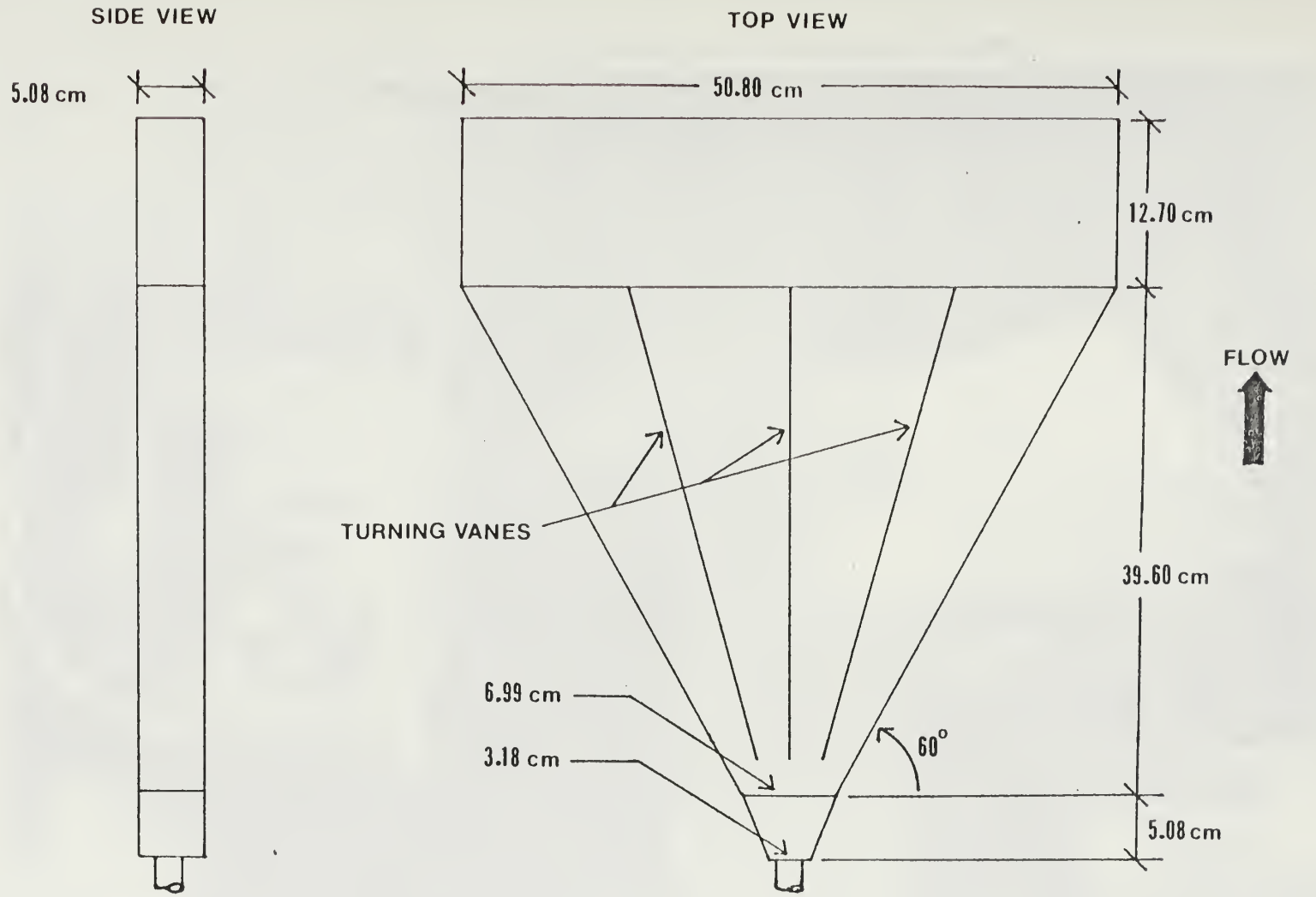

Figure 3. Diffuser Section

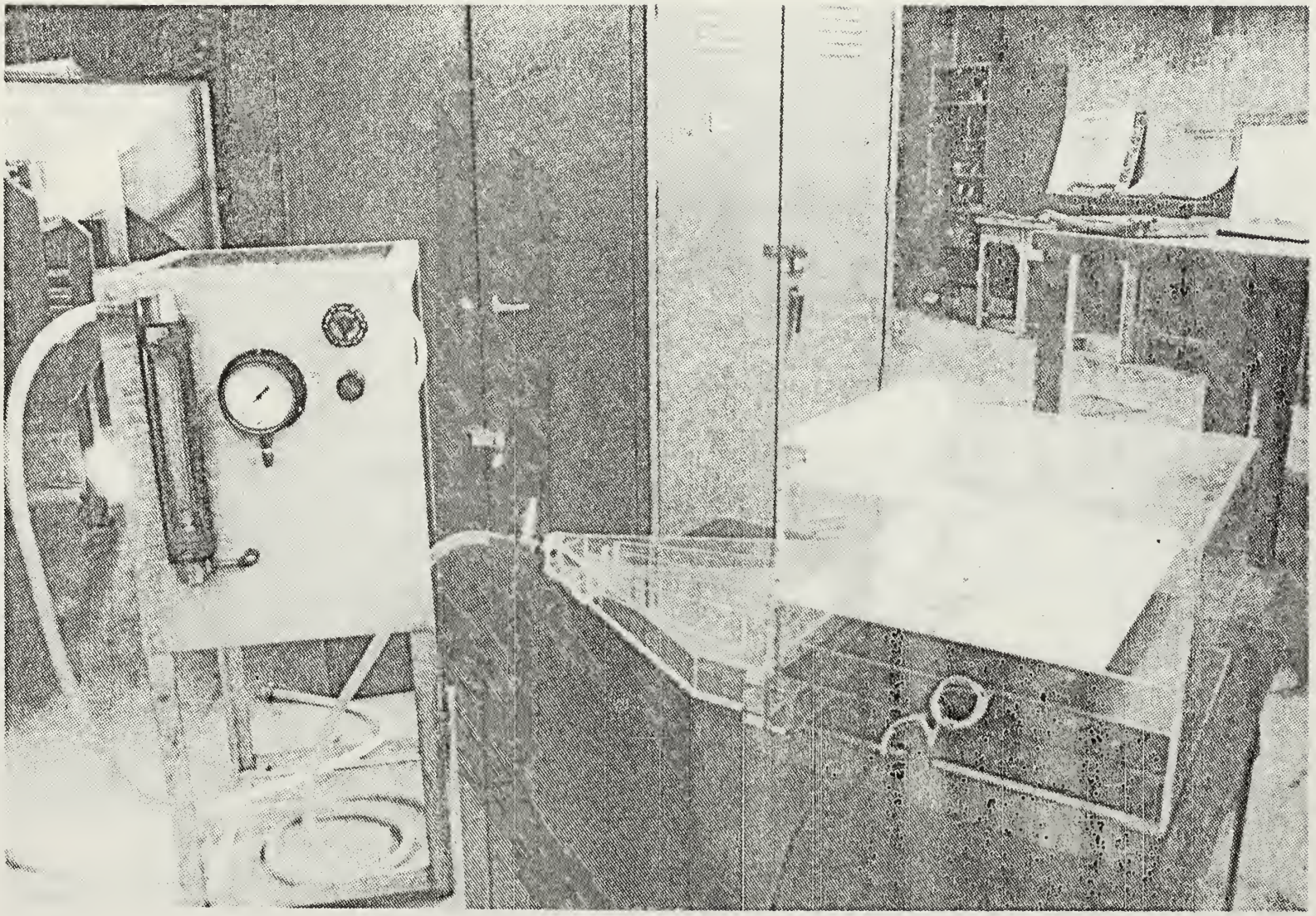

Figure 4. Photograph of Injection System

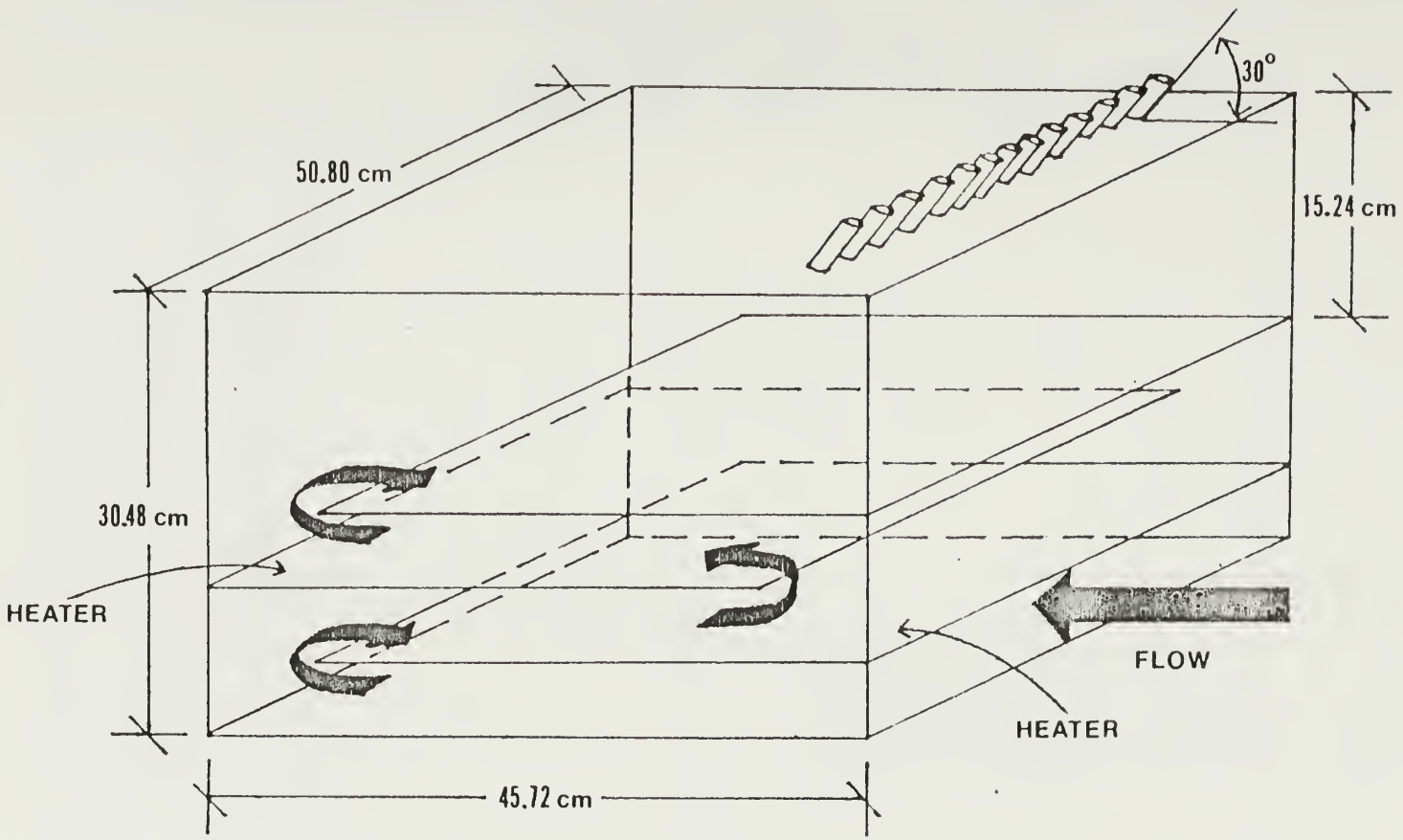

Figure 5. Injection Plenum Chamber

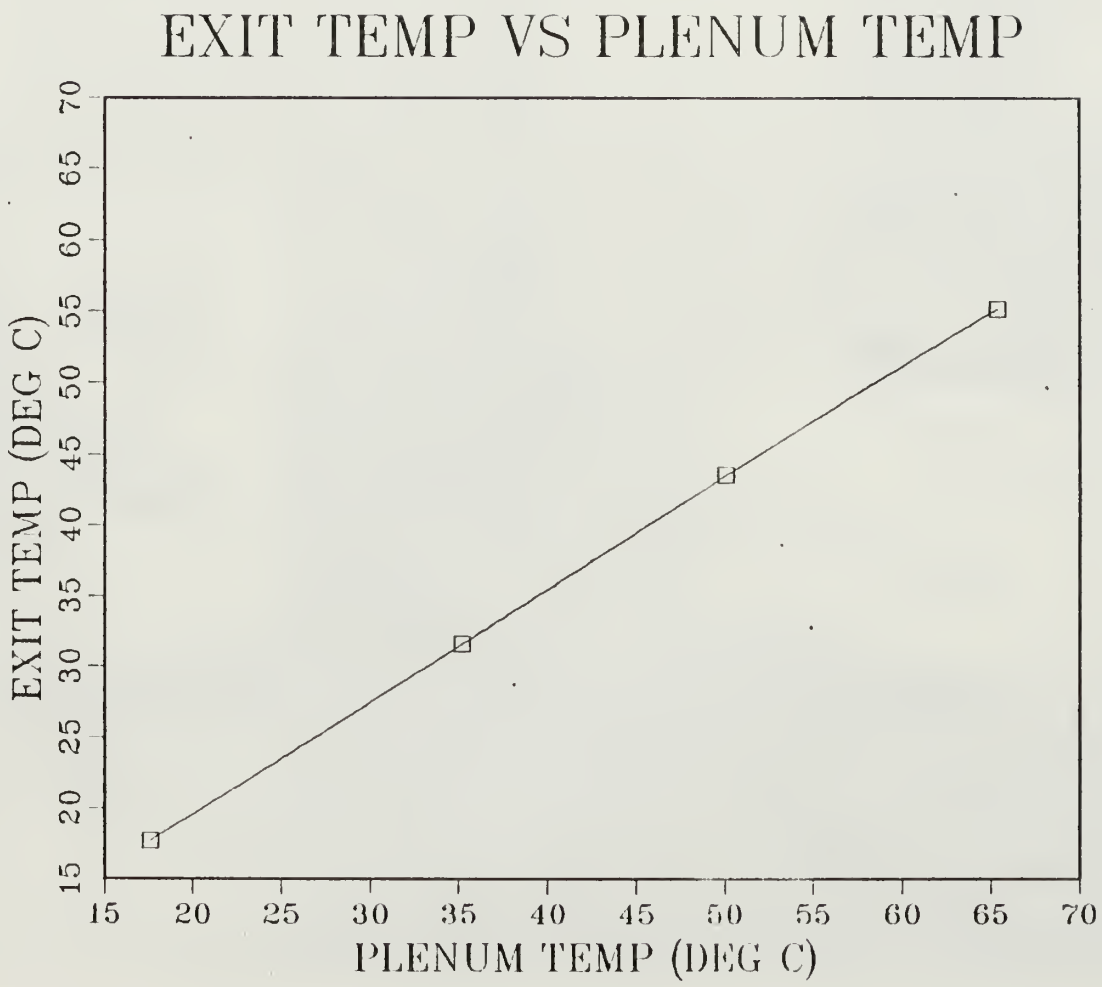

Figure 6. Coolant Temperature verses Plenum Temperature

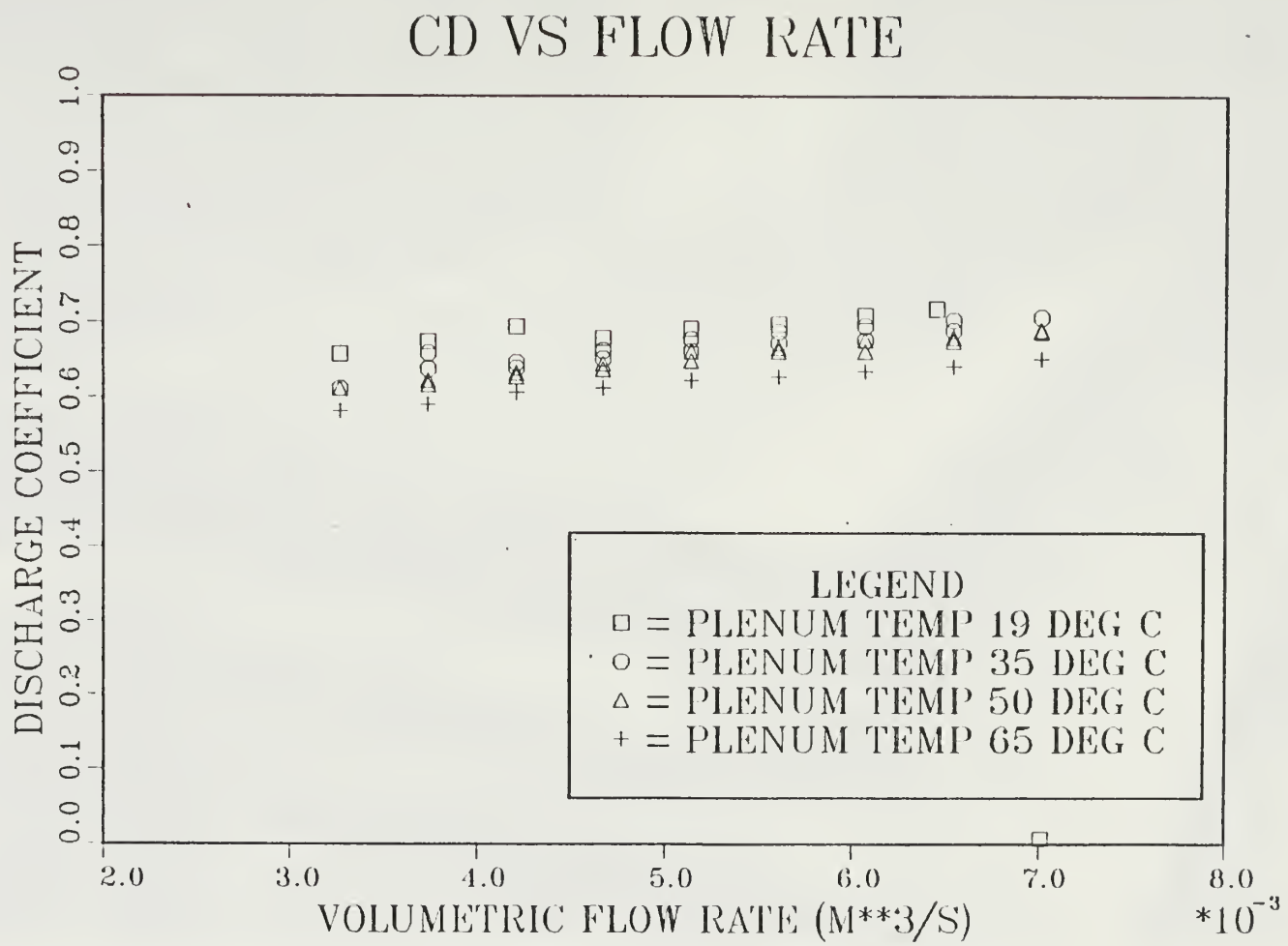

Figure 7. Discharge Coefficient verses Flow Rate

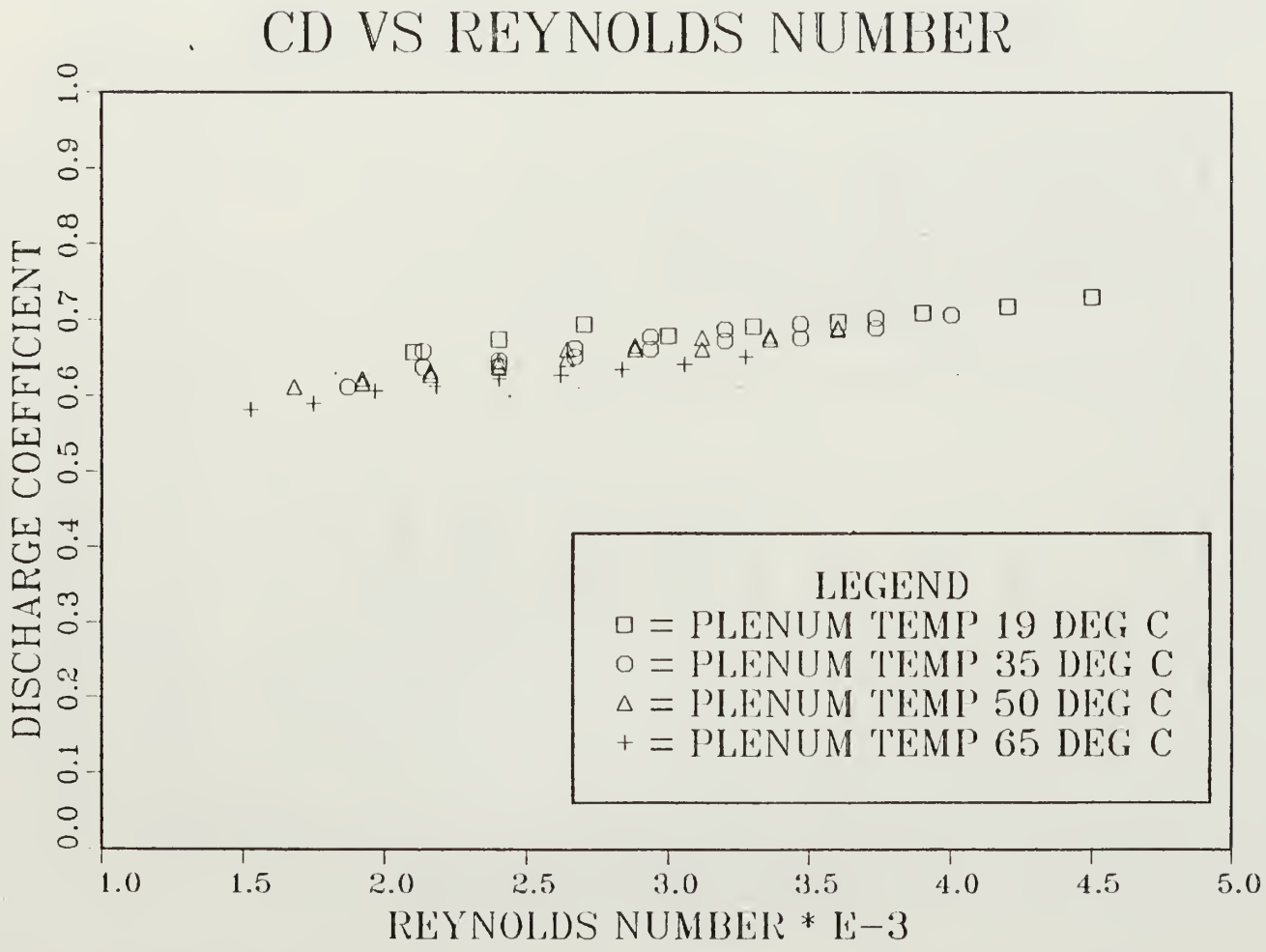

Figure 8. Discharge Coefficient verses Reynolds Number

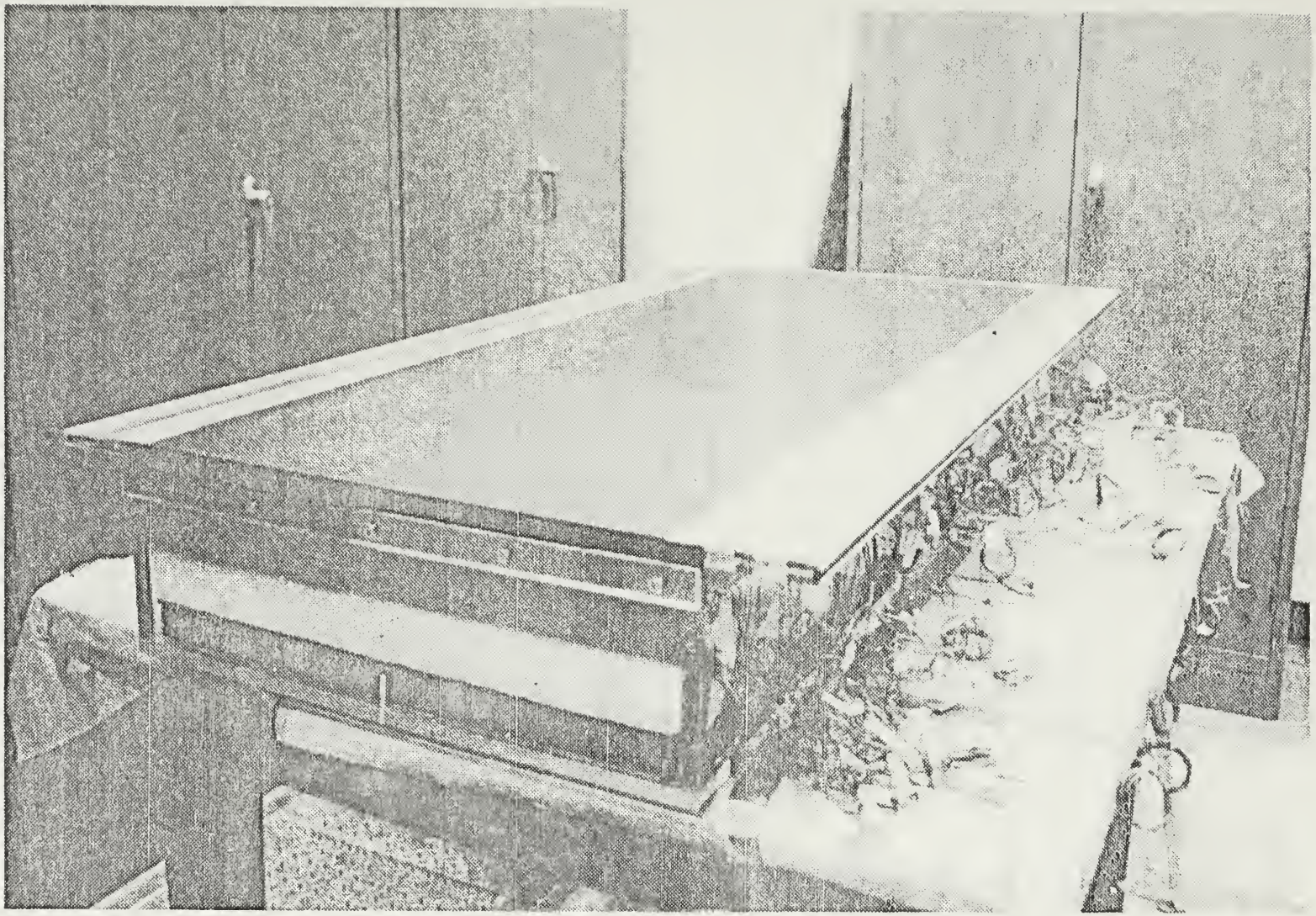

Figure 9. Photograph of Test Surface

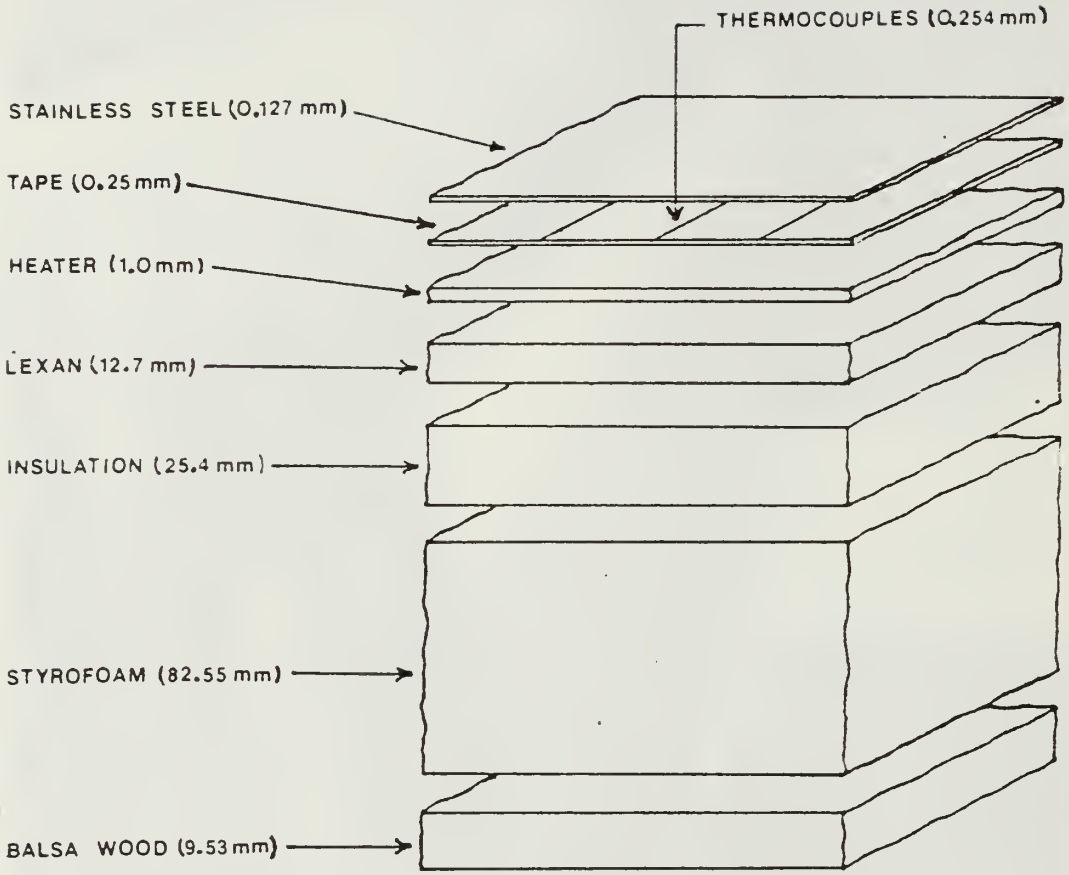

Figure 10. Cross Section of Test Surface

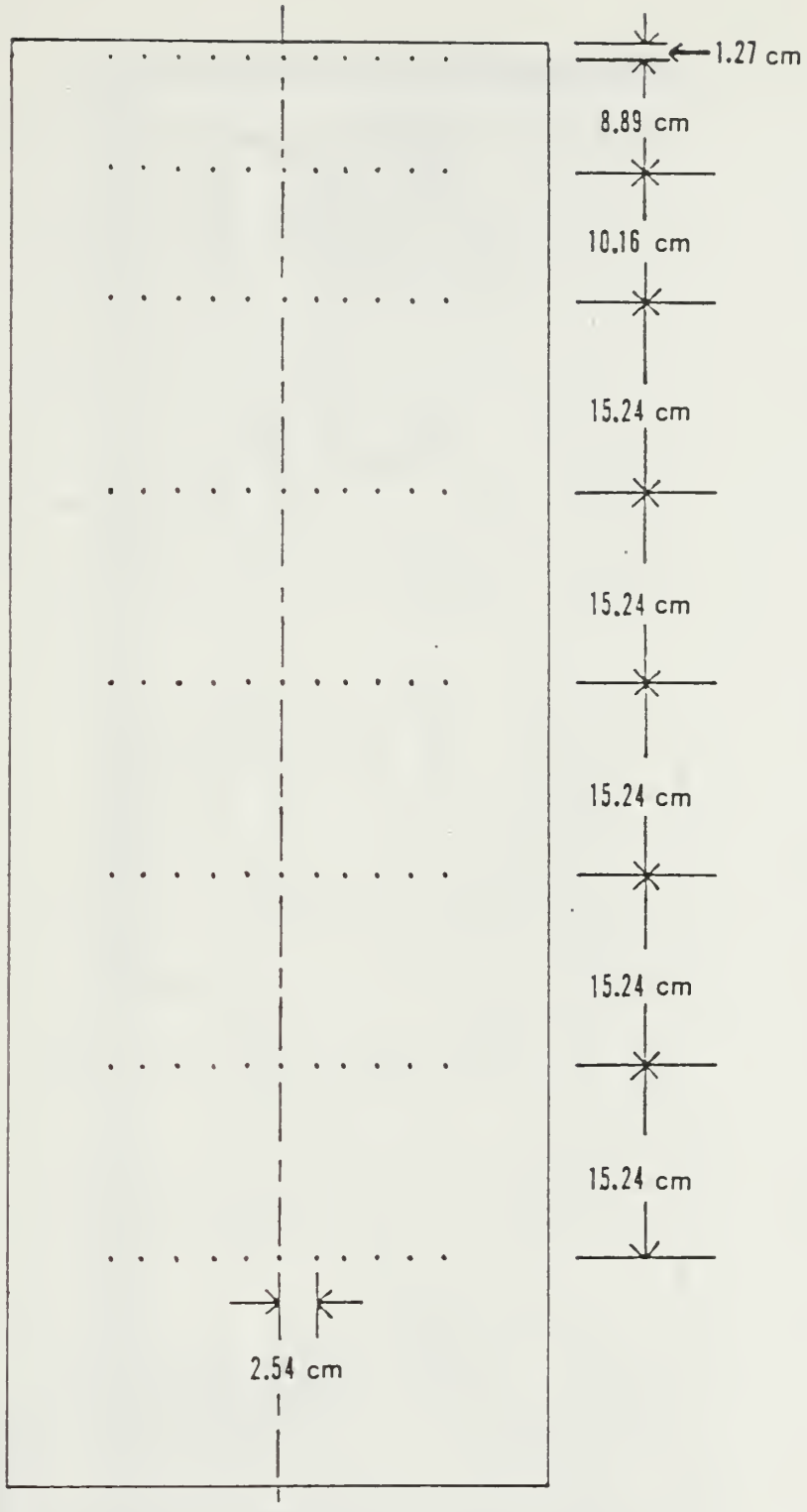

Figure 11. Test Section Thermocouple Placement

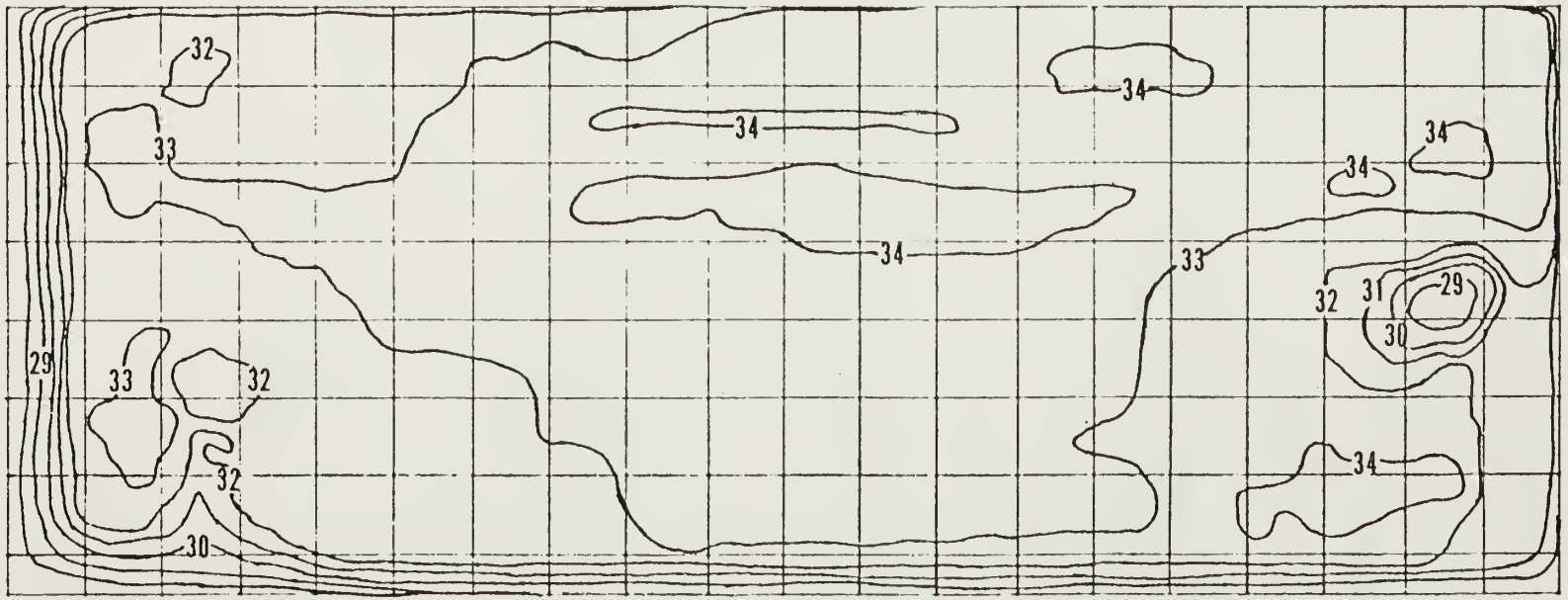

Figure 12. Isobars with Natural Convection ($T_w \approx 33\,^{\circ}C$)

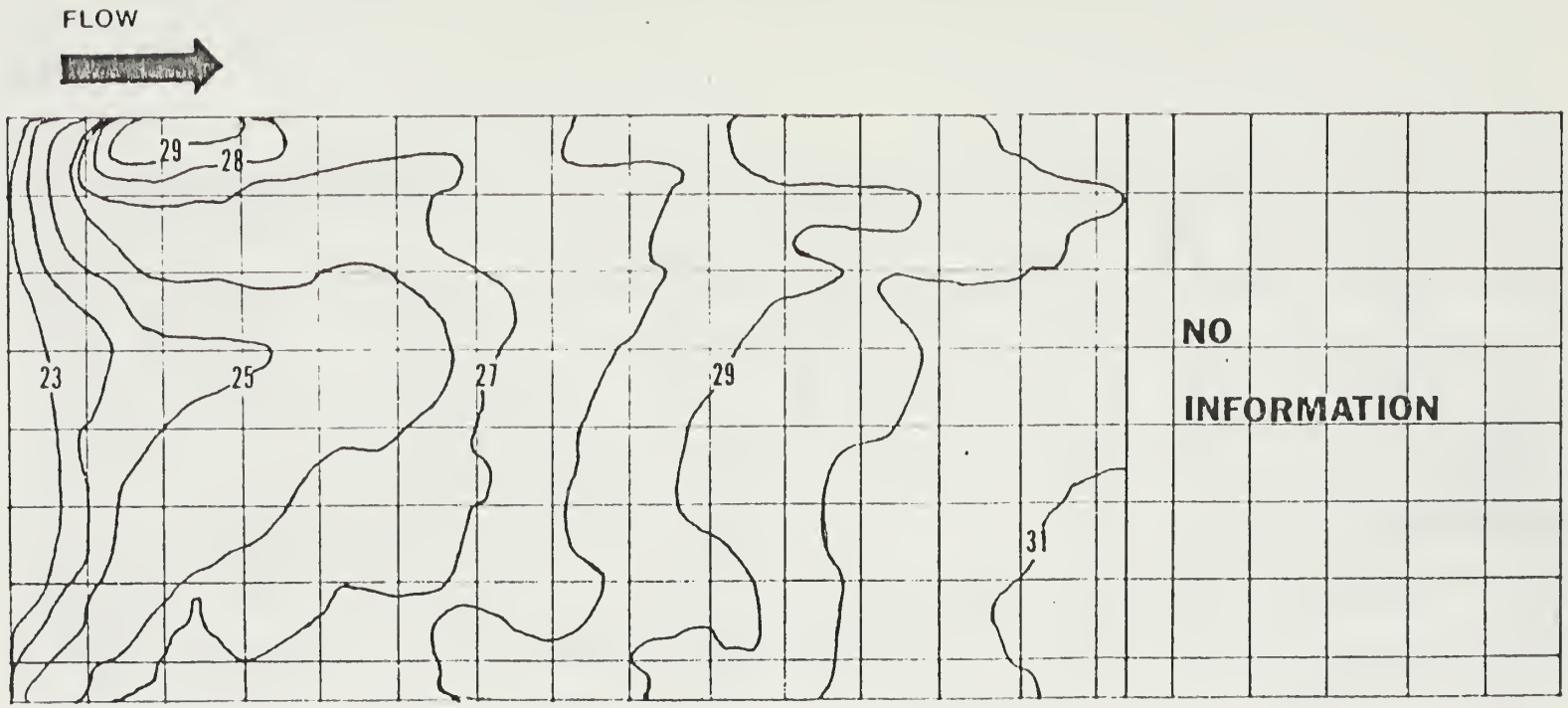

Figure 13. Isobars with Forced Convection ($T_w \approx 33\,^{\circ}C$)

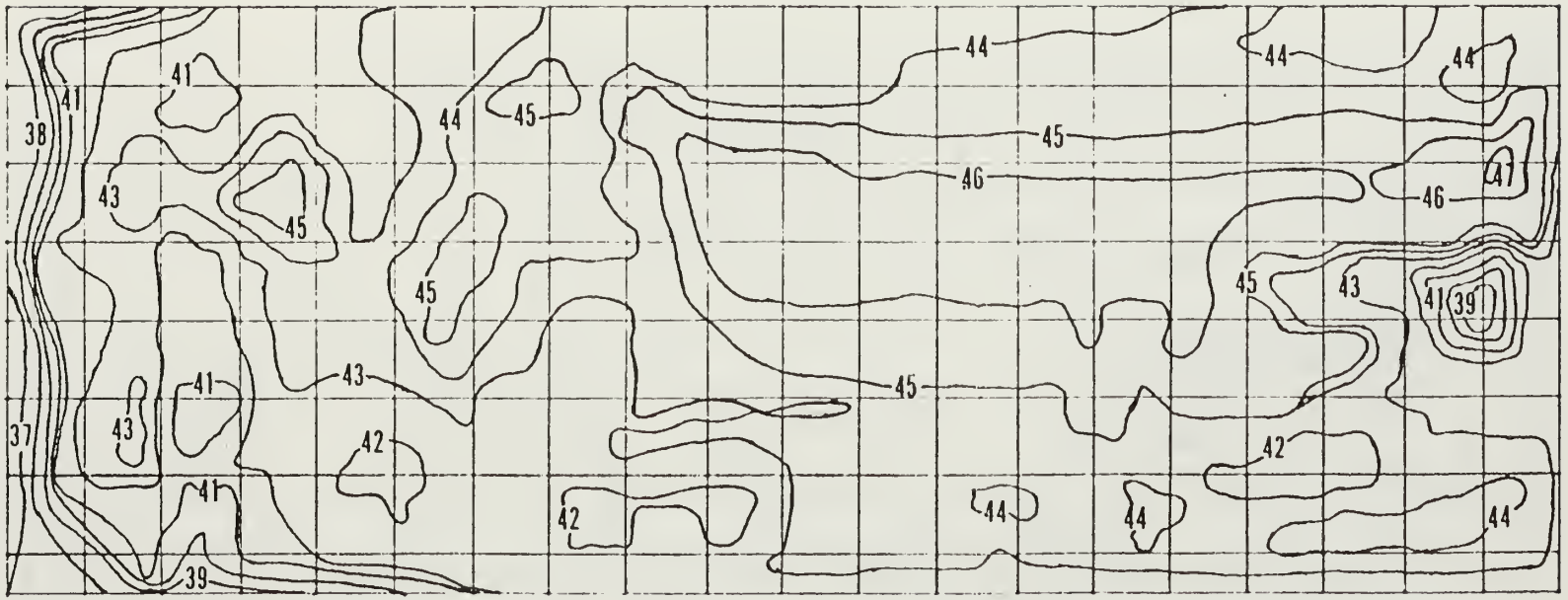

Figure 14. Isobars with Natural Convection ($T_w \approx 45\,^{\circ}C$)

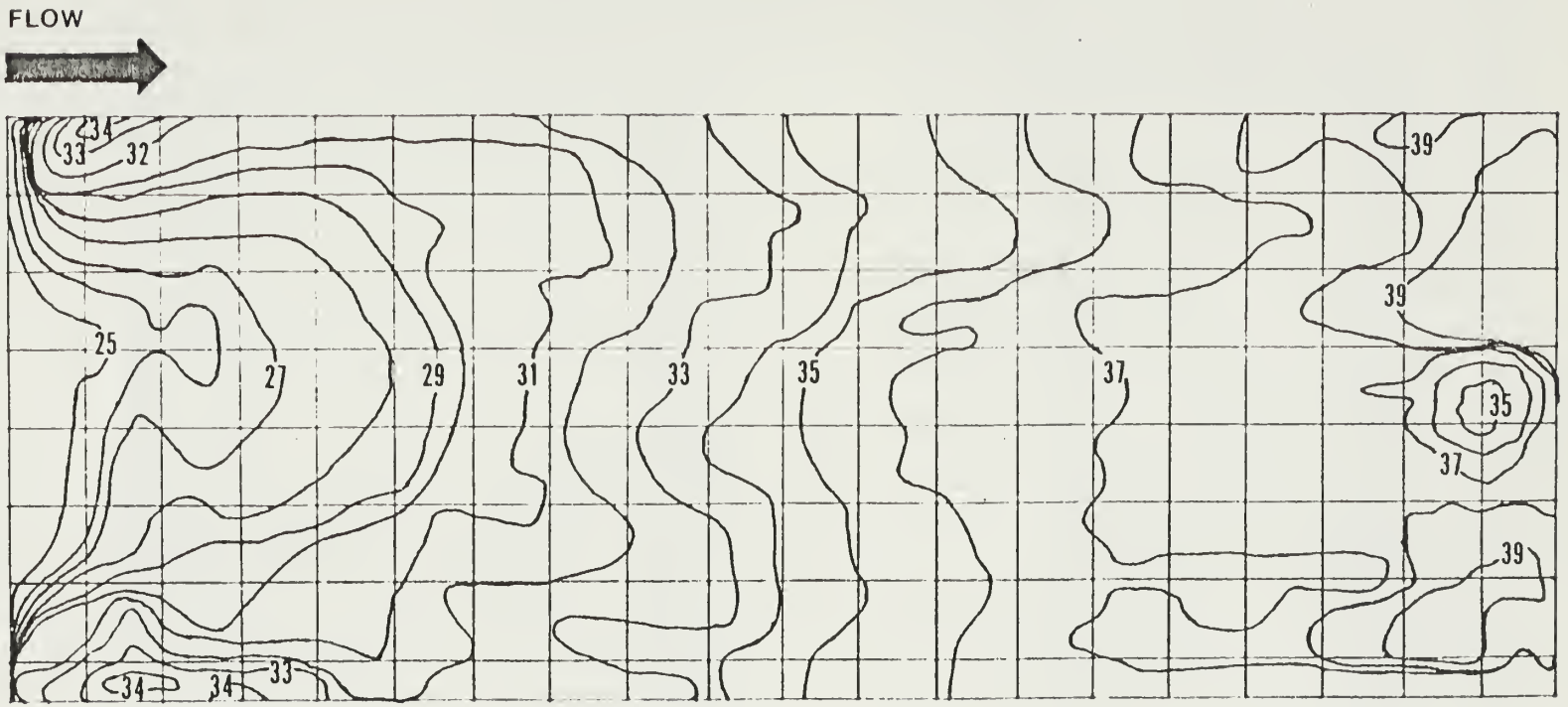

Figure 15. Isobars with Forced Convection ($T_w \approx 40\,^{\circ}C$)

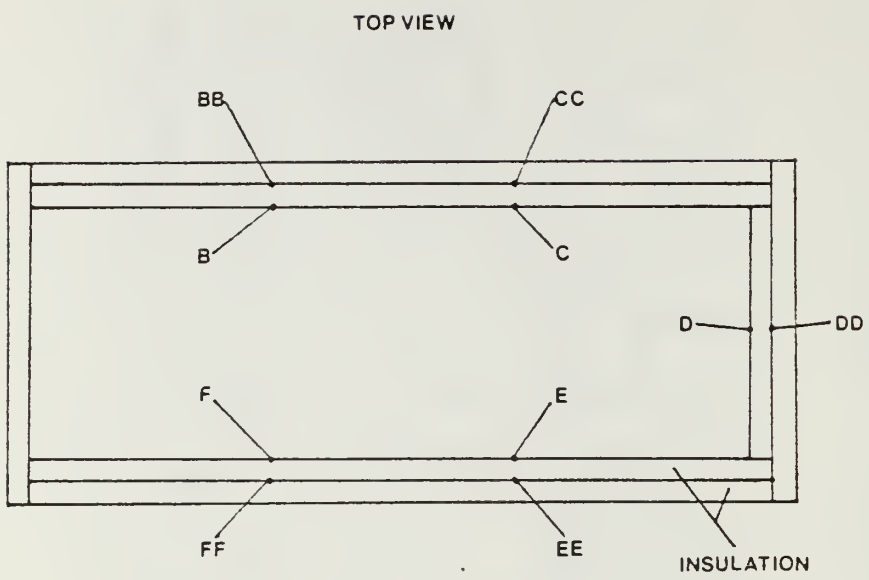

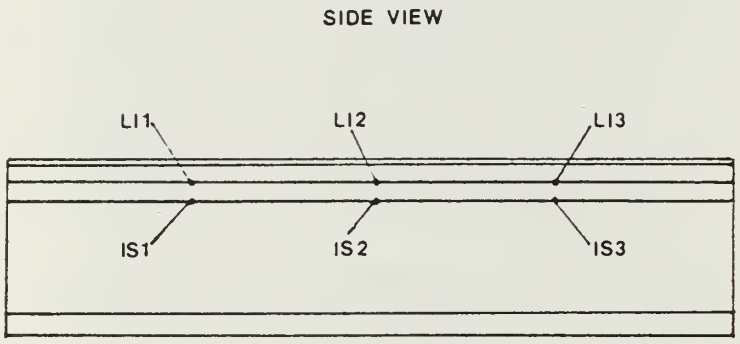

Figure 16. Energy Balance Thermocouple Placement

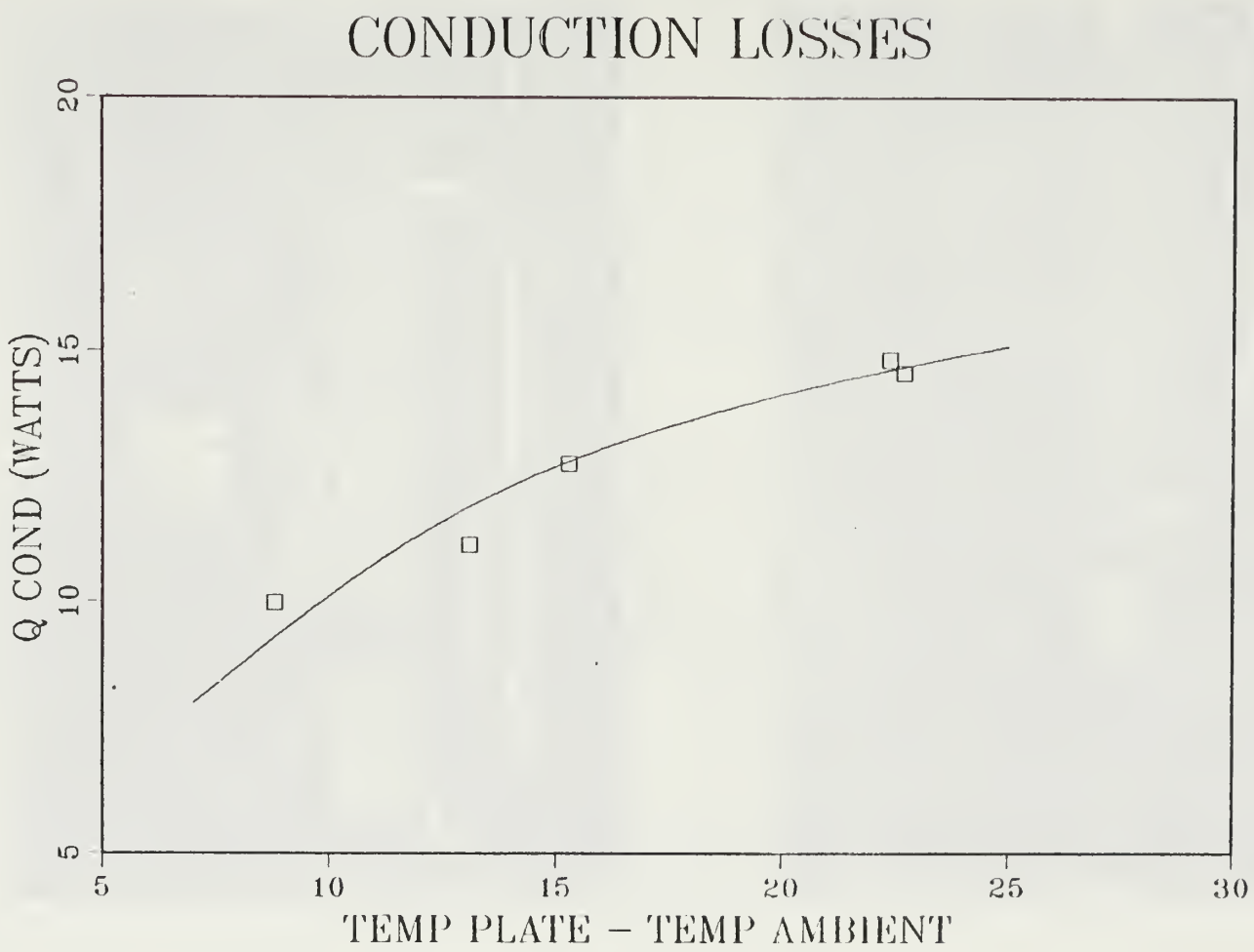

Figure 17. Conduction Losses

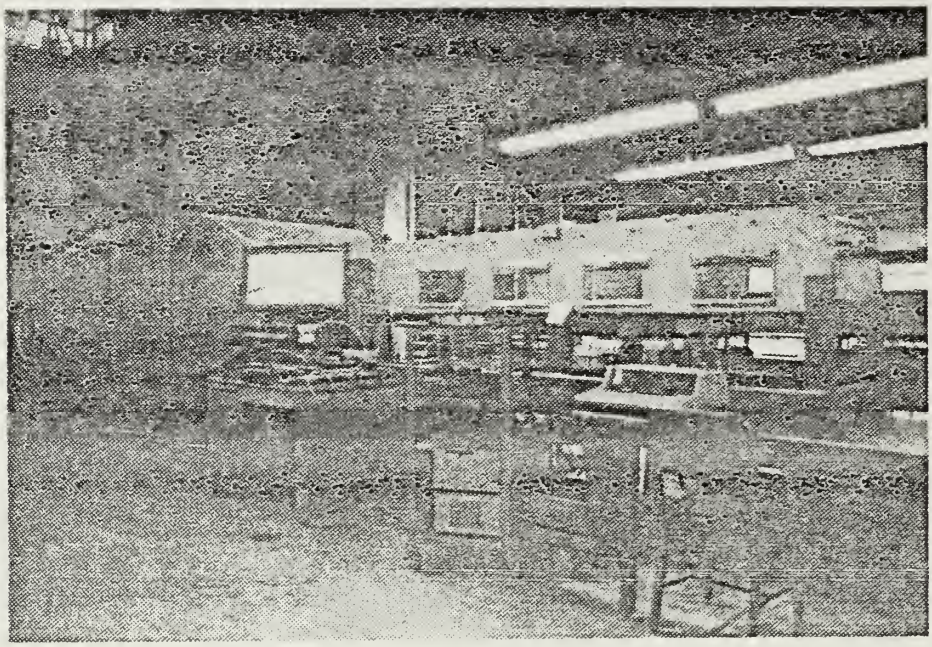

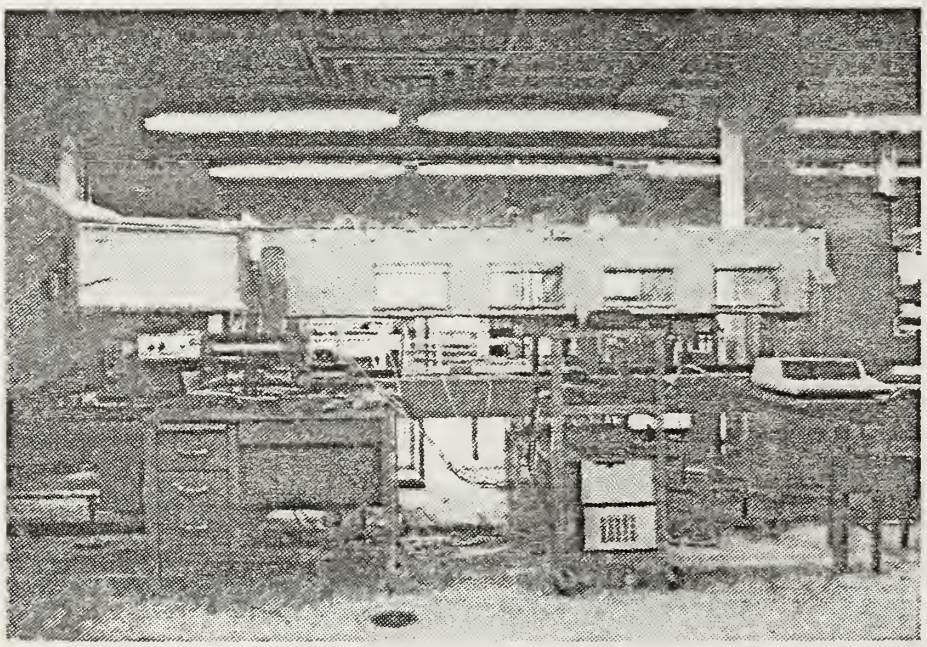

Figure 18. Photographs of Wind Tunnel

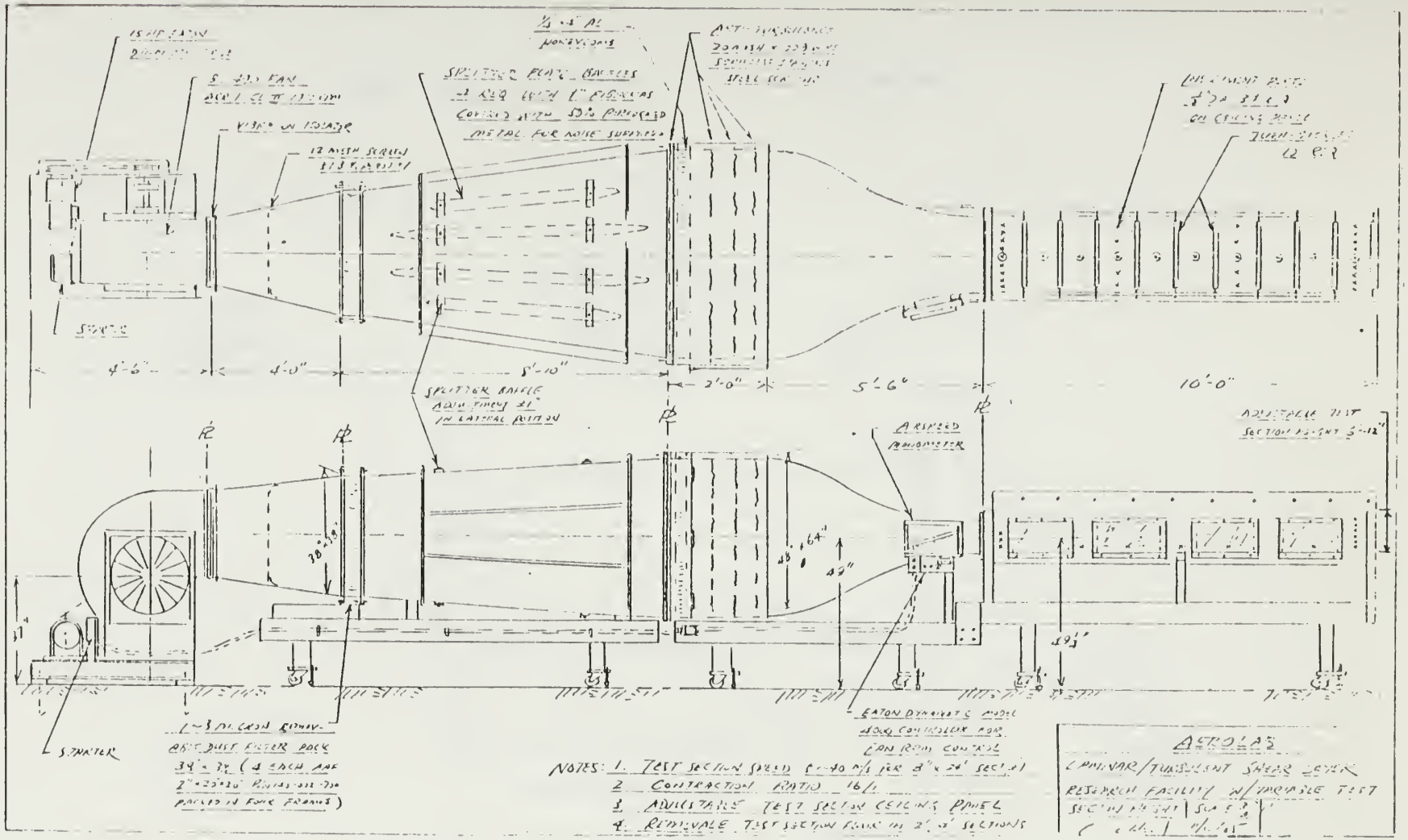

Figure 19. Schematic of Wind Tunnel

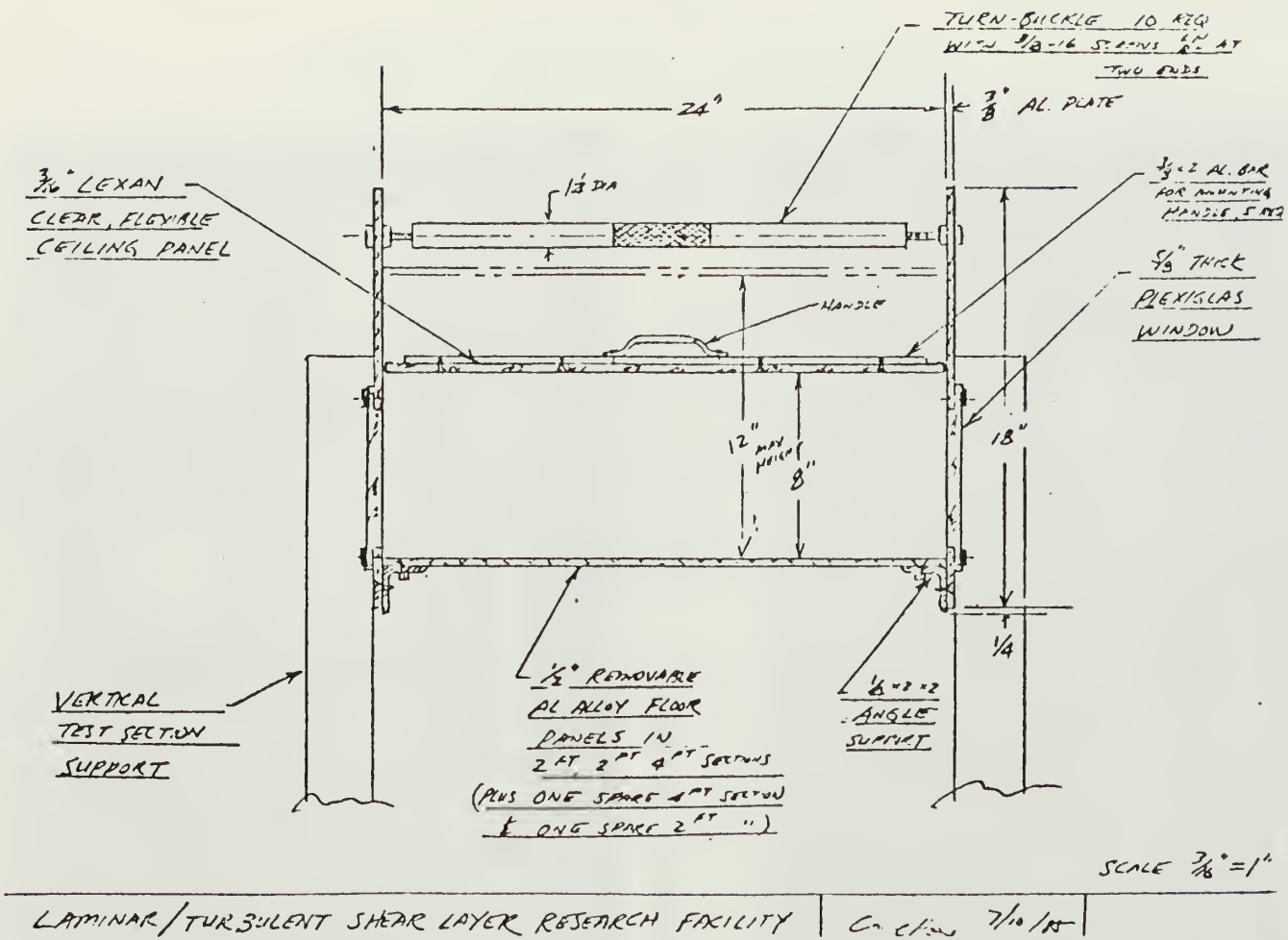

Figure 20. Cross Section of Wind Tunnel

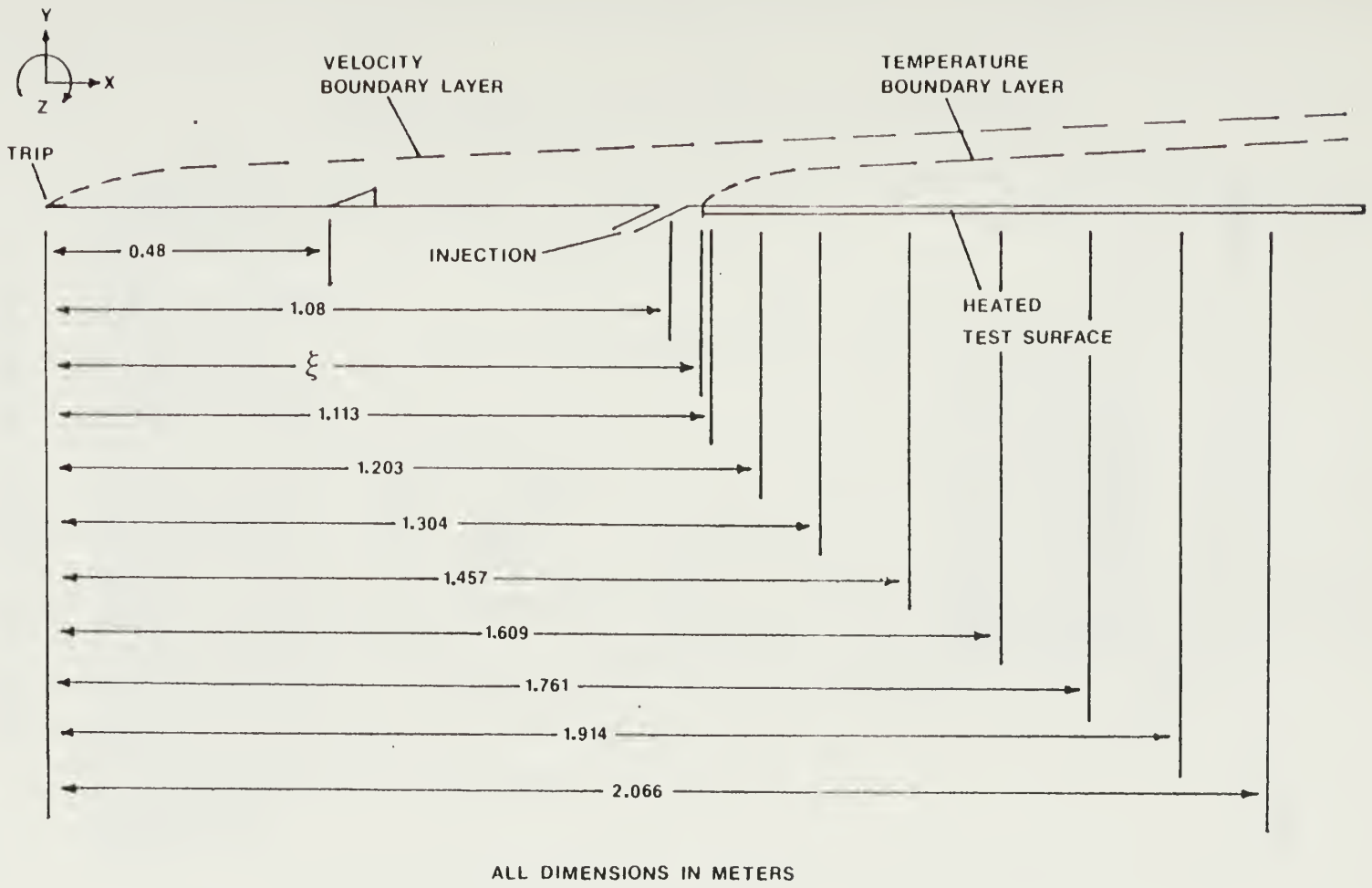

Figure 21. Coordinate System of Test Section

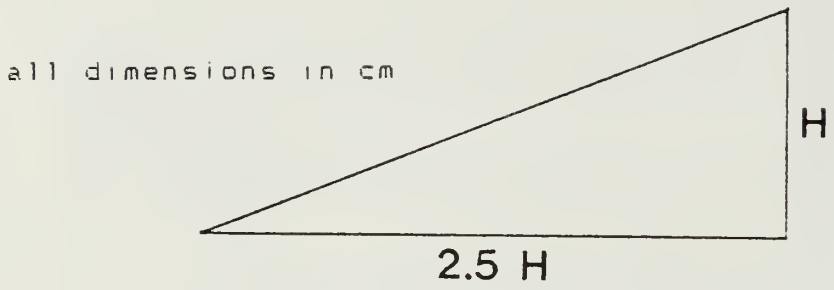

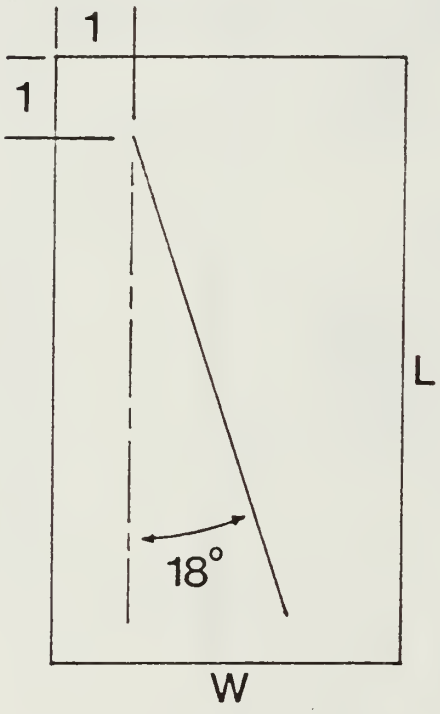

	H	2.5 H	L	W
#1	1.8	4.50	6.50	3.50
#2	3.0	7.50	9.50	4.50
#3	5.0	12.50	14.00	6.00
#4	7.0	17.50	19.00	7.50

Figure 22. Vortex Generators

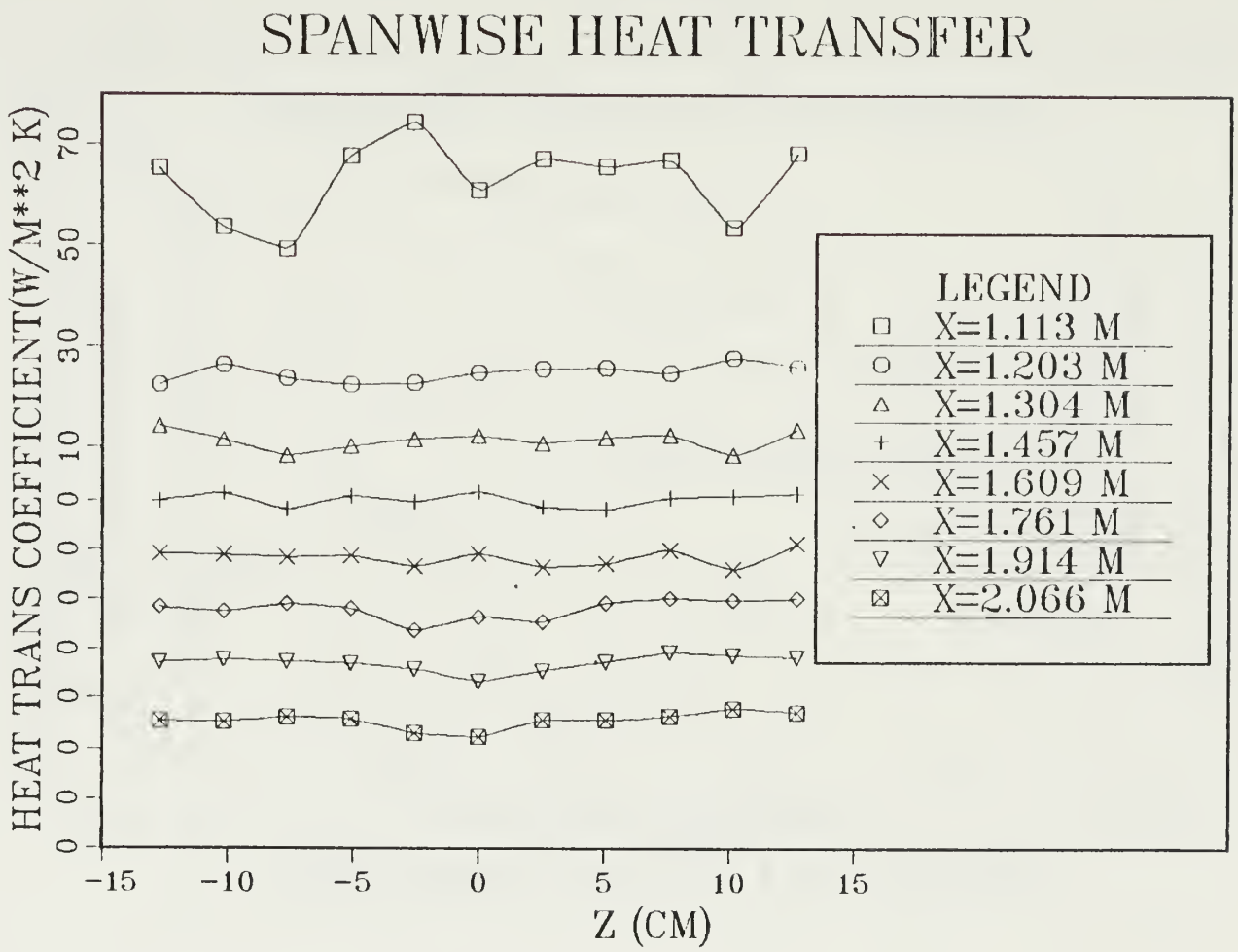

Figure 23. Spanwise Heat Transfer at 10 m/s

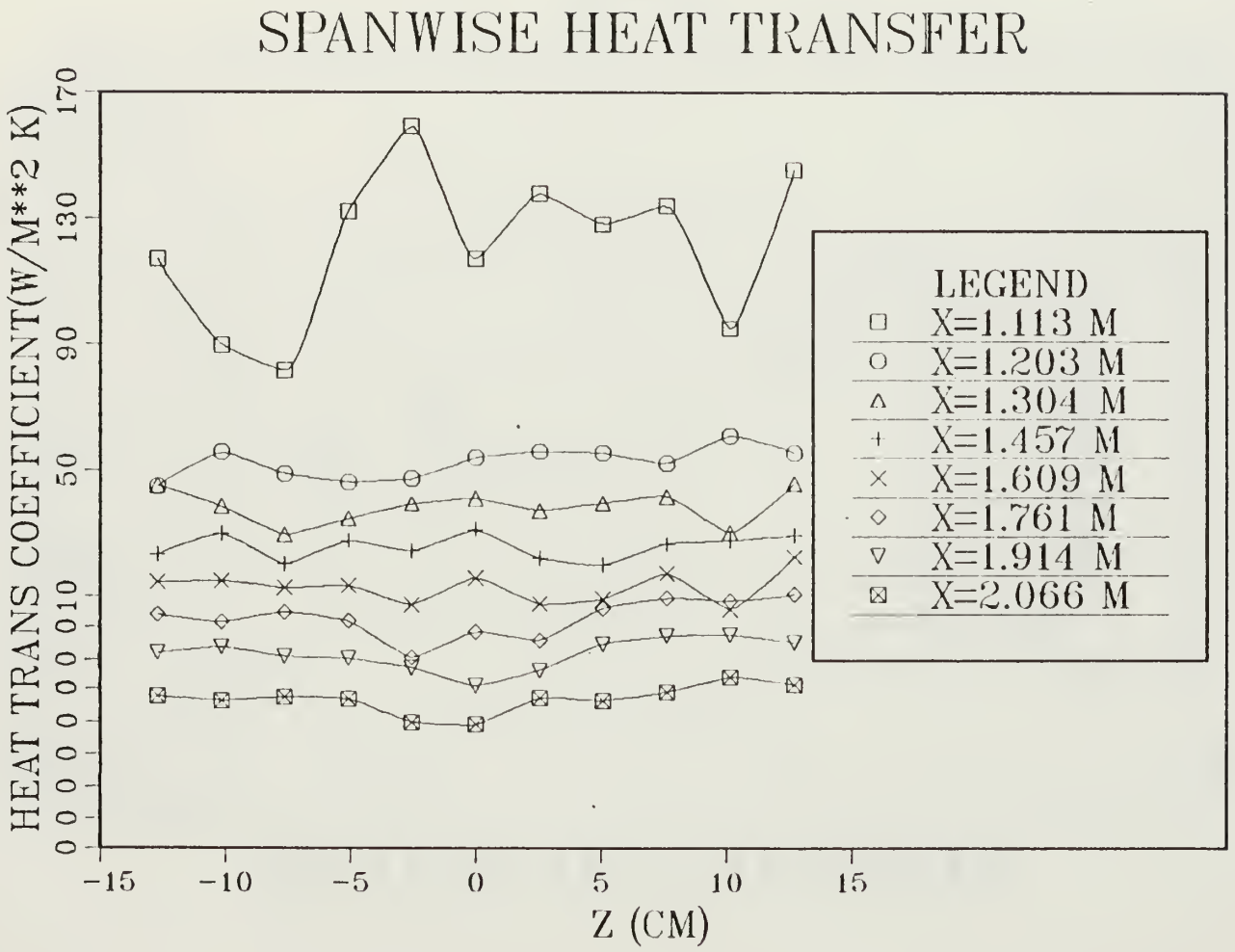

Figure 24. Spanwise Heat Transfer at 20 m/s

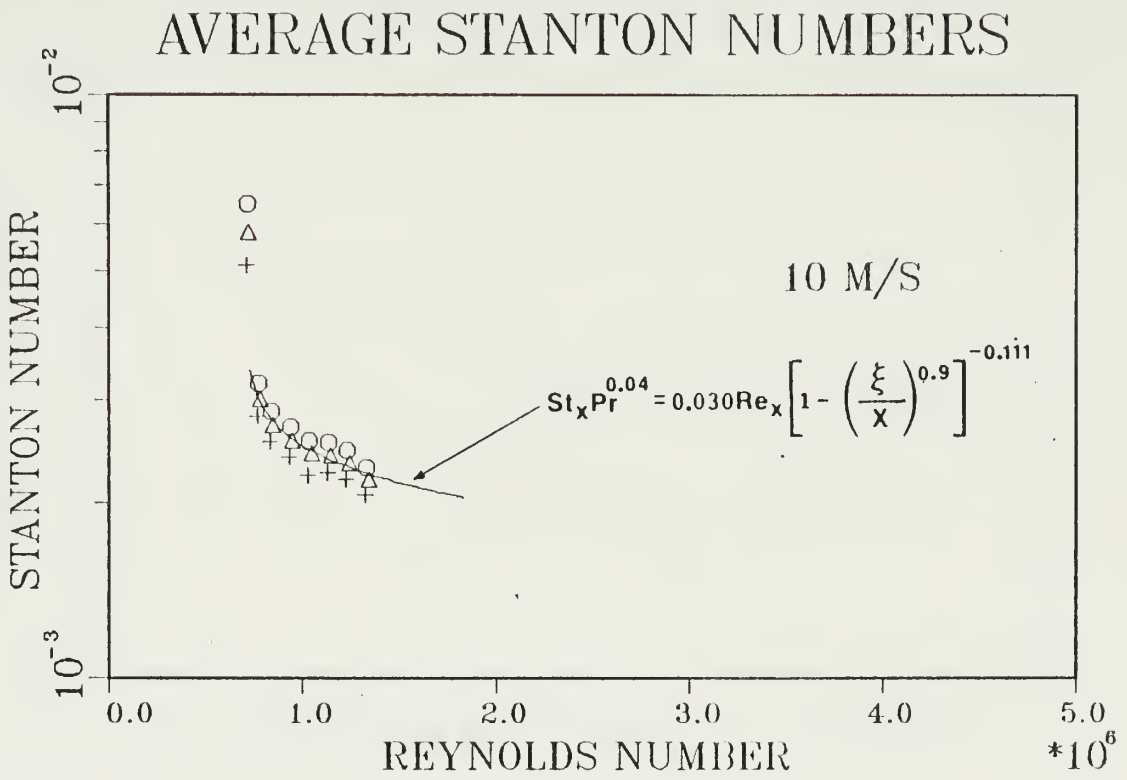

Figure 25. Spanwise Averaged Stanton Numbers at 10 m/s

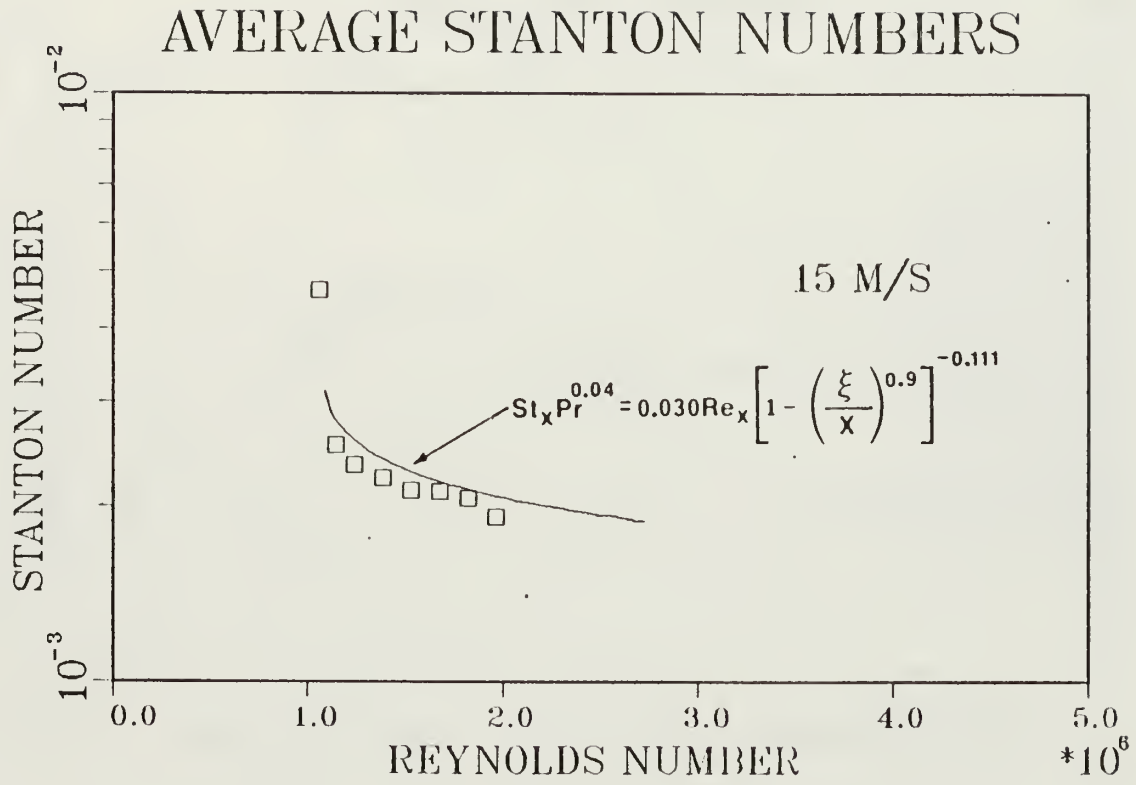

Figure 26. Spanwise Averaged Stanton Numbers at 15 m/s

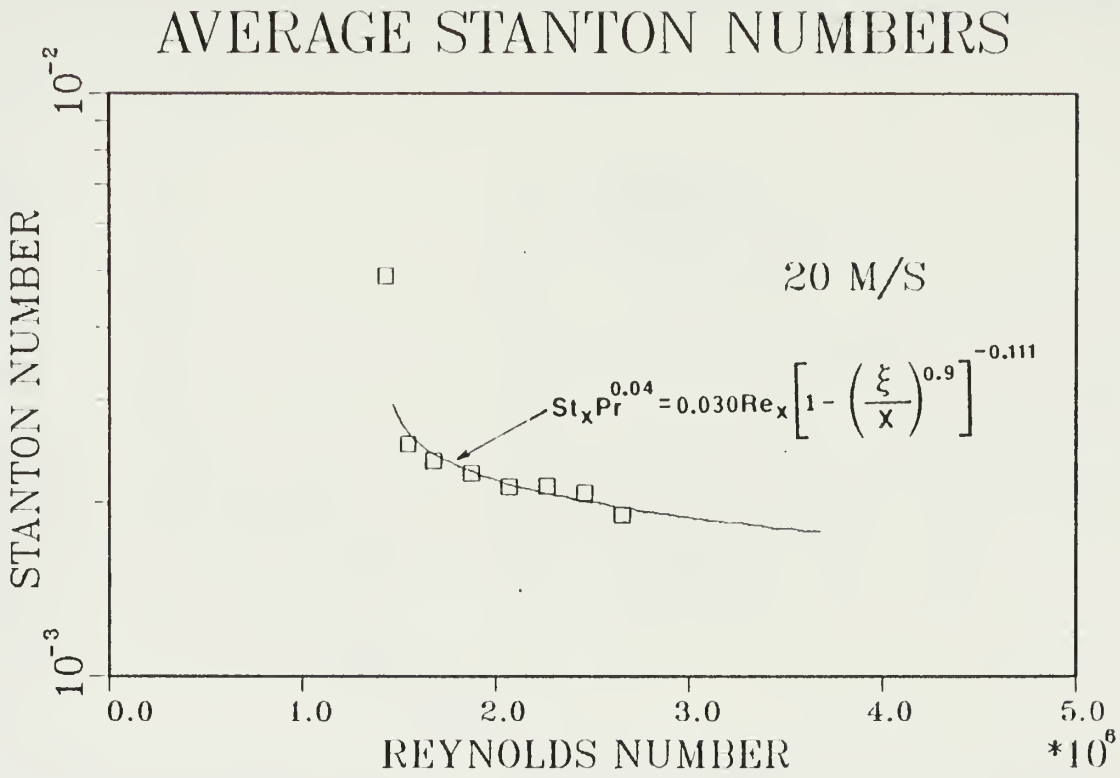

Figure 27. Spanwise Averaged Stanton Numbers at 20 m/s

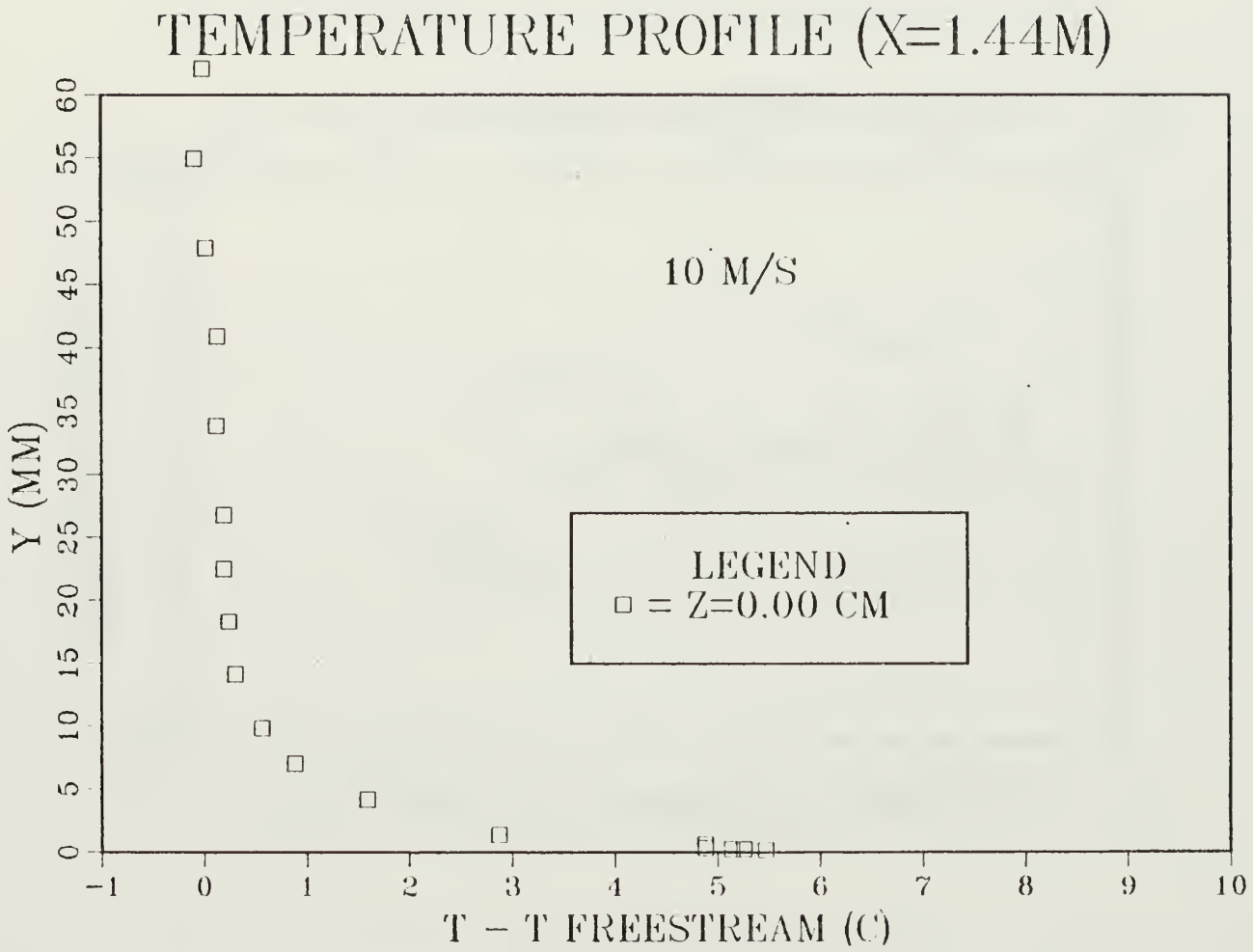

Figure 28. Temperature Profile of Turbulent Boundary Layer at X=1.44 m

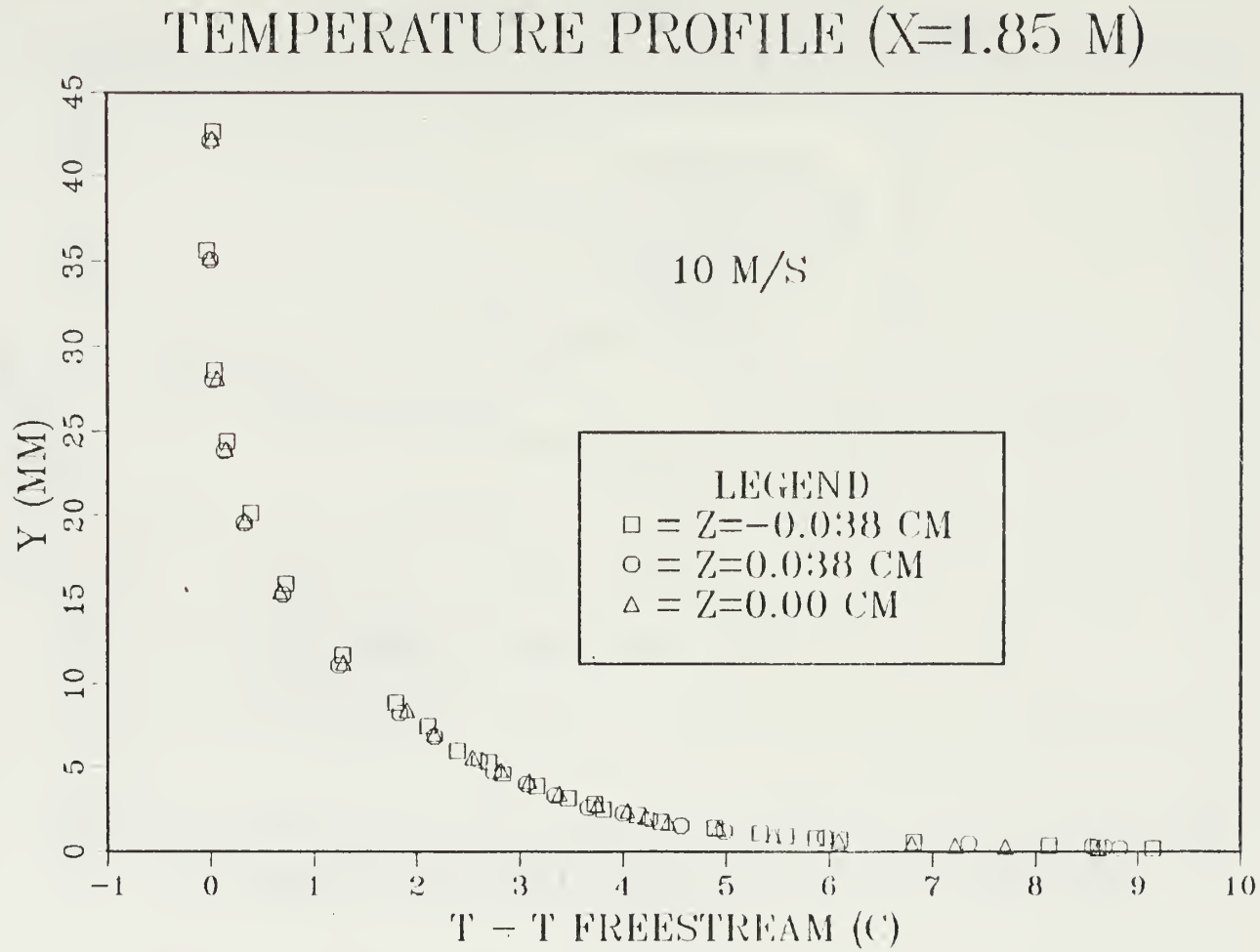

Figure 29. Temperature Profile of Turbulent Boundary Layer at X=1.85 m

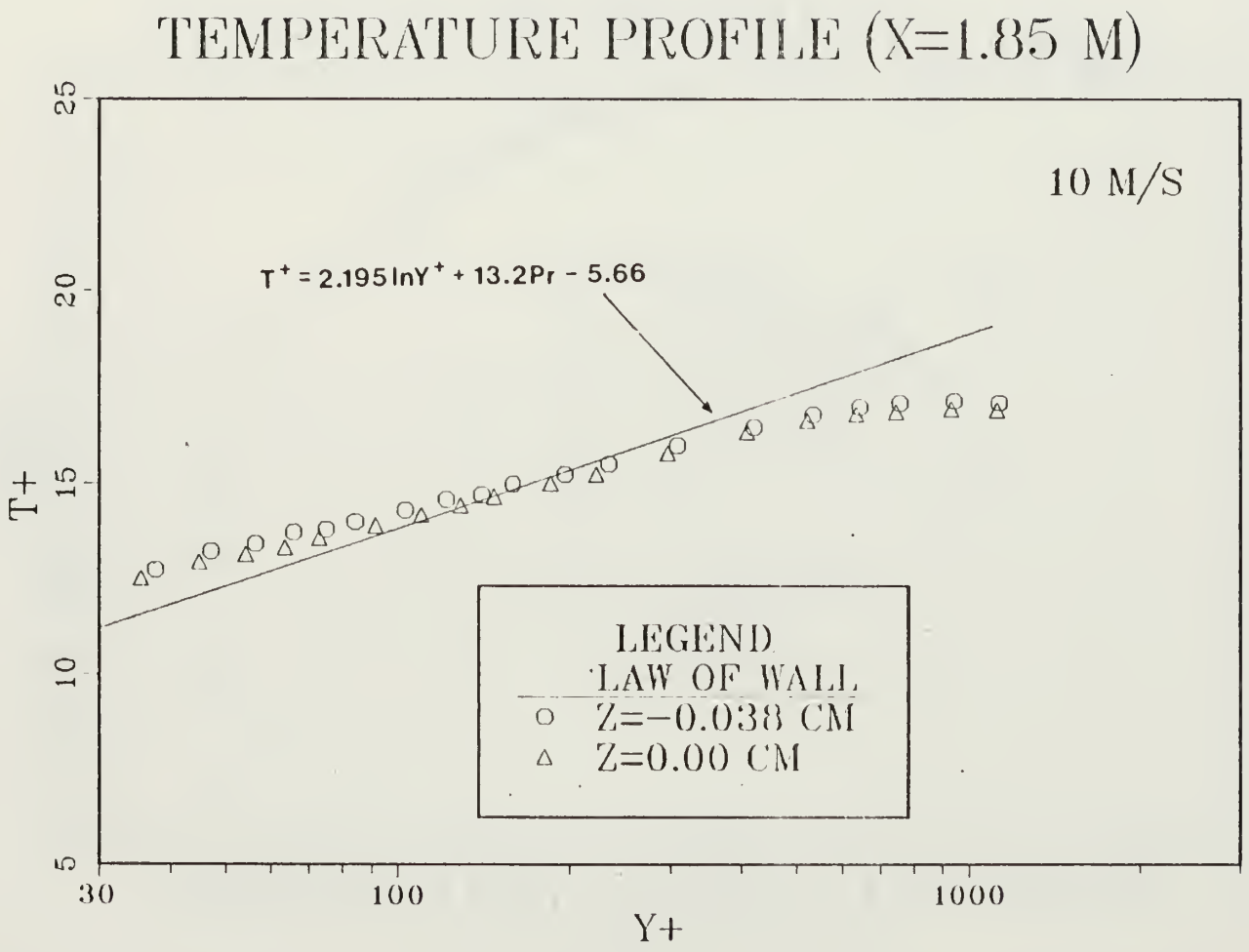

Figure 30. Temperature Profile Plotted in Wall Coordinates at X=1.85 m

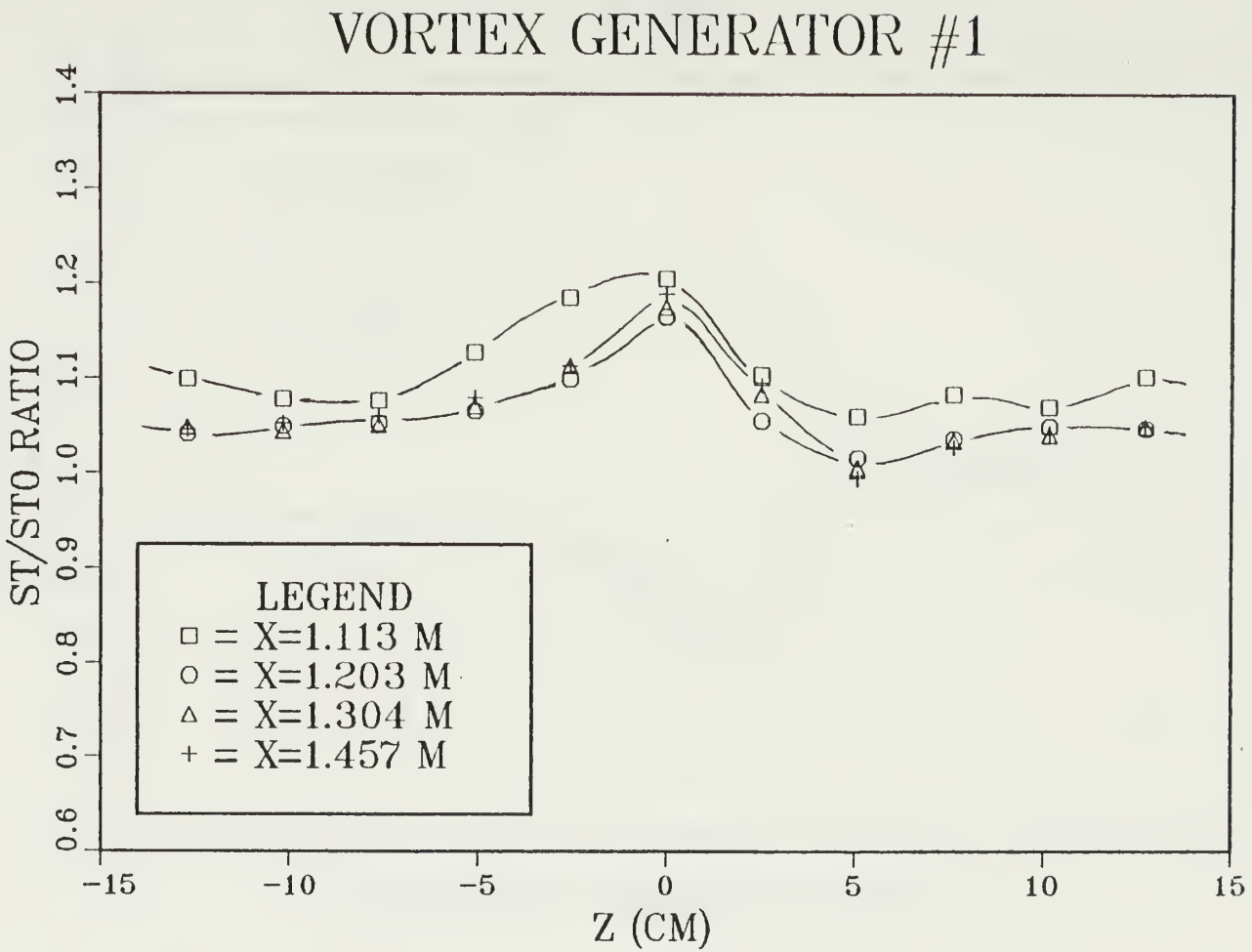

Figure 31. Vortex #1 at Z=-4.29 cm, Rows 1,2,3, and 4

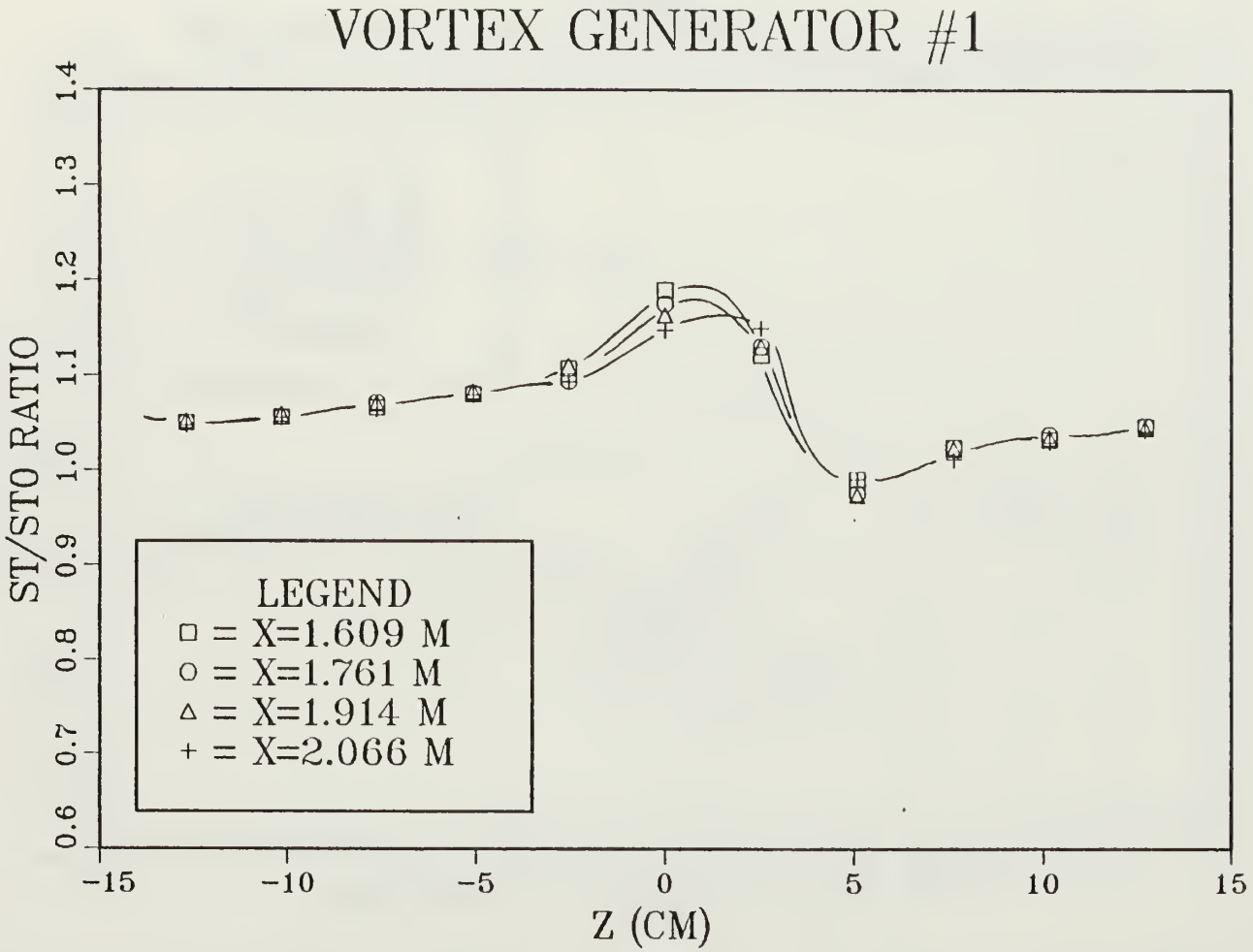

Figure 32. Vortex #1 at Z=-4.29 cm, Rows 5,6,7, and 8

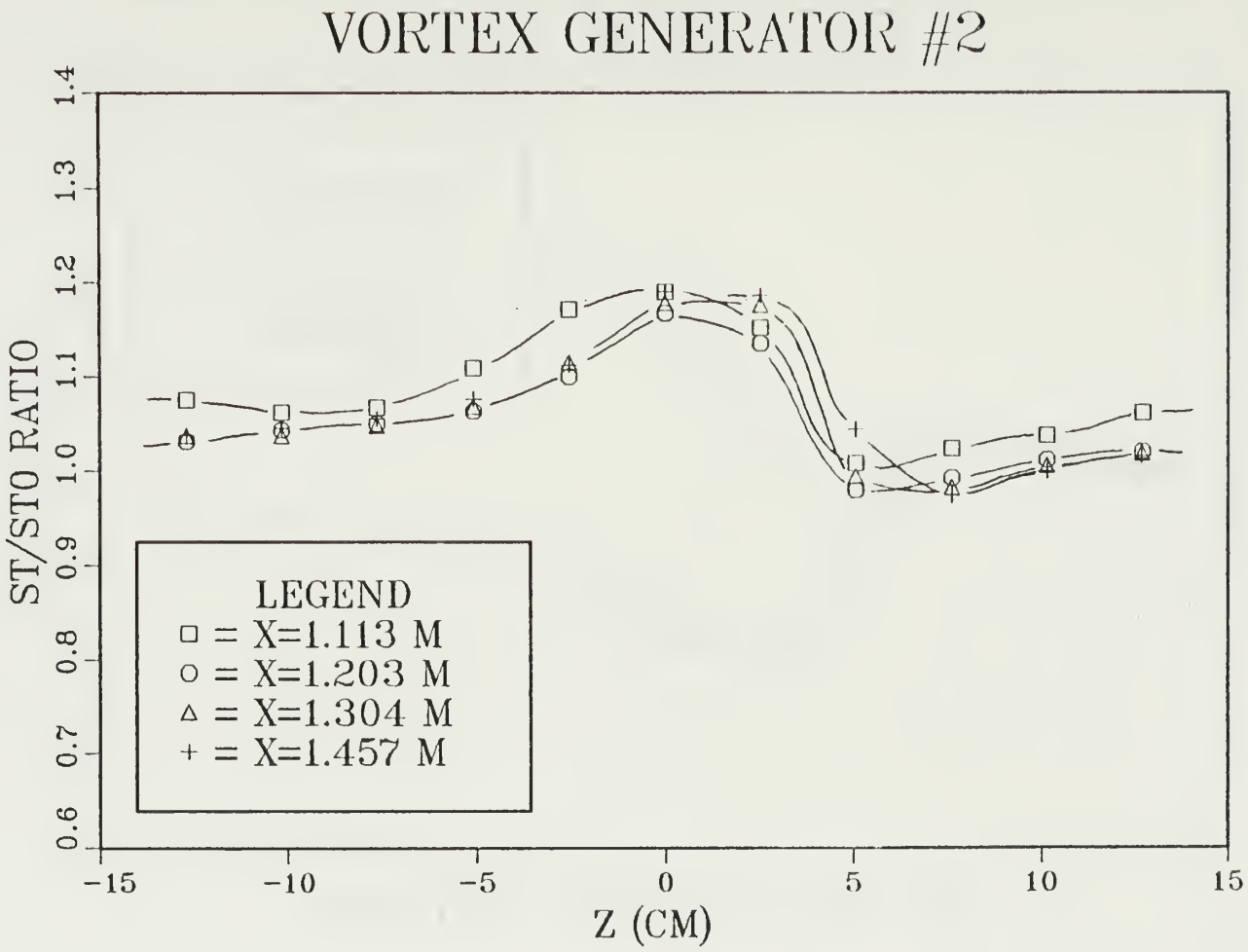

Figure 33. Vortex #2 at Z=-4.79 cm, Rows 1,2,3, and 4

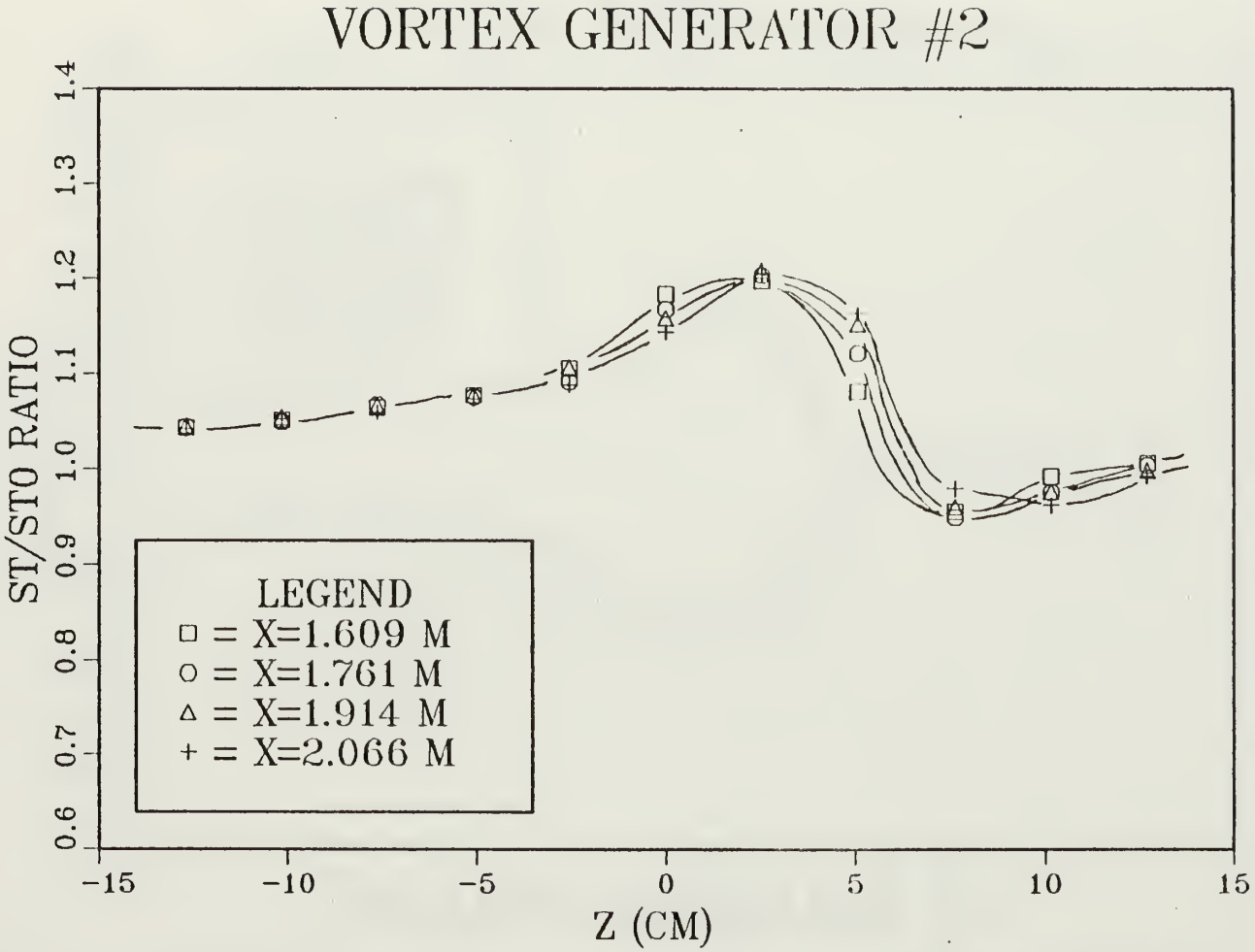

Figure 34. Vortex #2 at Z=-4.79 cm, Rows 5,6,7, and 8

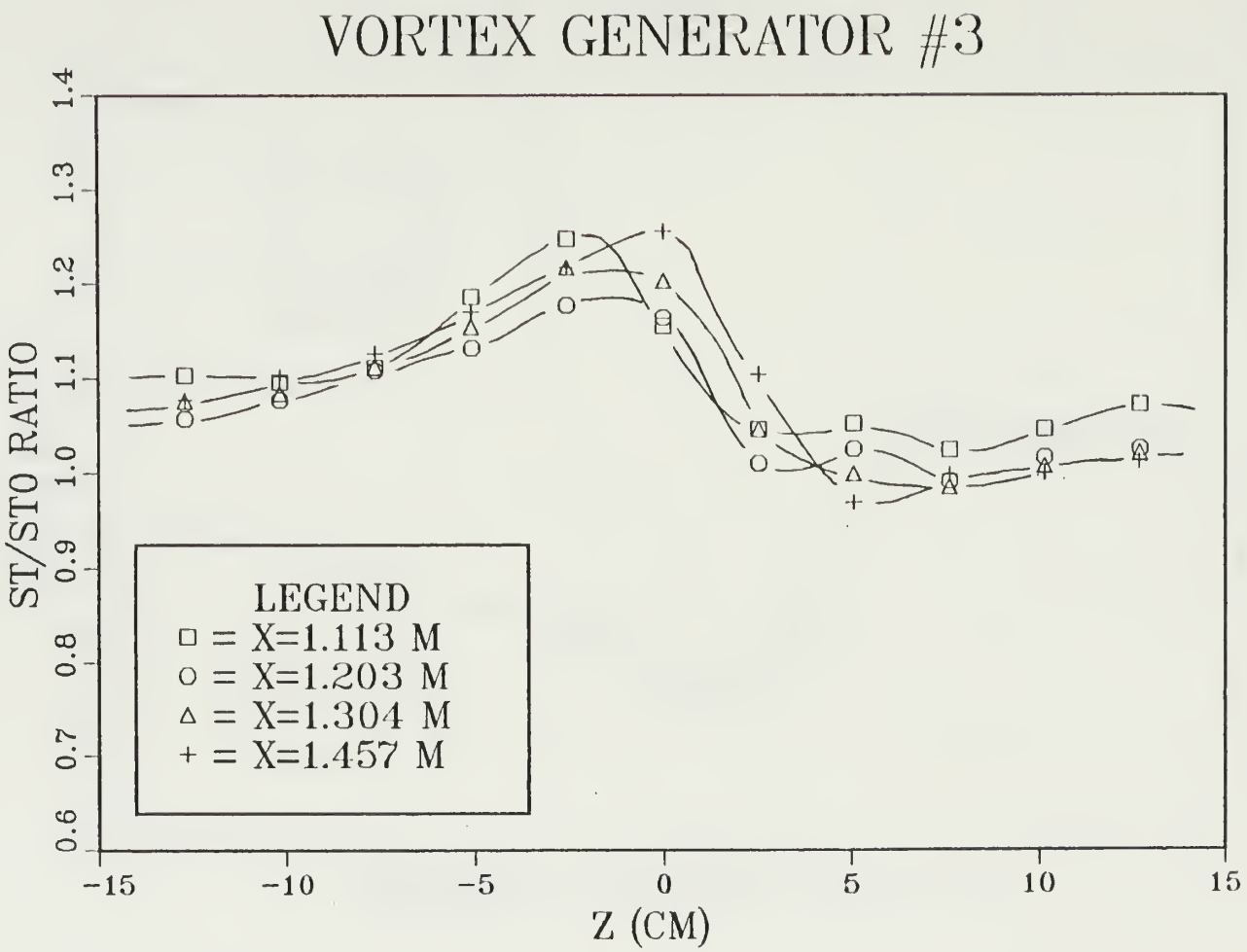

Figure 35. Vortex #3 at Z=-8.08 cm, Rows 1,2,3, and 4

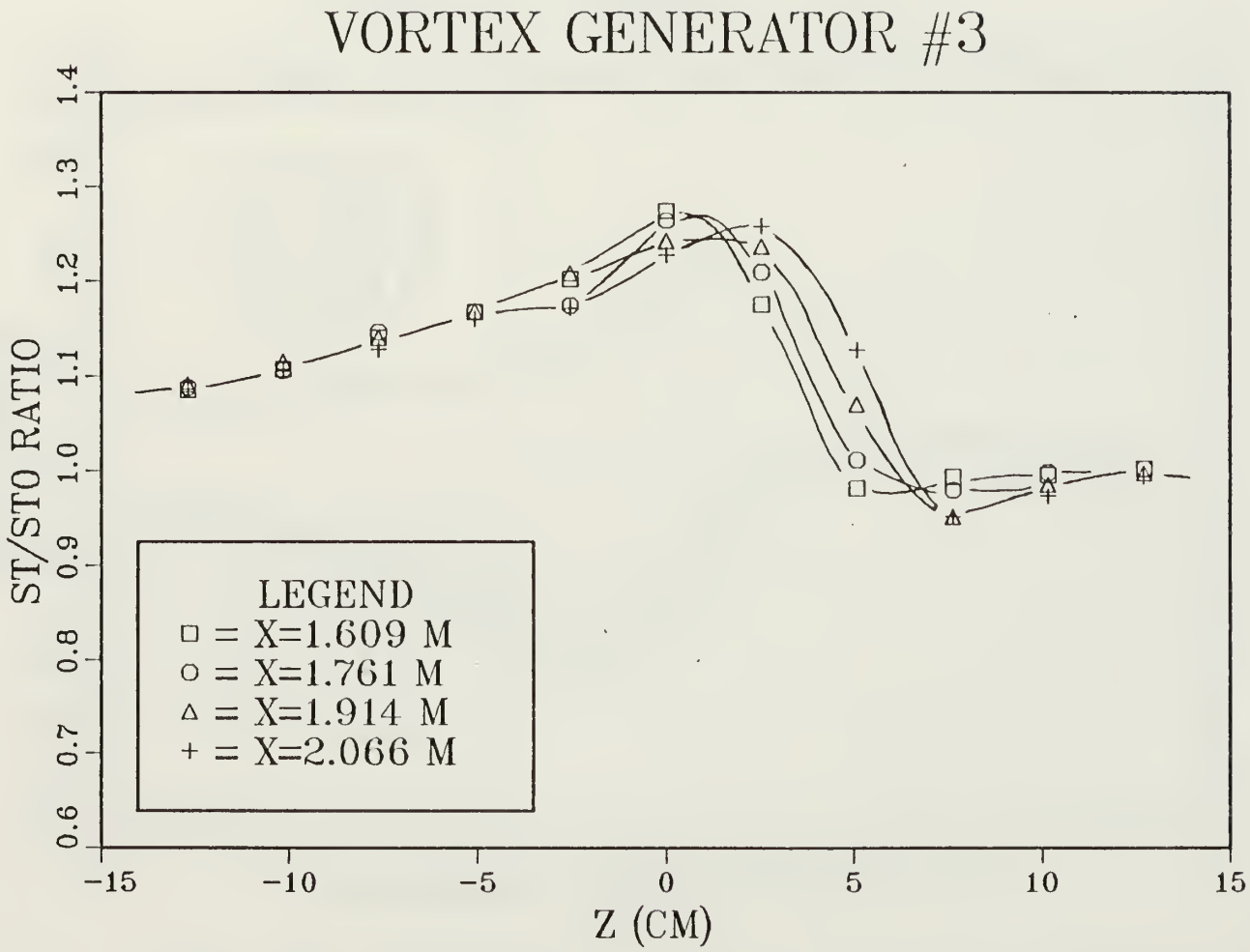

Figure 36. Vortex #3 at Z=-8.08 cm, Rows 5,6,7, and 8

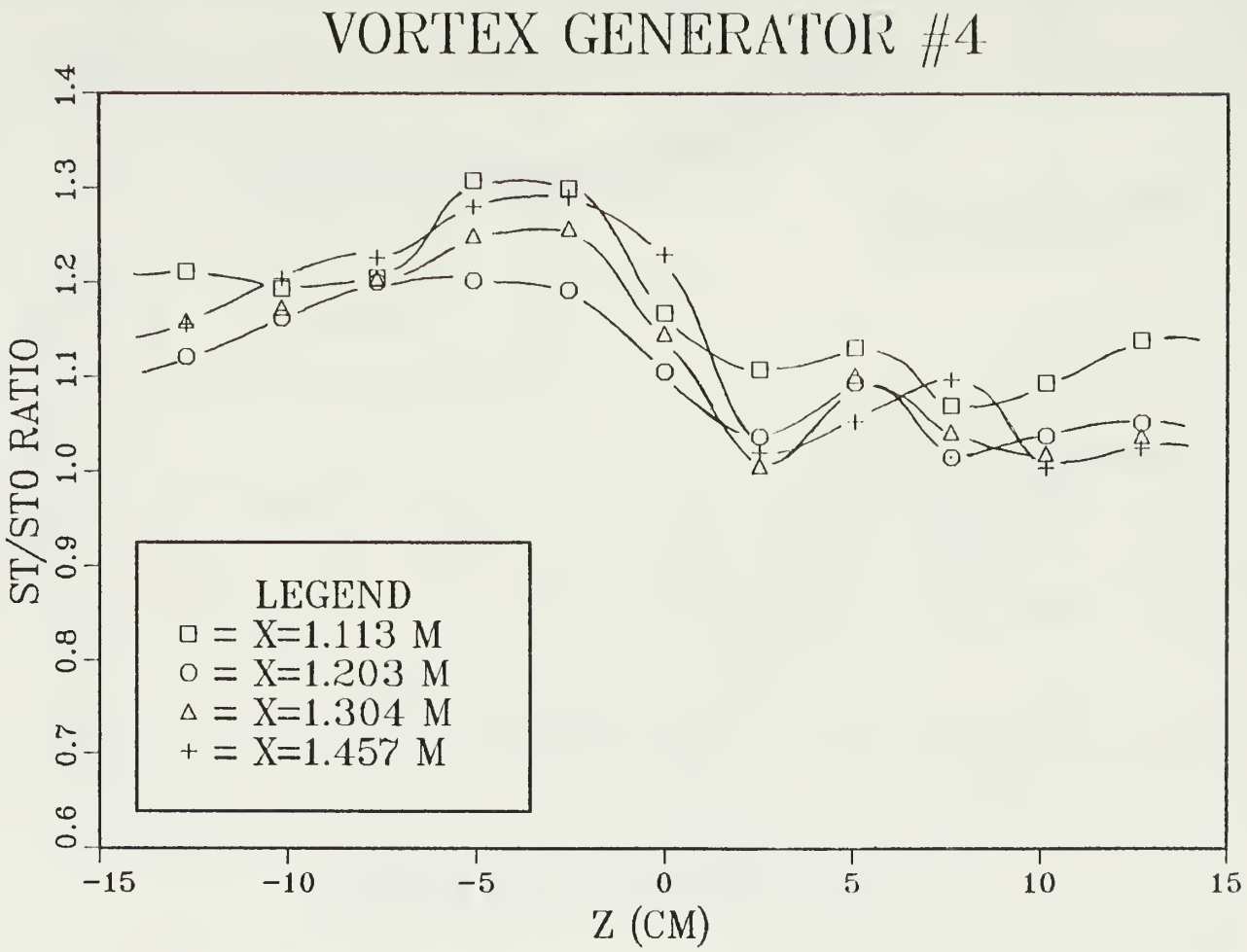

Figure 37. Vortex #4 at Z=-9.096 cm, Rows 1,2,3, and 4

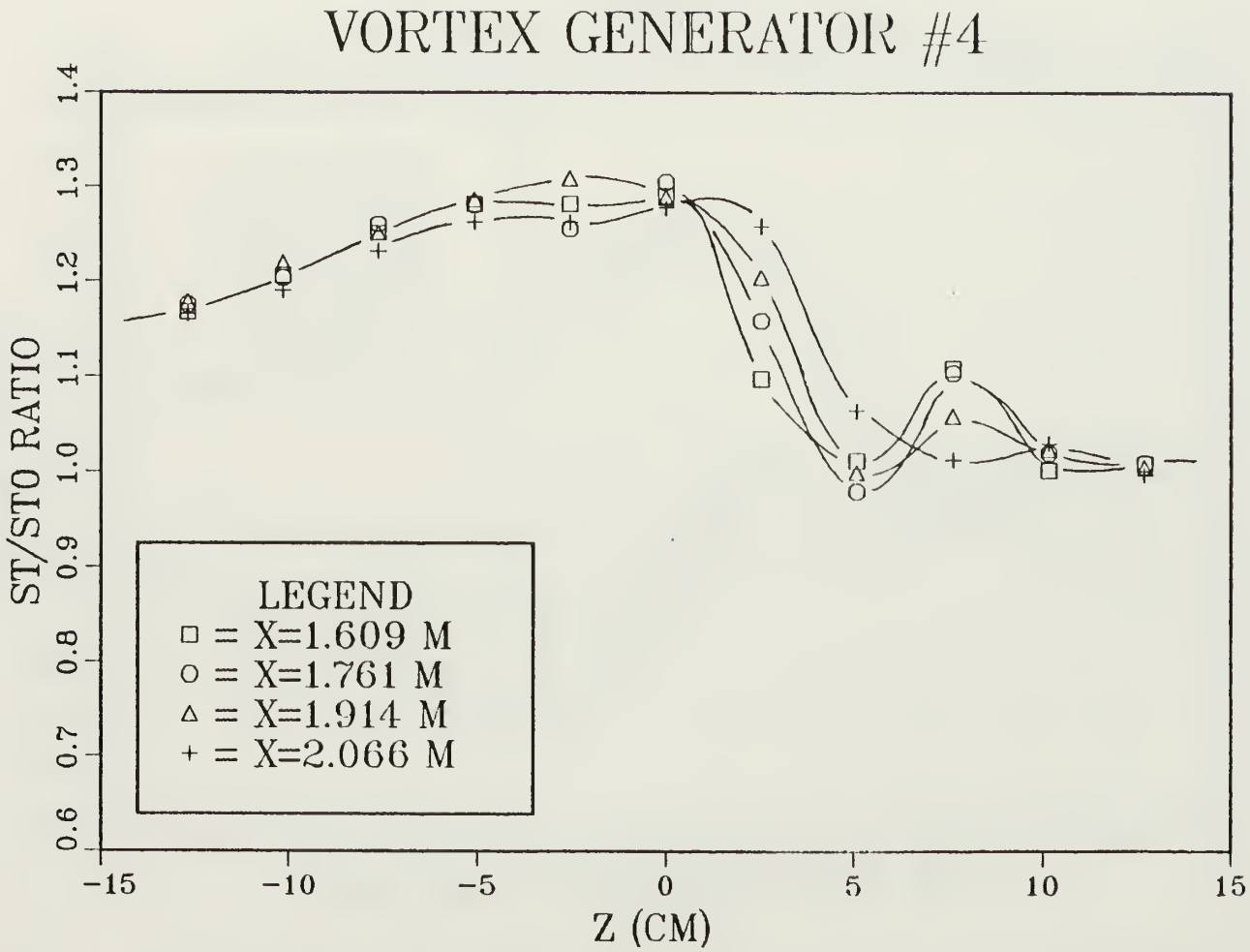

Figure 38. Vortex #4 at Z=-9.096 cm, Rows 5,6,7, and 8

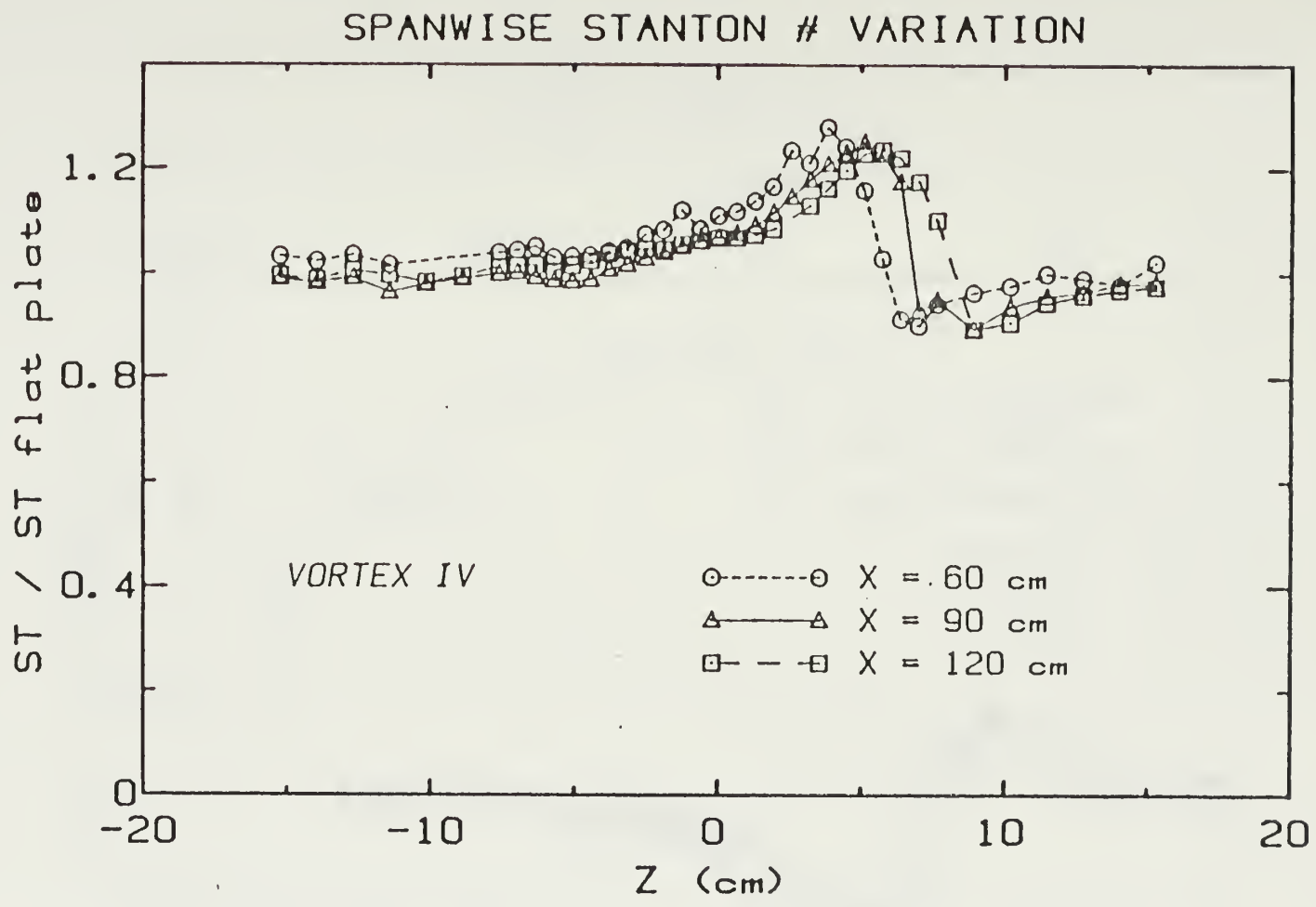

Figure 39. Stanton Number Variation, (Eibeck and Eaton, 1985)

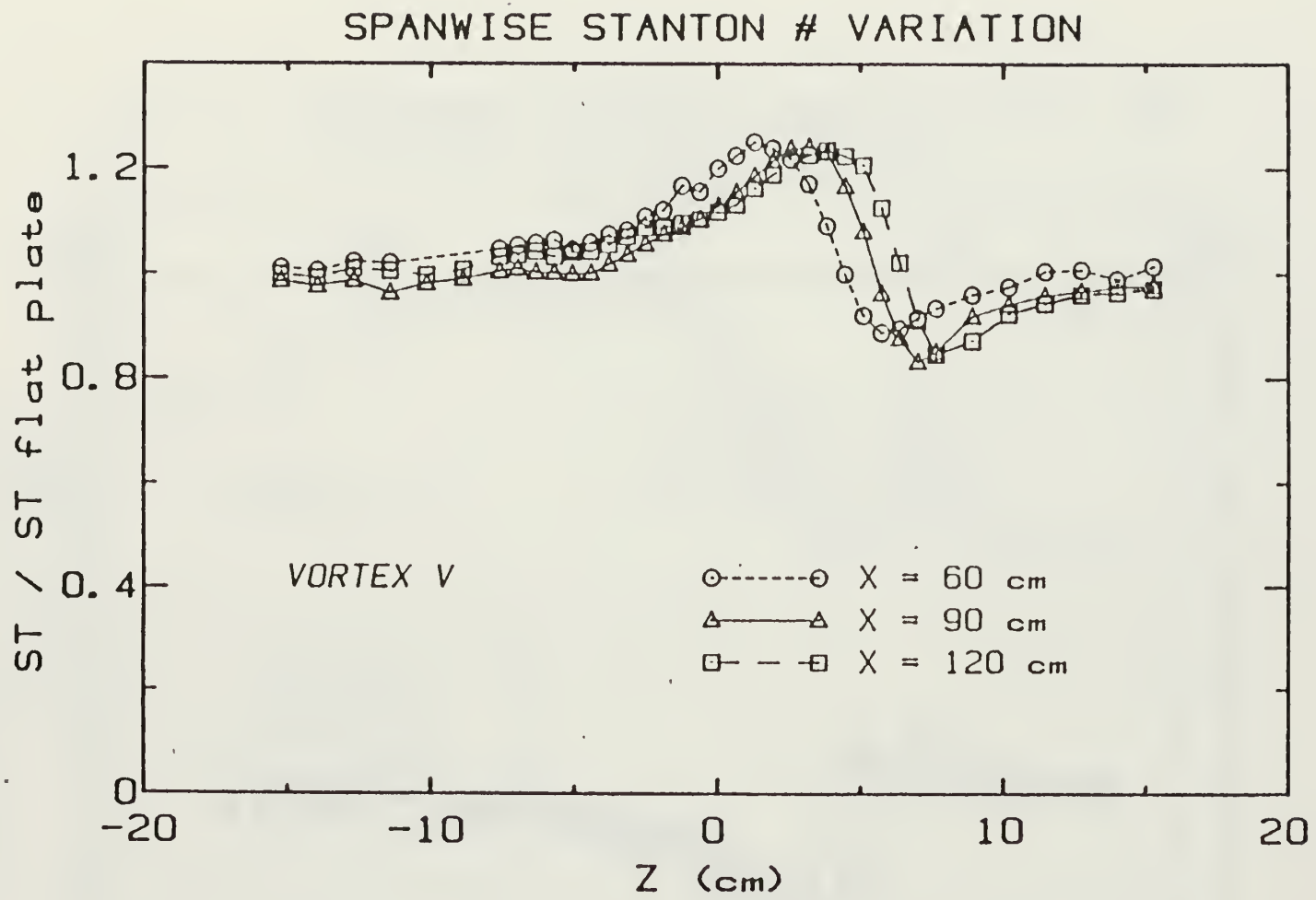

Figure 40. Stanton Number Variation, (Eibeck and Eaton, 1985)

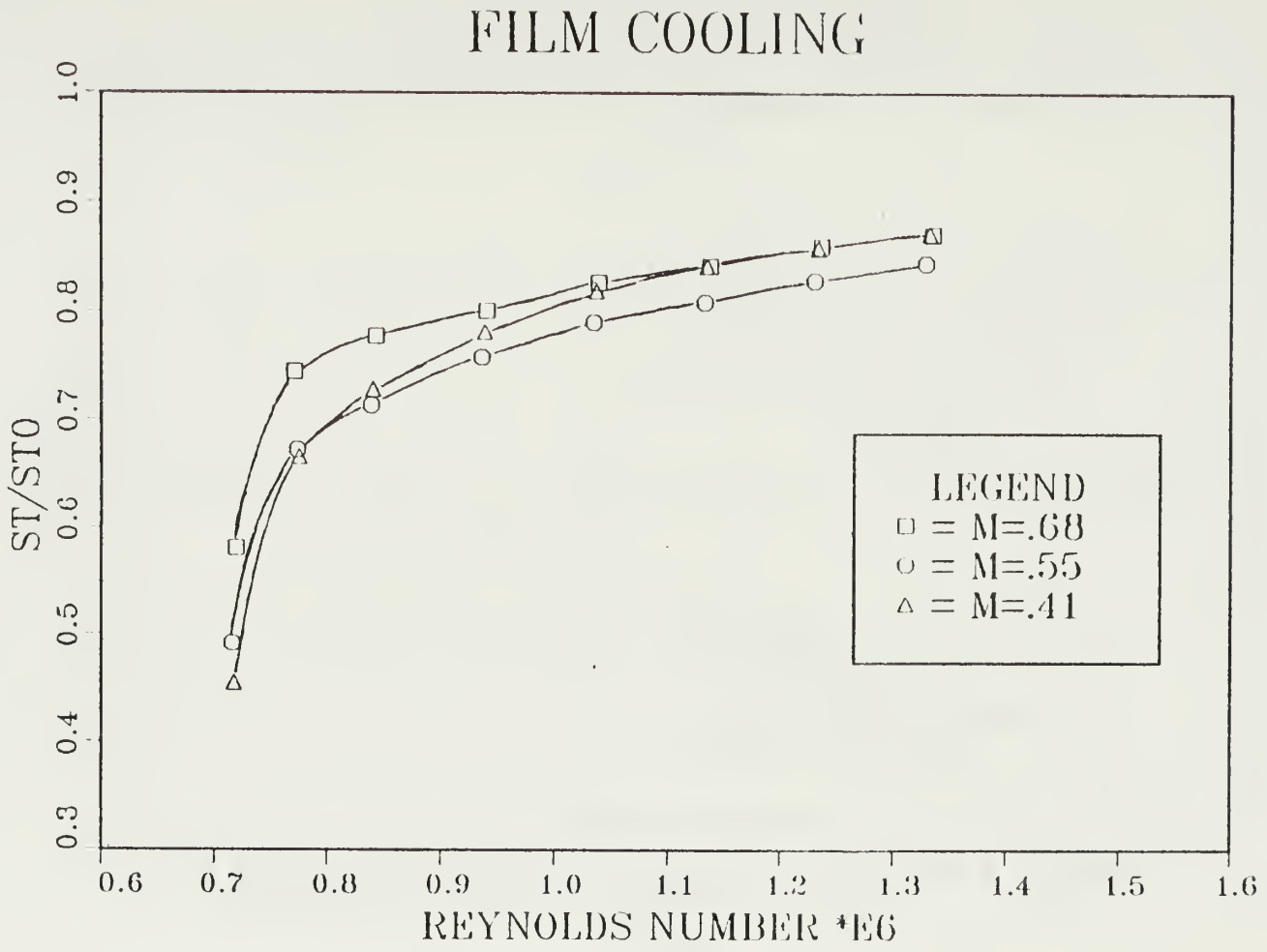

Figure 41. Film Cooling verses Reynolds Number

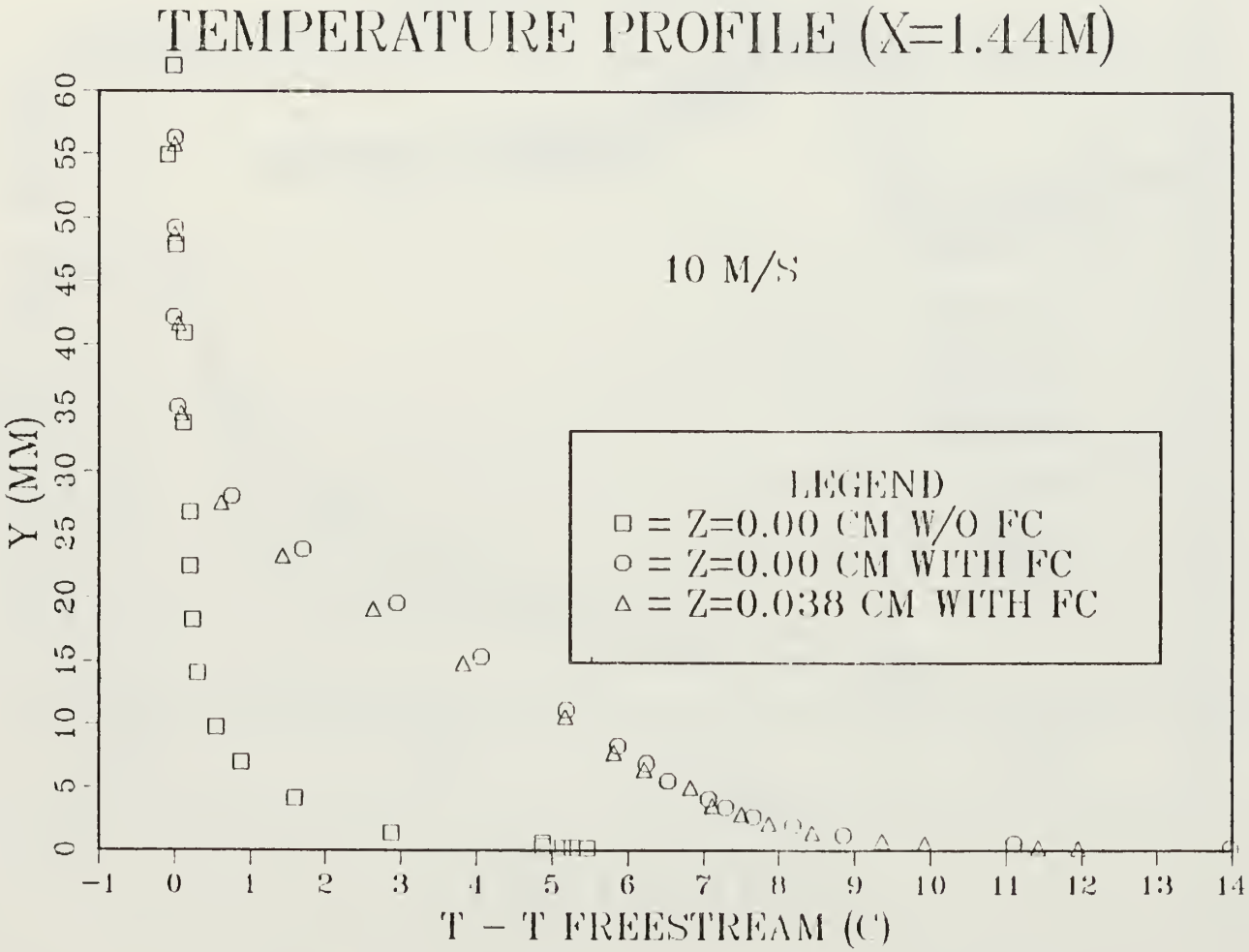

Figure 42. Temperature Profile with Film Cooling

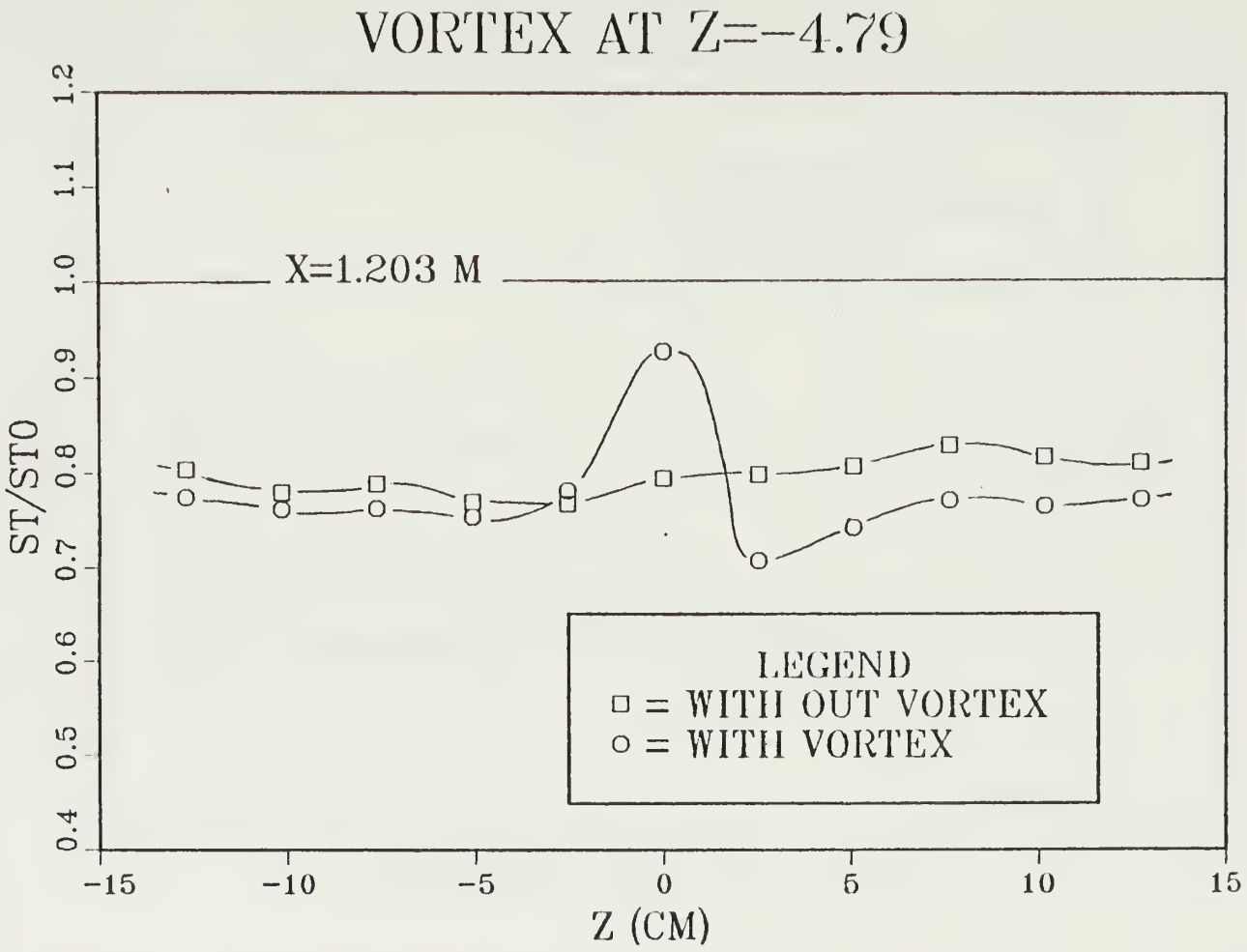

Figure 43. Vortex #2 at Z=-4.79 cm and X=1.203 m with Film Cooling

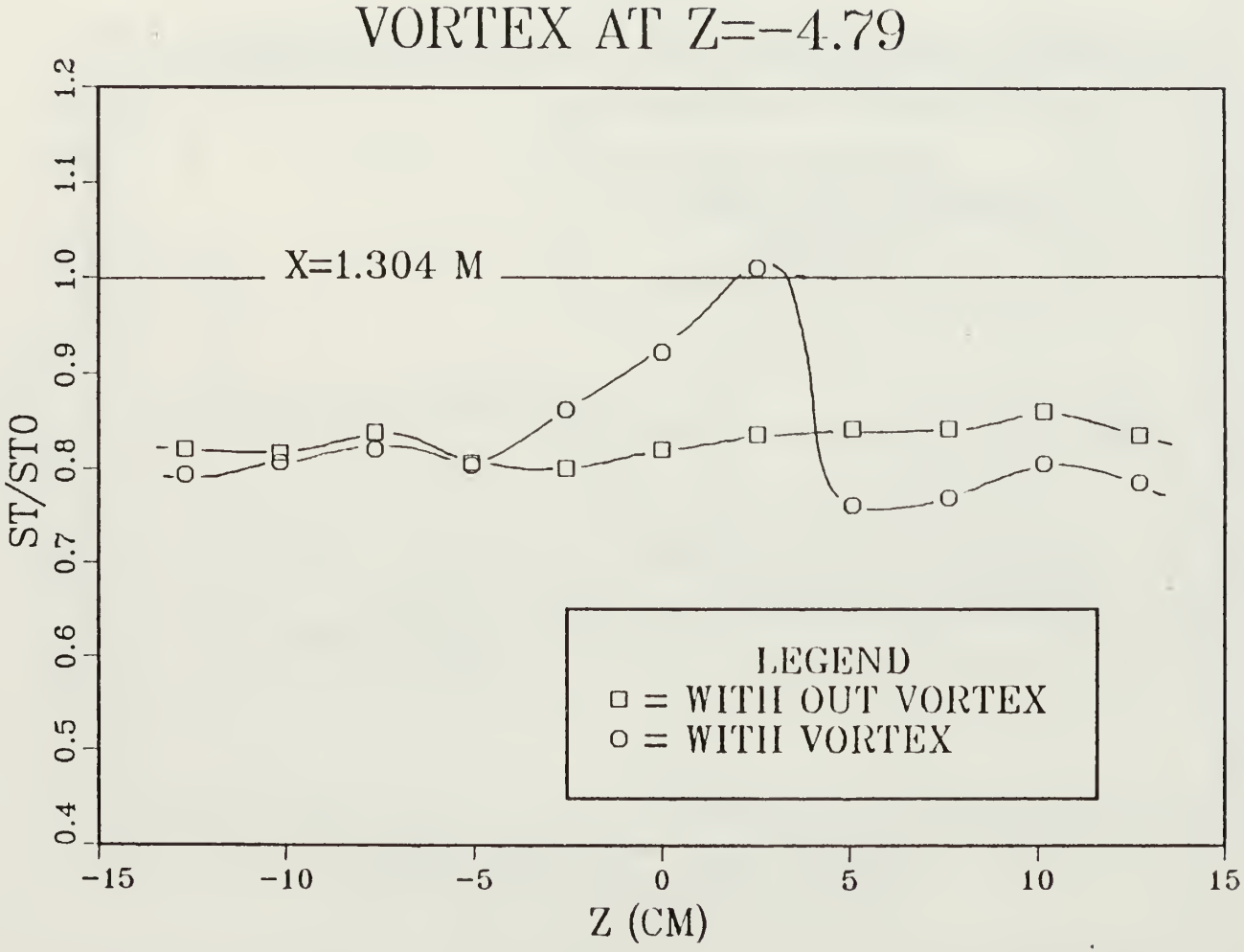

Figure 44. Vortex #2 at Z=-4.79 cm and X=1.304 m with Film Cooling

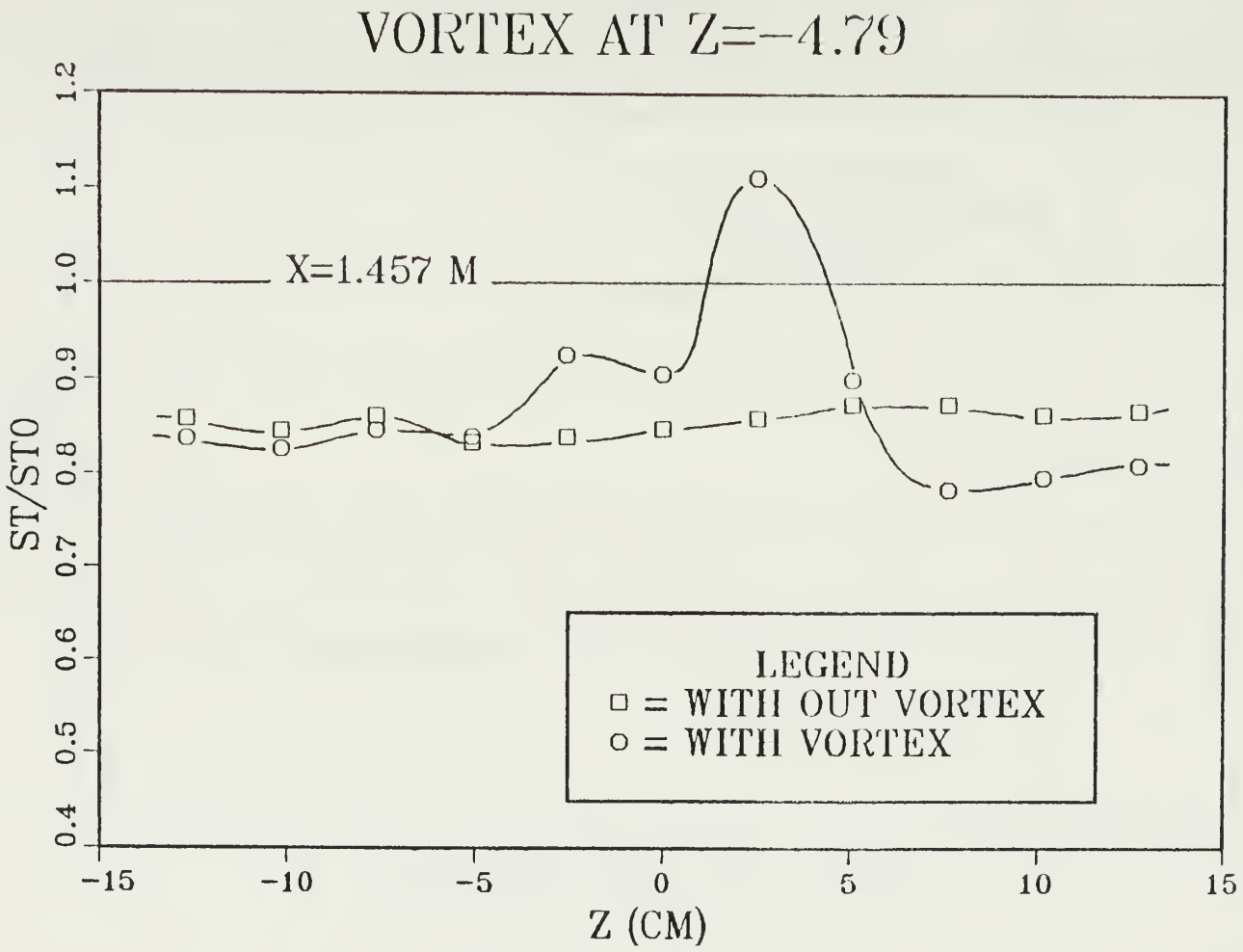

Figure 45. Vortex #2 at Z=-4.79 cm and X=1.457 m with Film Cooling

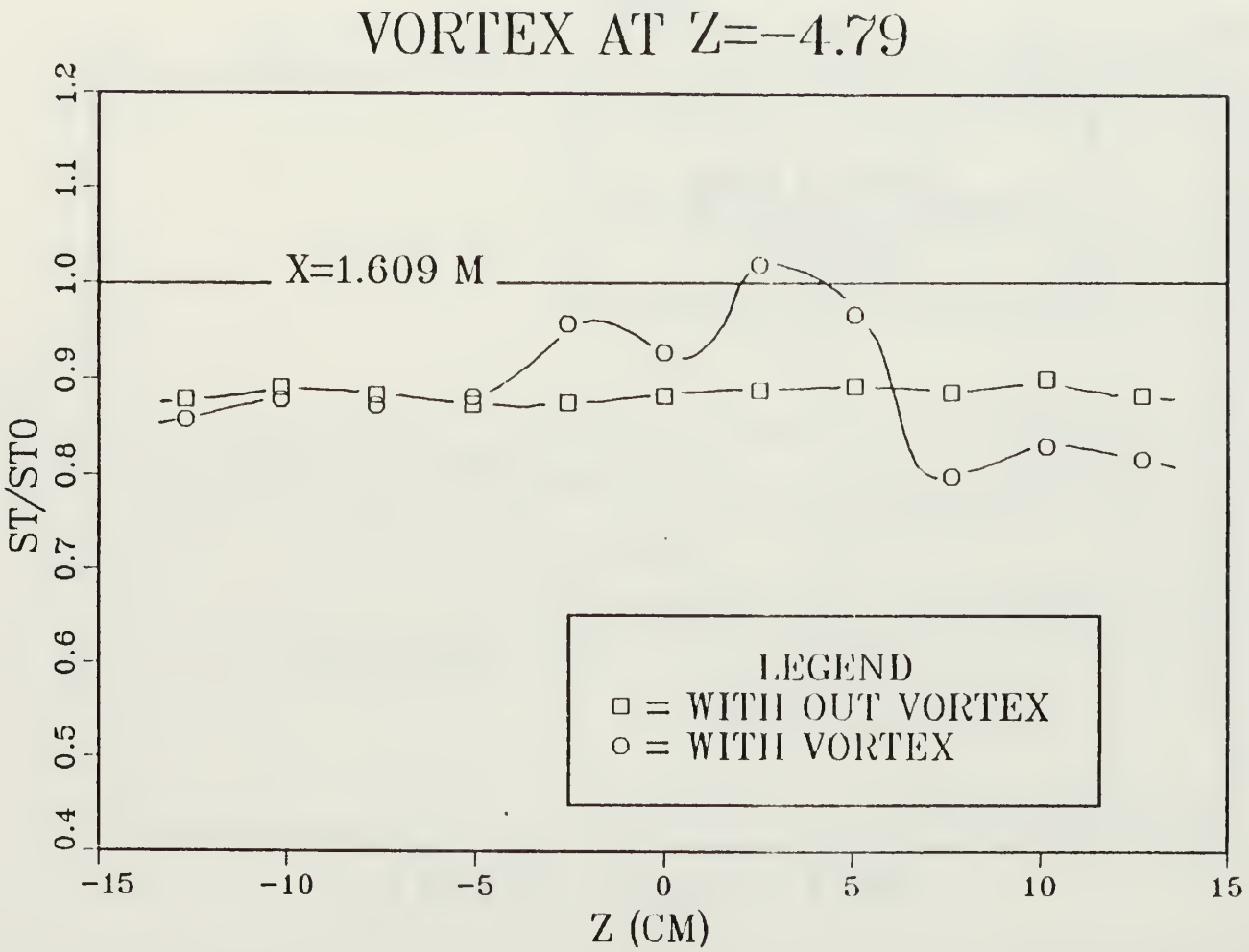

Figure 46. Vortex #2 at Z=-4.79 cm and X=1.609 m with Film Cooling

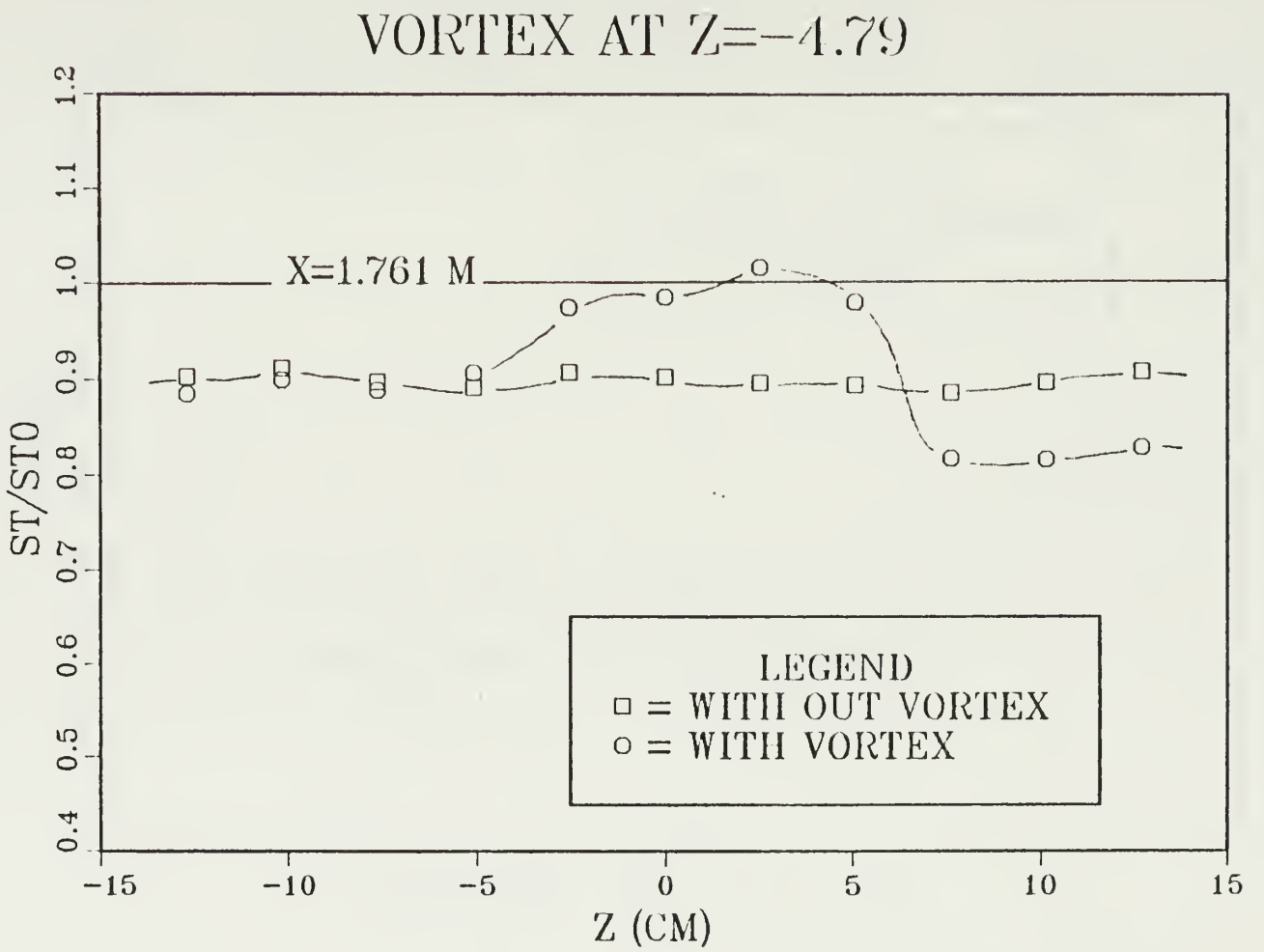

Figure 47. Vortex #2 at Z=-4.79 cm and X=1.761 m with Film Cooling

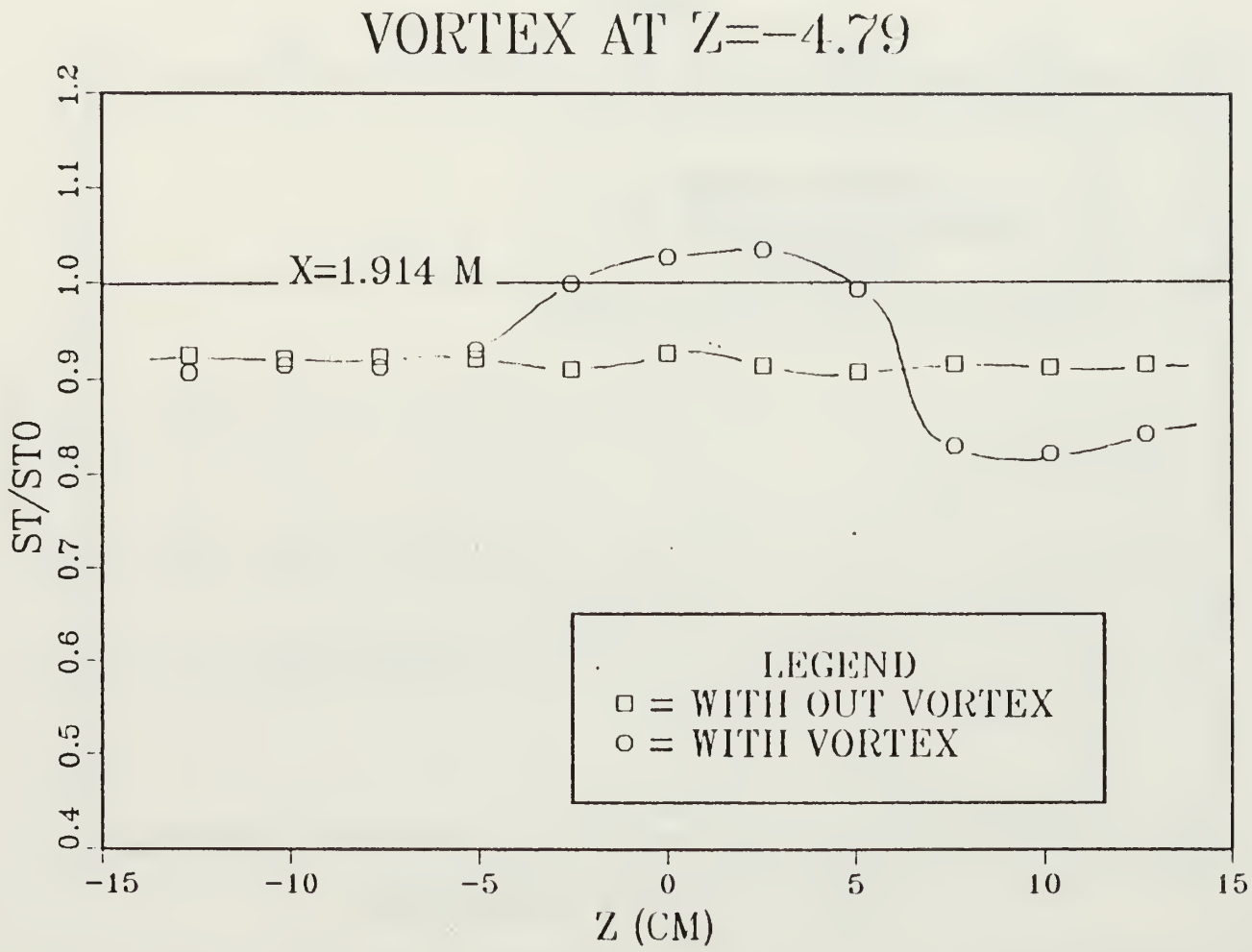

Figure 48. Vortex #2 at Z=-4.79 cm and X=1.914 m with Film Cooling

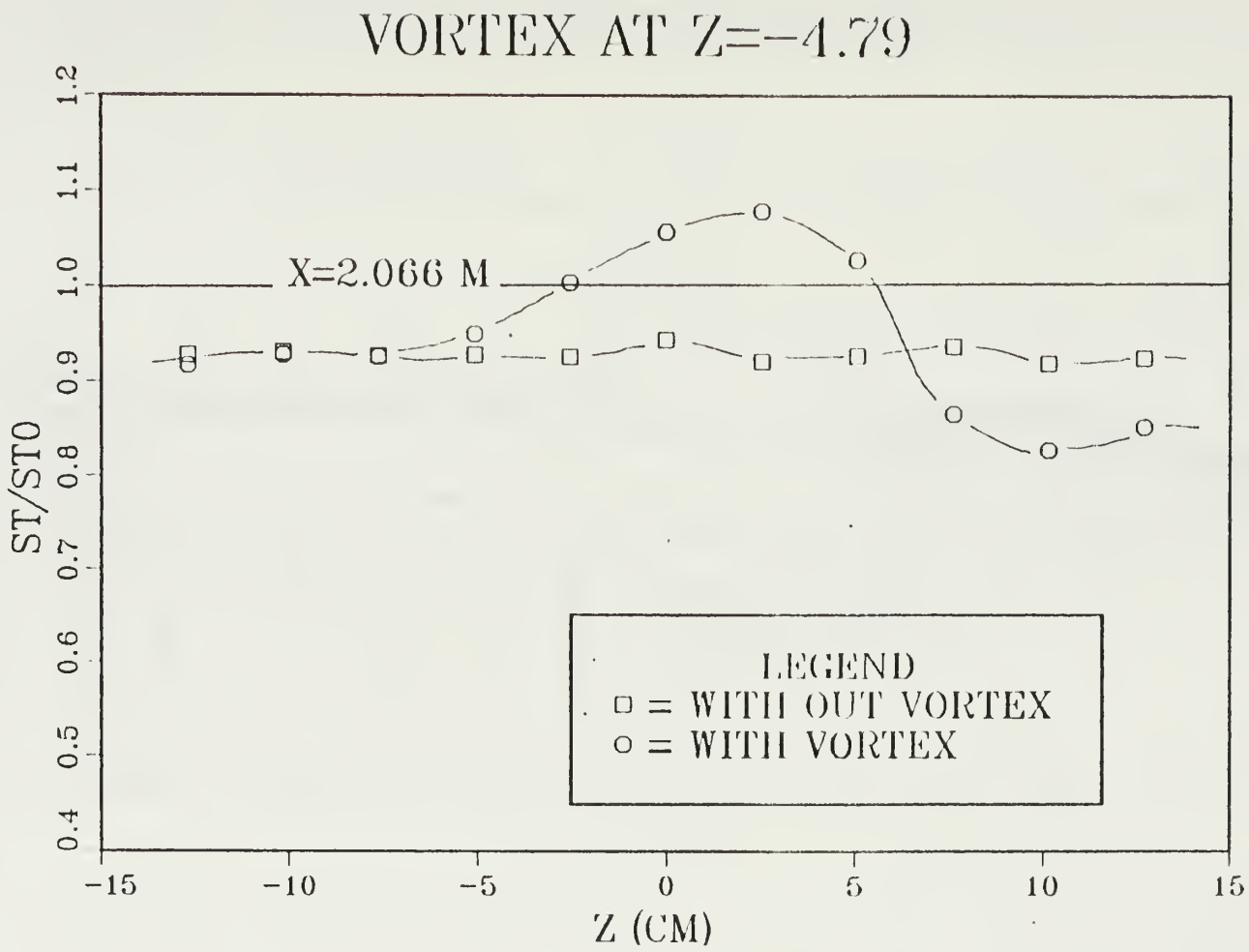

Figure 49. Vortex #2 at Z=-4.79 cm and X=2.066 m with Film Cooling

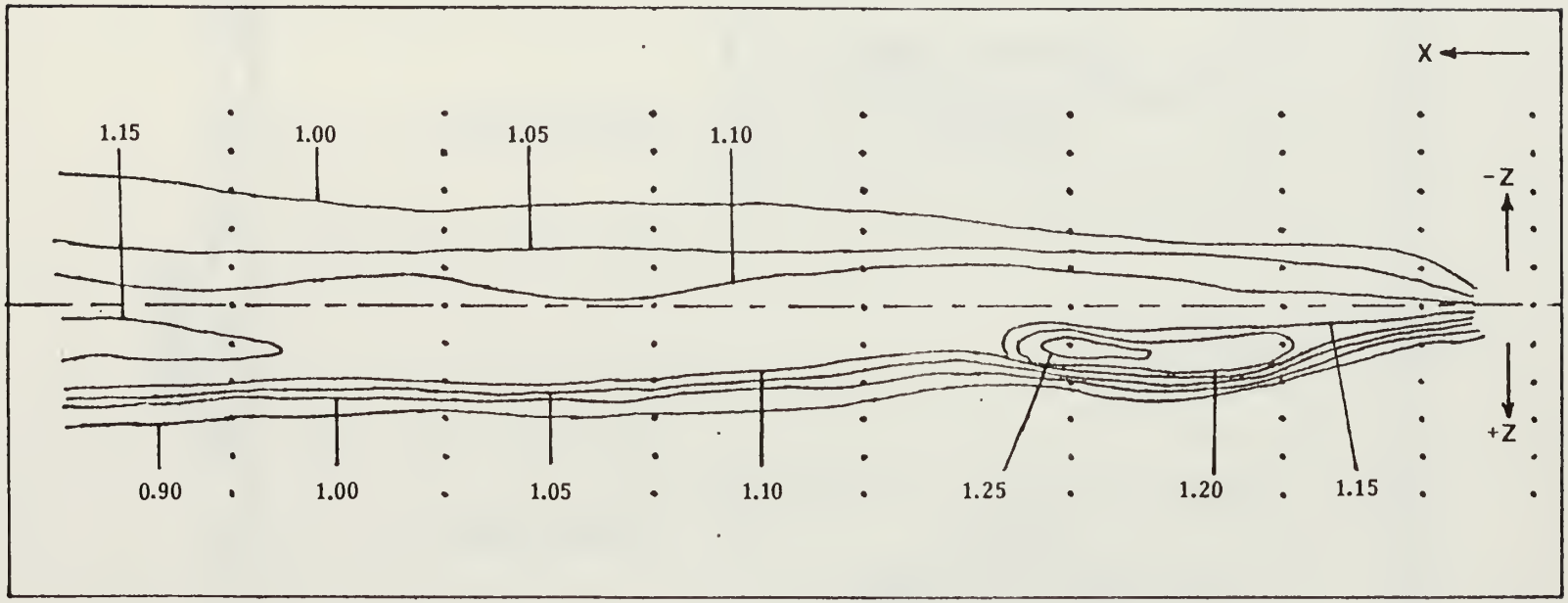

Figure 50. Surface Plot of St/St_f with Vortex at Z=-4.79 cm

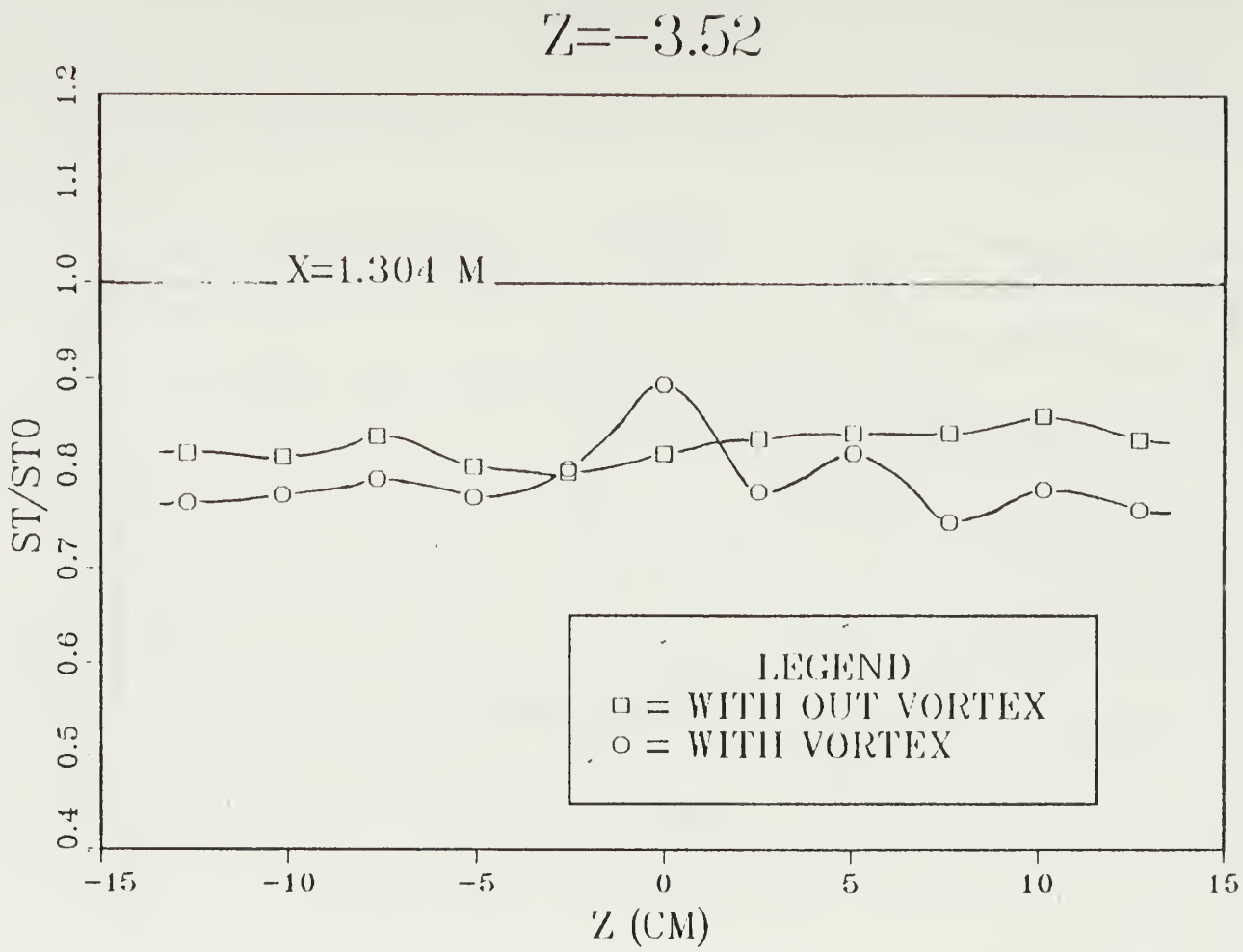

Figure 51. Vortex #2 at Z=-3.52 cm and X=1.304 m with Film Cooling

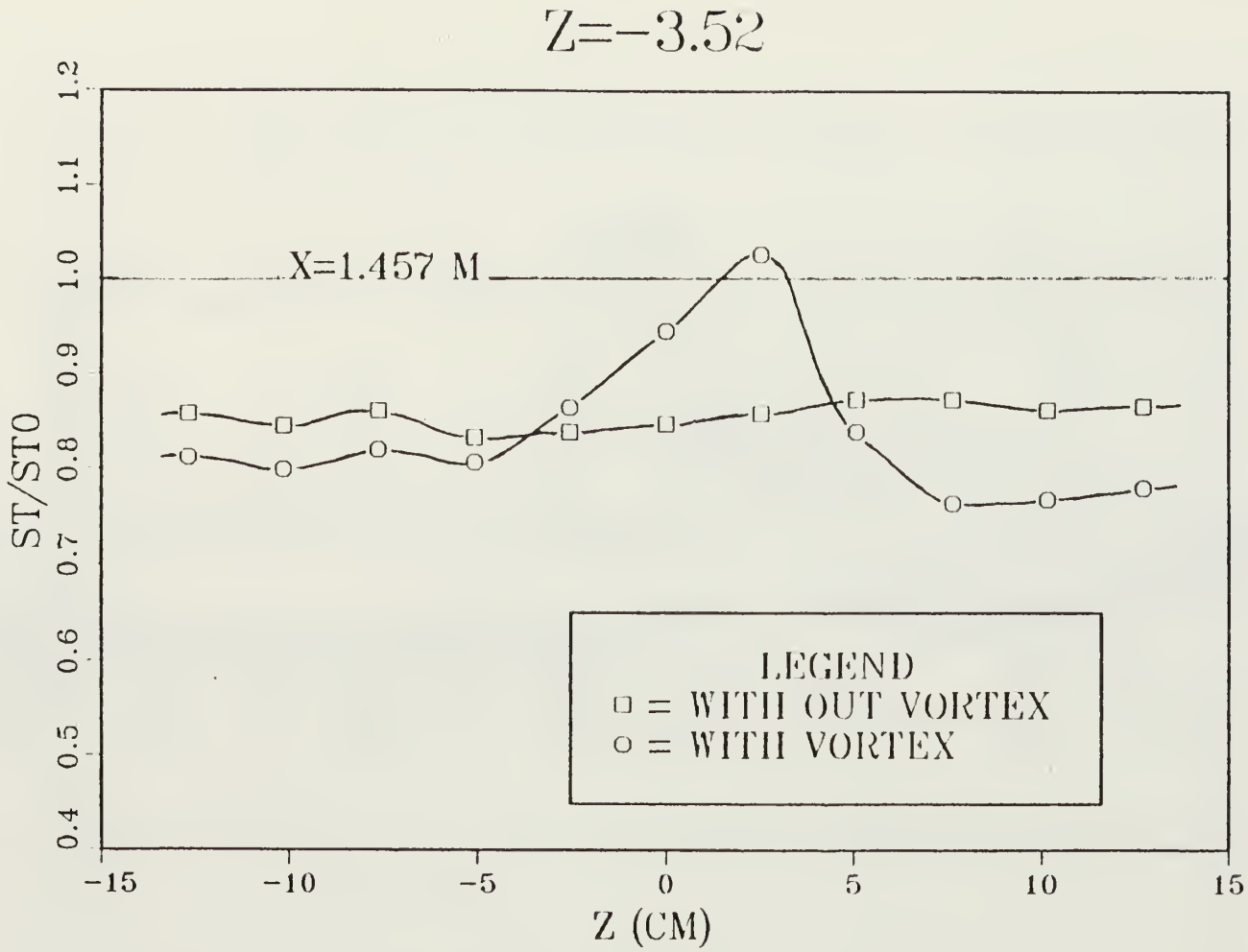

Figure 52. Vortex #2 at Z=-3.52 cm and X=1.457 m with Film Cooling

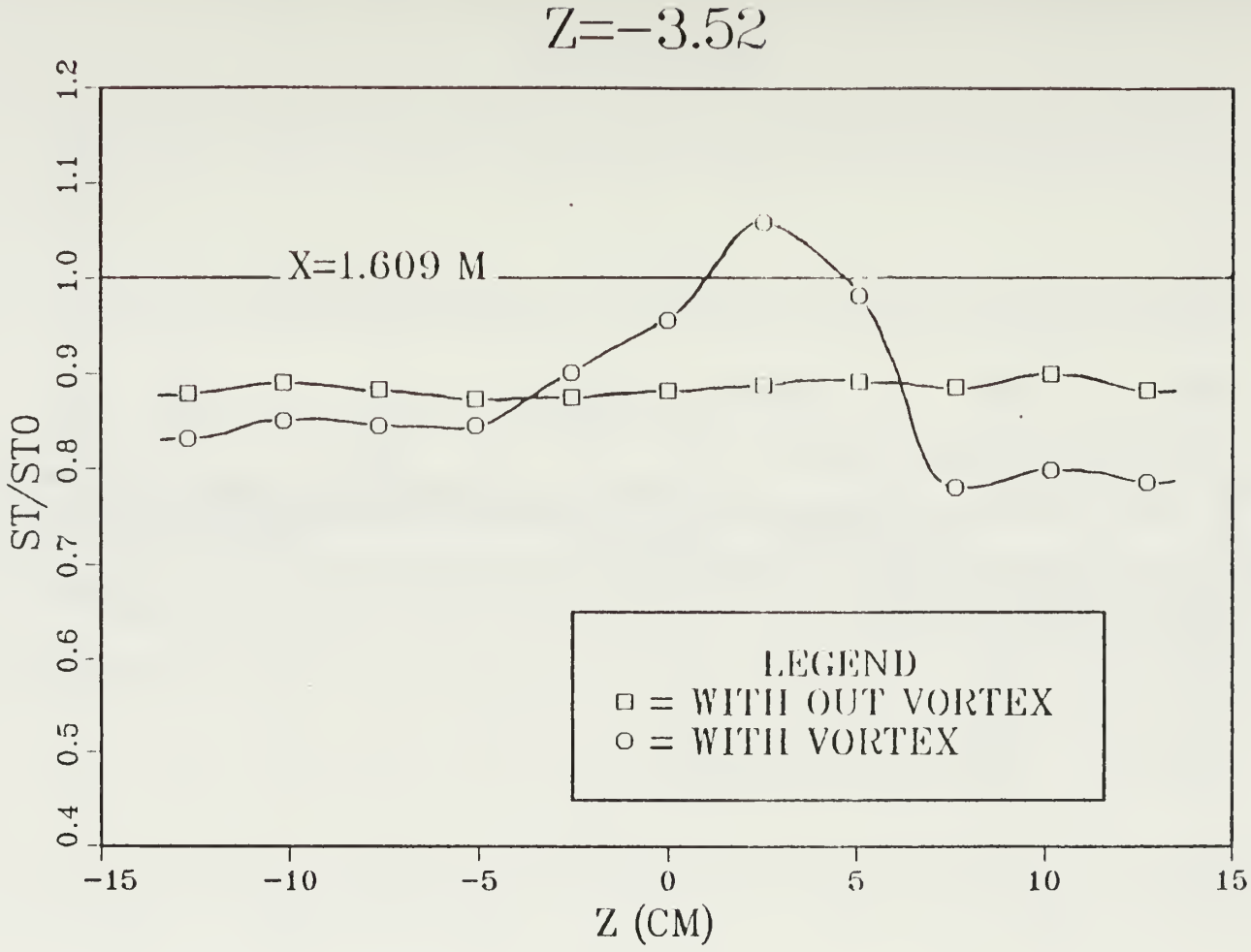

Figure 53. Vortex #2 at Z=-3.52 cm and X=1.609 m with Film Cooling

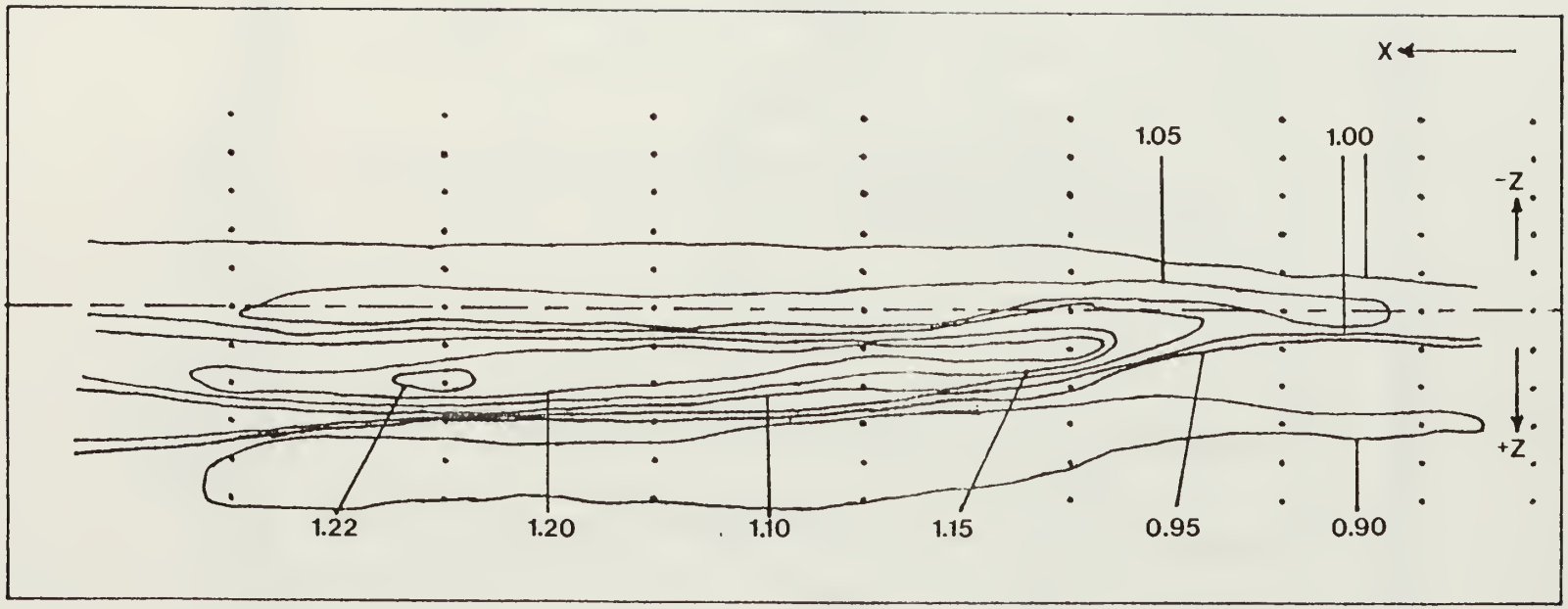

Figure 54. Surface Plot of St/St_f with Vortex at Z=-3.52 cm

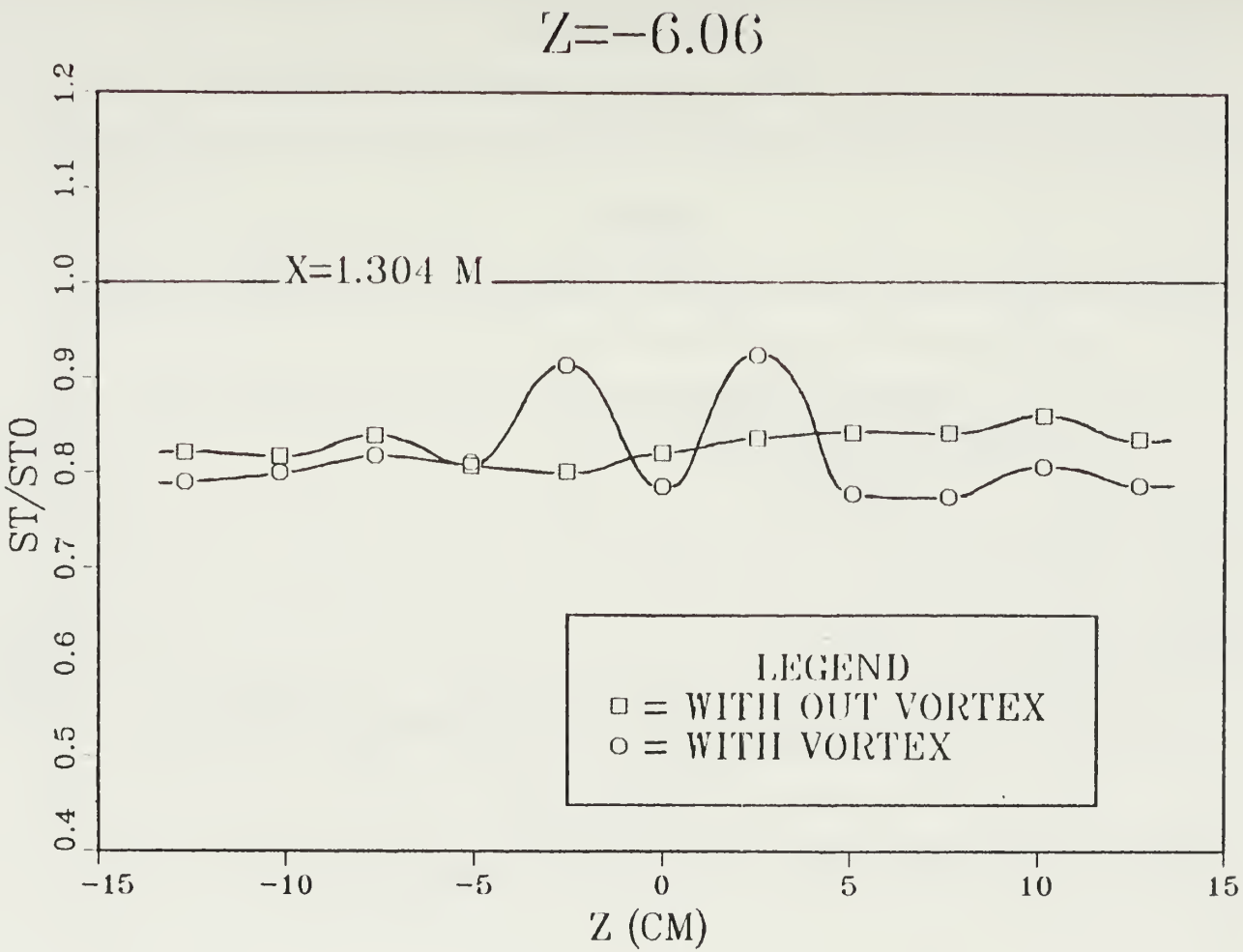

Figure 55. Vortex #2 at Z=-6.06 cm and X=1.304 m with Film Cooling

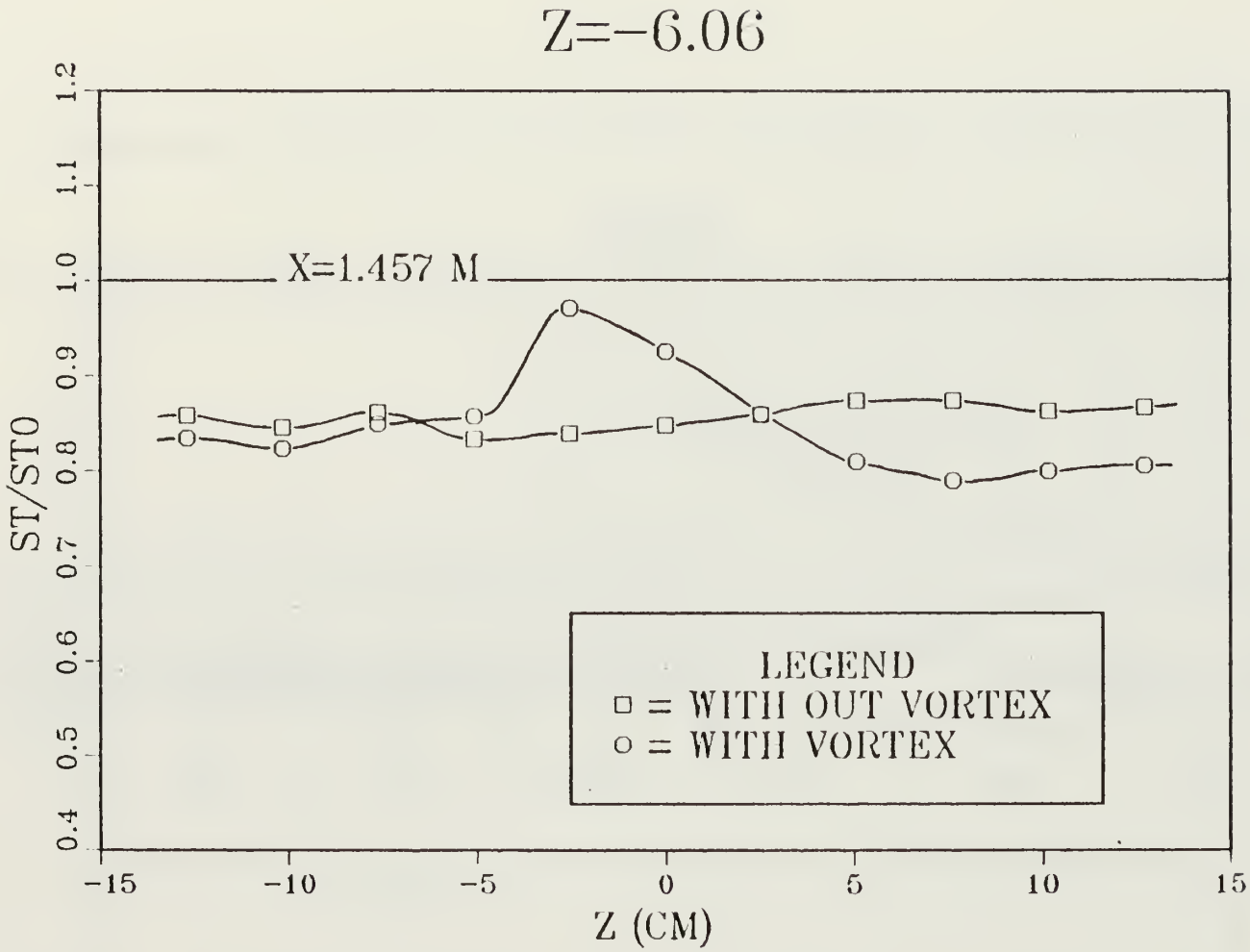

Figure 56. Vortex #2 at Z=-6.06 cm and X=1.457 m with Film Cooling

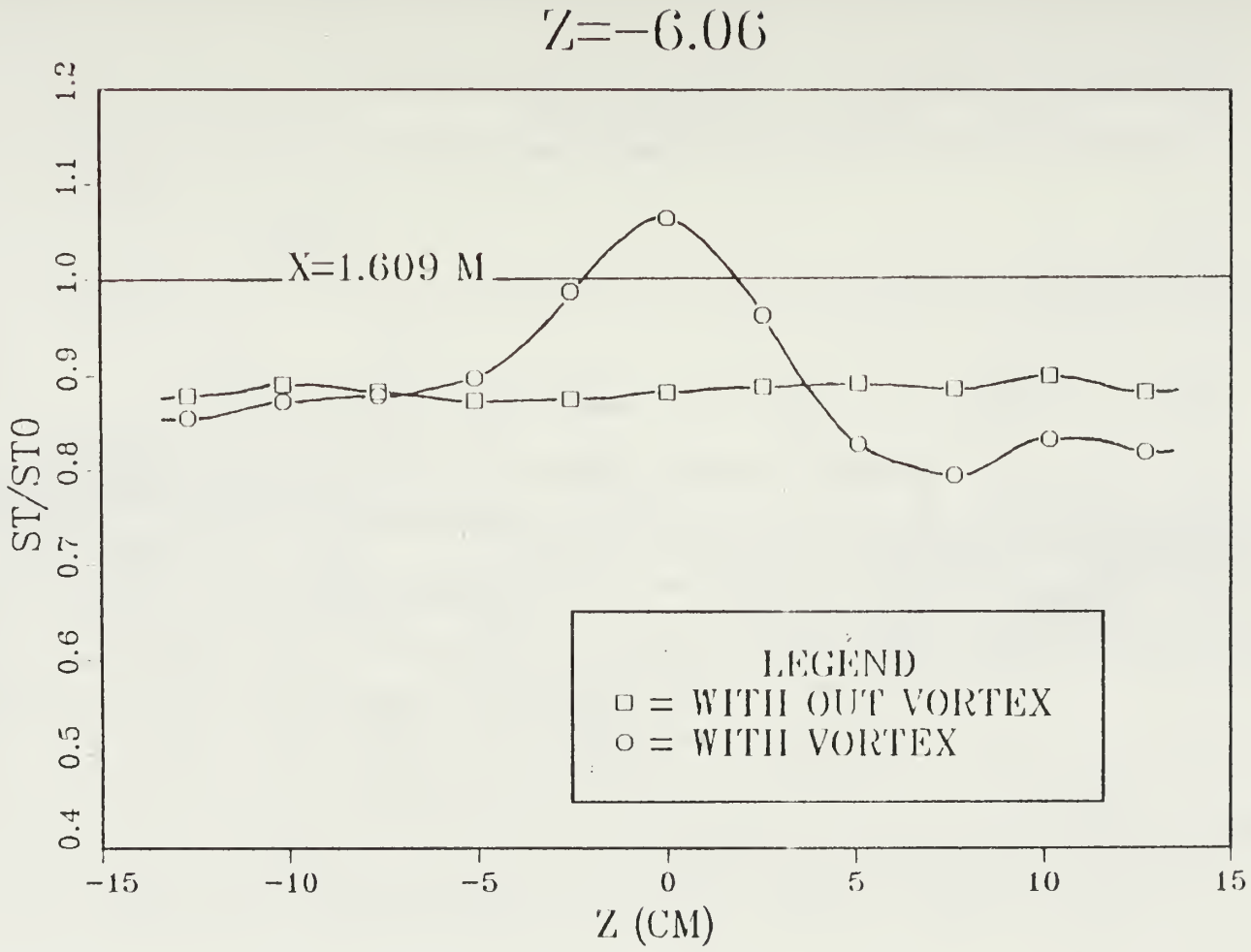

Figure 57. Vortex #2 at Z=-6.06 cm and X=1.609 m with Film Cooling

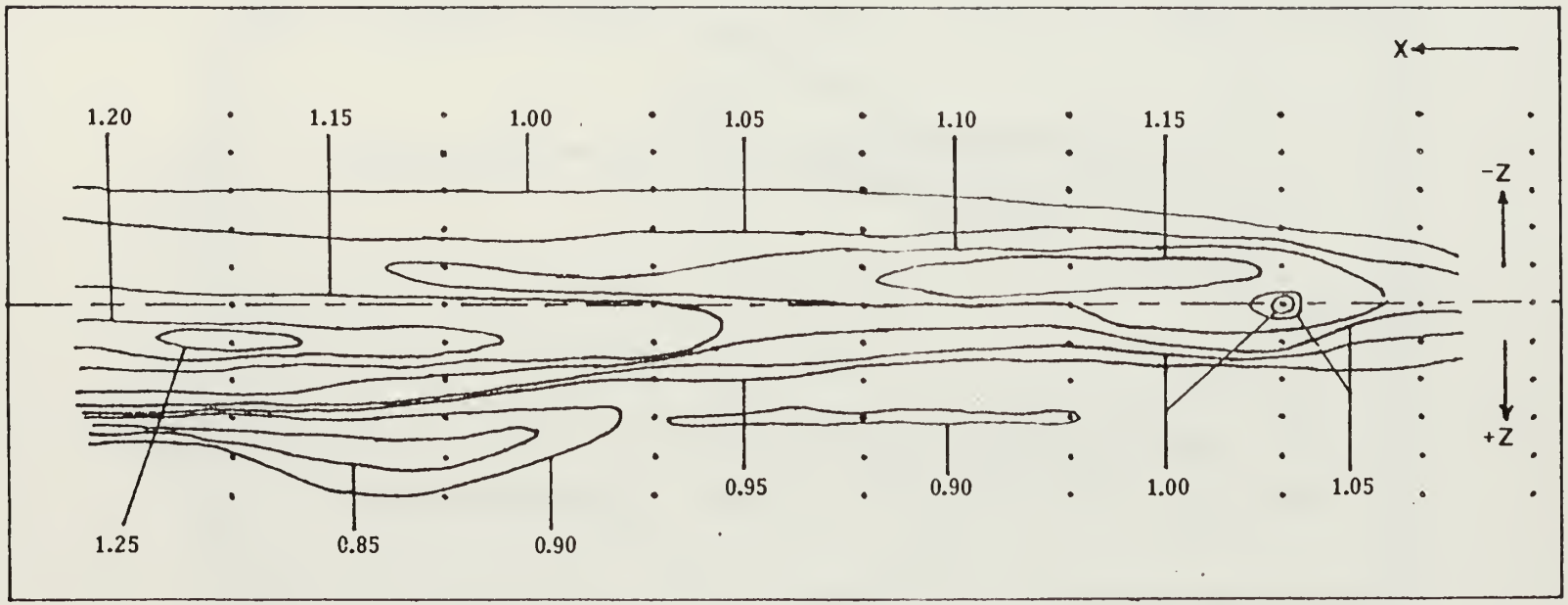

Figure 58. Surface Plot of St/St_f with Vortex at Z=-6.06 cm

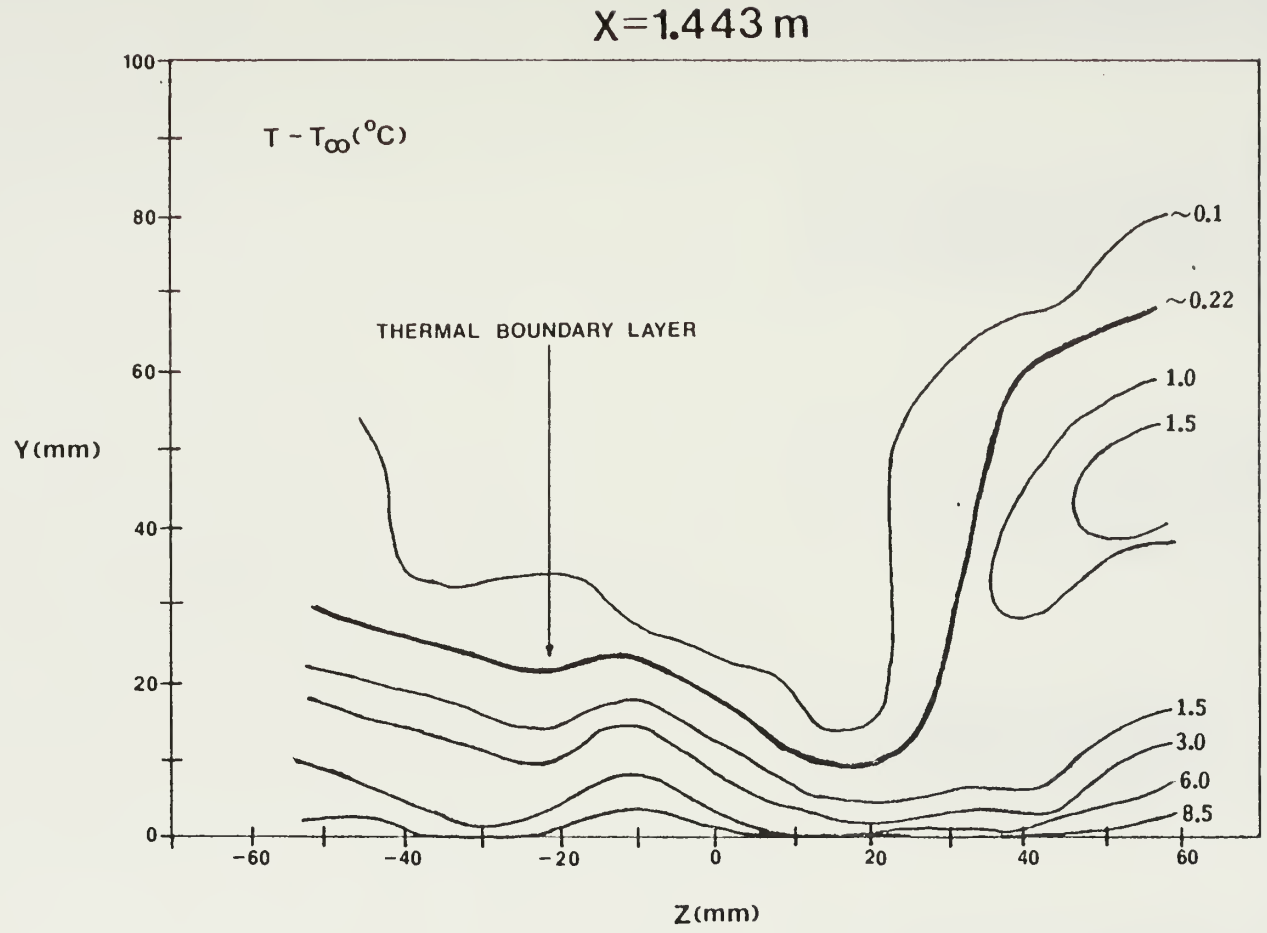

Figure 59. Temperature Profile in the Y, Z Plane with Vortex #2 and Film Cooling

APPENDIX B

TABLES

TABLE 1. INJECTION SYSTEM DATA ($T_{oc} \approx 19\,^{\circ}C$)

FLOW RATE (m^3/s)	MASS FLUX (kg/m^2*s)	EXIT TEMP. (deg C)	DISCHARGE COEFFICIENT	REYNOLDS NUMBER
0.701E-2	0.915E+1	18.8	0.730	4504.5
0.654E-2	0.854E+1	18.7	0.718	4204.2
0.607E-2	0.793E+1	18.8	0.709	3930.9
0.561E-2	0.732E+1	18.8	0.698	3603.6
0.514E-2	0.671E+1	18.8	0.691	3303.3
0.467E-2	0.610E+1	18.9	0.679	3003.0
0.421E-2	0.548E+1	19.2	0.694	2702.7
0.374E-2	0.487E+1	19.2	0.674	2402.4
0.327E-2	0.426E+1	19.2	0.658	2101.1

TABLE 2. INJECTION SYSTEM DATA ($T_{oc} \approx 32\,^{\circ}C$)

FLOW RATE (m^3/s)	MASS FLUX (kg/m^2*s)	EXIT TEMP. (deg C)	DISCHARGE COEFFICIENT	REYNOLDS NUMBER
0.701E-2	0.895E+1	31.8	0.707	4004.0
0.654E-2	0.835E+1	32.0	0.689	3737.1
0.607E-2	0.775E+1	32.0	0.677	3470.1
0.561E-2	0.716E+1	32.0	0.673	3203.2
0.514E-2	0.656E+1	32.0	0.661	2936.3
0.467E-2	0.597E+1	31.9	0.651	2669.3
0.421E-2	0.537E+1	32.1	0.639	2402.4
0.374E-2	0.477E+1	31.9	0.659	2135.5
0.327E-2	0.418E+1	31.9	0.612	1868.5
0.374E-2	0.477E+1	32.2	0.638	2135.5
0.421E-2	0.537E+1	32.2	0.647	2402.4
0.467E-2	0.596E+1	32.2	0.663	2669.3
0.514E-2	0.657E+1	31.7	0.678	2936.3
0.561E-2	0.716E+1	31.8	0.688	3203.2
0.607E-2	0.776E+1	31.9	0.695	3470.1
0.654E-2	0.835E+1	32.0	0.703	3737.1
0.701E-2	0.895E+1	32.0	0.707	4004.0

TABLE 3. INJECTION SYSTEM DATA (T_{oc}≈43.5 °C)

FLOW RATE (m^3/s)	MASS FLUX (kg/m^2*s)	EXIT TEMP. (DEG C)	DISCHARGE COEFFICIENT	REYNOLDS NUMBER
0.701E-2	0.862E+1	43.6	0.688	3603.6
0.654E-2	0.805E+1	43.5	0.675	3363.4
0.607E-2	0.747E+1	43.5	0.661	3123.1
0.561E-2	0.690E+1	43.5	0.661	2882.9
0.514E-2	0.632E+1	43.5	0.649	2642.7
0.467E-2	0.575E+1	43.5	0.638	2402.4
0.421E-2	0.517E+1	43.5	0.628	2162.2
0.374E-2	0.460E+1	43.4	0.617	1921.9
0.327E-2	0.402E+1	43.5	0.611	1681.7
0.374E-2	0.460E+1	43.6	0.623	1921.9
0.421E-2	0.517E+1	43.9	0.633	2162.2
0.467E-2	0.575E+1	43.5	0.645	2402.2
0.514E-2	0.633E+1	43.3	0.661	2642.7
0.561E-2	0.690E+1	43.5	0.666	2882.9
0.607E-2	0.747E+1	43.6	0.676	3123.1
0.654E-2	0.805E+1	43.5	0.680	3363.4
0.701E-2	0.863E+1	43.3	0.690	3603.6

TABLE 4. INJECTION SYSTEM DATA ($T_{oc} \approx 55\ ^{\circ}C$)

FLOW RATE (m^3/s)	MASS FLUX (kg/m^2*s)	EXIT TEMP. (DEG C)	DISCHARGE COEFFICIENT	REYNOLDS NUMBER
0.701E-2	0.814E+1	54.4	0.652	3276.0
0.654E-2	0.759E+1	54.6	0.642	3057.6
0.607E-2	0.706E+1	54.1	0.635	2839.2
0.561E-2	0.652E+1	54.1	0.628	2620.8
0.514E-2	0.597E+1	54.4	0.623	2402.4
0.467E-2	0.541E+1	55.0	0.613	2184.0
0.421E-2	0.486E+1	55.7	0.606	1965.6
0.374E-2	0.433E+1	55.4	0.590	1747.2
0.327E-2	0.378E+1	55.9	0.581	1528.8

TABLE 5. MATERIAL PROPERTIES FOR CONDUCTION LOSSES

MATERIAL	k (W/m^2*K)	A (m^2)	ΔX (m)
INSULATION	0.04	0.04897	0.0254
INSULATION	0.04	0.0848	0.0254
PLEXIGLASS	0.184	0.416	0.1524
GREASE	0.20	8.0E-5	0.0127
STEEL	15.0	5.8E-5	0.00254

TABLE 6. CONDUCTION LOSSES

POWER (W)	Qup(W)	Qcond(W)	ΔT(C)
12.00	2.02	9.98	8.8
14.28	3.15	11.13	13.1
16.52	3.78	12.74	15.3
20.44	5.77	14.67	22.7
20.45	5.62	14.83	22.4

APPENDIX C

UNCERTAINTY ANALYSIS

Uncertainty analysis was performed using the method proposed in 1953 by Kline and McClintock [Ref. 20]. This is the root sum square method, where the uncertainty, W_F , of some function F, is a function of the independent variables X_n.

$$W_F=\left[\sum_i\left(\frac{\partial F}{\partial X_i}W_i\right)^2\right]^{1/2} \qquad (1)$$

To calculate the uncertainty of the heat transfer coefficient, h, the following independent variable uncertainties where determined: $W_q = \pm 16$ W/m , $W_{Tw} = \pm 0.5$ °C, and $W_{T\infty} = \pm 0.1$ °C. Here the uncertainity of convection was based on a 2% error in radiation losses and a 1% error in conduction losses. The uncertainty of T_w is higher than T_∞ due to higher uncertainty inherent in our calculation of contact resistance. From these parameters the uncertainty of h was determined to be ± 0.73 W/m^{2}K or approximately 2.5% based on an h value of 30 W/m^{2}K.

To calculate the uncertainty of the Stanton number, the uncertainty of the heat transfer coefficient along with the following independent variable uncertainties were determined: $W_{\rho_\infty} = \pm 0.005$ kg/m^3 , $W_{U\infty} = \pm 0.1$ m/s and $W_{Cp} = 2$ J/kgK. The uncertainty of C_p was based on the assumption of

constant properties. From these parameters the uncertainty of the Stanton numbers was calculated to be ± 1.8E-4 or approximately 5% based on a Stanton number of 3.6E-3.

APPENDIX D

SOFTWARE

NOMENCLATURE

A	-	P amb
A1	-	T amb
C	-	$P_{oc} - P_{\infty}$
C1()	-	thermocouple temperatures ($^{\circ}C$)
D1	-	$T_w - T_{\infty}$
D2	-	$\rho_c U_c$
D3	-	$(\rho_c U_c)_i$
D4	-	Cd
D5	-	contact resistance temperature correction
F1	-	$\dot{V}_c$
F2	-	Re_d
H()	-	h_o, h_f
H1()	-	spanwise averaged h_o, h_f
I1	-	current
N9	-	run number
Q	-	q convection (W/m^2)
Q1	-	q conduction (W)
Q2	-	q radiation (W)
Q3	-	power (W)
R1	-	ρ_{∞}
R2	-	ρ_c
R3	-	ρ_{ci}

R2() - Re_x

S() - Stanton numbers

S0() - baseline Stanton numbers

S1() - spanwise averaged Stanton numbers

T1 - T_∞

T5 - T_p

T6 - T_c

T8 - T_{oc}

T9 - T_w

U1 - U_∞

U2 - U_c

U3 - U_{ci}

V - voltage

X1() - downstream distance (m)

Z - contact resistance (K/W)

```
 10 REM PROGRAM STDAT1
 20 REM
 30 REM THIS PROGRAM
 40 REM ACQUIRES MULTIPLE
 50 REM CHANNEL THERMOCOUPLE
 60 REM DATA
 70 REM AND CALCULATES HEAT
 80 REM TRANSFER
 90 REM
100 REM LIGRANI/ORTIZ/JOSEPH VER
    SION
110 REM NOVEMBER 1986
120 REM
130 REM
140 REM
150 CLEAR
160 DIM C1(140),X1(8)
170 DIM A(110),U(110),W(110)
180 DIM H(140),S(140)
190 DISP "(HIT <CONT>.)"
200 PAUSE
210 CLEAR
220 REM
230 REM
240 REM CH 0-79,100-139
250 REM COPPER CONSTANTAN THERMO
    COUPLES
260 REM
270 REM
280 REM
290 FOR I=0 TO 139
300 C1(I)=I
310 NEXT I
320 REM
330 REM
340 REM
350 REM ENTER AMPS AND VOLTS
360 REM
370 REM
380 DISP "ENTER RUN NO (MMDDYY.H
    HMM)"
390 INPUT N9
400 DISP "ENTER CURRENT(AMPS)"
410 INPUT I1
420 DISP "ENTER VOLTAGE(VOLTS)"
430 INPUT V
440 DISP "RUN #=",N9
450 DISP "I(AMPS)=",I1
460 DISP "V(VOLTS)=",V
470 REM
480 REM
490 REM ENTER DEL P, AMB CNDTNS
500 REM
510 REM
520 DISP "ENTER PAMB(IN HG)"
530 INPUT A
540 DISP "ENTER DEL P(IN H2O)"
550 INPUT C
560 DISP "ENTER TAMB(C)"
570 INPUT A1
```

```
580 DISP "PAMB(IN HG)=",A
590 DISP "DEL P(IN H2O)=",C
600 DISP "THERMOMETER AMB(C)",A1
610 REM
620 REM
630 REM
640 REM
650 DISP "(HIT (CONT))"
660 PAUSE
670 PRINT "STANTON NO RESULTS"
680 PRINT
690 PRINT "RUN #",N9
700 PRINT
710 L1=0
720 REM CONTINUE THE LOOP
730 L1=L1+1
740 REM
750 OUTPUT 709 ;"AI";C1(L1);"VT1
    "
760 ENTER 709 ; X
770 GOSUB 2170
780 C1(L1)=T
790 BEEP 10,10
800 REM
810 CLEAR
820 REM
830 REM
840 REM
850 REM CONTINUE TO LOOP FOR ALL
     THERMOCOUPLES
860 REM
870 IF L1<79 THEN GOTO 720
880 IF L1=79 THEN L1=L1+20
890 IF L1<>139 THEN GOTO 720
900 GOSUB 2280
910 BEEP 10,10
920 A(0)=U
930 PRINT "AMBIENT T(C):",A(0)
940 PRINT
950 REM TRANSFORM TO SI UNITS
960 A=A*3385.82
970 C=C*248.7
980 T1=C1(109)+273.15
990 R1=A/(287*T1)
1000 U1=(2*C/R1)^.5
1010 REM
1020 REM
1030 REM
1040 REM PRINT OUT DATA
1050 REM
1060 PRINT "DENSITY (KG/M3)"
1070 PRINT R1
1080 PRINT "VELOCITY (M/S)"
1090 PRINT U1
1100 PRINT "PAMB (N/M2)"
1110 PRINT A
1120 PRINT "FS TEMP (K)"
1130 PRINT T1
1140 PRINT "THERMOMETER AMB(C)"
1150 PRINT A1
```

```
1160 REM
1170 REM AVG PLATE TEMP
1180 REM
1190 REM
1200 REM
1210 T9=0
1220 FOR I=1 TO 79
1230 T9=T9+C1(I)
1240 NEXT I
1250 FOR I=100 TO 108
1260 T9=T9+C1(I)
1270 NEXT I
1280 T9=T9/88
1290 PRINT "AVG PLATE TEMP,MEASU
     RED,(C)"
1300 PRINT T9
1310 REM
1320 REM
1330 REM ENERGY BALANCE
1340 REM
1350 D1=T9-U
1360 Q1=.093+1.45*D1-.051*D1^2+.
     00058*D1^3
1370 K9=T9+273.15
1380 U9=U+273.15
1390 Q2=.000000002169*(K9^4-U9^4)
1400 Q3=I1*V
1410 Q=Q3-Q1-Q2
1420 REM
1430 REM
1440 PRINT "T PLATE-T AMB (C)"
1450 PRINT D1
1460 PRINT "POWER IN (WT)"
1470 PRINT Q3
1480 PRINT "COND LOSS (WT)"
1490 PRINT Q1
1500 PRINT "RAD LOSS (WT)"
1510 PRINT Q2
1520 PRINT "CONV LOSS (WT)"
1530 PRINT Q
1540 PRINT "CURRENT (AMPS)"
1550 PRINT I1
1560 PRINT "VOLTAGE (VOLTS)"
1570 PRINT V
1580 REM
1590 REM
1600 REM
1610 C9=1005
1620 REM
1630 REM WALL TEMP. CORRECTIONS
1640 REM
1650 Z=.016
1660 D5=Q*Z
1670 Q=Q/.4897
1680 REM
1683 PRINT "AVG PLATE TEMP,CORRE
     CTED,(C)"
1685 PRINT T9-D5
1690 PRINT
1700 PRINT "No        ST
      H"
```

```
1710 REM CALCULATE HEAT TRANSFER
     COEFFICIENTS AND STANTON NU
     MBERS
1720 FOR J=1 TO 2
1730 IF J=1 THEN GOTO 1750
1740 GOTO 1790
1750 M=1
1760 M1=79
1770 M2=0
1780 GOTO 1820
1790 M=100
1800 M1=108
1810 M2=20
1820 FOR I=M TO M1
1830 C1(I)=C1(I)-05
1840 H(I)=Q/(C1(I)-C1(100))
1850 S(I)=H(I)/(R1*01*C9)
1860 J1=I-M2
1870 PRINT USING 1880 ; J1,S(I),
     H(I)
1880 IMAGE 2D,2X,SD.DDDE,2X,SD.D
     DDE
1890 NEXT I
1900 NEXT J
1910 REM
1920 REM CALCULATE LOCAL REYNOLD
     S NUMBER
1930 REM
1940 PRINT
1950 REM
1960 N1=.0000156
1970 F=U1/N1
1980 X1(1)=1.11329
1990 X1(2)=1.20269
2000 X1(3)=1.30429
2010 X1(4)=1.45669
2020 X1(5)=1.60909
2030 X1(6)=1.76149
2040 X1(7)=1.91389
2050 X1(8)=2.06629
2060 PRINT "ROW #      RE"
2070 FOR I=1 TO 8
2080 R2(I)=X1(I)*F
2090 PRINT USING 2100 ; I,R2(I)
2100 IMAGE DD,3X,D.4DE
2110 NEXT I
2120 !
2130 ! CALCULATE AVG STANTON NO
2140 GOSUB 2420
2150 END
2160 !
2170 ! SUBROUTINE
2180 !
2190 !
2200 ! VOLTAGE TO TEMPERATURE
2210 ! CONVERSION
2220 !
2230 ! V(MV) TO T(C)
2240 !
2250 E=X*1000
```

```
2260 T=25.573*E-1.936879*E*E+.99
     785*E*E*E-.261277*E*E*E*E
2270 RETURN
2280 !
2290 ! FIND THE AMBIENT TEMPERAT
     URE
2300 !
2310 OUTPUT 709 ;"AI";C1(0);"VT1
     "
2320 ENTER 709 ; X
2330 GOSUB 2170
2340 U=T
2350 OUTPUT 709 ;"AI";C1(0);"VT1
     "
2360 ! U = AMBIENT TEMP.
2370 !
2380 RETURN
2390 REM   U=AMBIENT TEMP.
2400 REM
2410 RETURN
2420 !
2430 ! SUBROUTINE TO FIND AVG ST
     ANTON NO
2440 !
2450 FOR I=1 TO 7
2460 H1(I)=0
2470 M=I*11-10
2480 FOR J=M TO I*11
2490 H1(I)=H1(I)+H(J)
2500 NEXT J
2510 H1(I)=H1(I)/11
2520 S1(I)=H1(I)/(R1*U1*C9)
2530 NEXT I
2540 H1(8)=0
2550 FOR I=78 TO 79
2560 H1(8)=H1(8)+H(I)
2570 NEXT I
2580 FOR I=100 TO 108
2590 H1(8)=H1(8)+H(I)
2600 NEXT I
2610 H1(8)=H1(8)/11
2620 S1(8)=H1(8)/(R1*U1*C9)
2630 !
2640 ! PRINT AVG STANTON NO
2650 PRINT
2660 PRINT "ROW #  AVG ST NO"
2670 FOR I=1 TO 8
2680 PRINT USING 2690 ; I,S1(I)
2690 IMAGE DD,3X,D.4DE
2700 NEXT I
2710 RETURN
```

```
 10 REM PROGRAM STDAT3
 20 REM
 30 REM THIS PROGRAM
 40 REM ACQUIRES MULTIPLE
 50 REM CHANNEL THERMOCOUPLE
 60 REM DATA
 70 REM AND CALCULATES HEAT
 80 REM TRANSFER
 90 REM
100 REM LIGRANI/ORTIZ/JOSEPH VER
    SION
110 REM NOVEMBER 1986
120 REM
130 REM
140 REM
150 CLEAR
160 DIM C1(140),X1(8)
170 DIM A(110),U(110),W(110)
180 DIM H(110),S(110),S0(110)
190 DISP "(HIT <CONT>.)"
200 ASSIGN# 2 TO "STFC3"
210 PAUSE
220 CLEAR
230 REM
240 REM
250 REM CH.0-79,100-139
260 REM COPPER CONSTANTAN THERMO
    COUPLES
270 REM
280 REM
290 REM
300 FOR I=0 TO 139
310 C1(I)=I
320 NEXT I
330 REM
340 REM
350 REM
360 REM ENTER AMPS AND VOLTS
370 REM
380 REM
390 DISP "ENTER RUN NO (MMDDYY.H
    HMM)"
400 INPUT N9
410 DISP "ARE YOU WORKING (1)WIT
    H OR (2) WITHOUT FILMCOOLING
    "
420 INPUT Z1
430 IF Z1=1 THEN GOSUB 2850
440 DISP "ENTER CURRENT(AMPS)"
450 INPUT I1
460 DISP "ENTER VOLTAGE(VOLTS)"
470 INPUT V
480 DISP "RUN #=",N9
490 DISP "I(AMPS)=",I1
500 DISP "V(VOLTS)=",V
510 REM
520 REM
530 REM ENTER DEL P, AMB CNDTNS
540 REM
550 REM
```

```
560 DISP "ENTER PAMB(IN HG)"
570 INPUT A
580 DISP "ENTER DEL P(IN H2O)"
590 INPUT C
600 DISP "ENTER TAMB(C)"
610 INPUT A1
620 DISP "PAMB(IN HG)=",A
630 DISP "DEL P(IN H2O)=",C
640 DISP "THERMOMETER AMB(C)",A1
650 REM
660 REM
670 REM
680 REM
690 DISP "(HIT (CONT))"
700 PAUSE
710 PRINT "STANTON NO RESULTS"
720 PRINT
730 PRINT "RUN #",N9
740 PRINT
750 L1=0
760 REM CONTINUE THE LOOP
770 L1=L1+1
780 REM
790 OUTPUT 709 ;"AI";C1(L1);"VT1
    "
800 ENTER 709 ; X
810 GOSUB 2300
820 C1(L1)=T
830 BEEP 10,10
840 REM
850 CLEAR
860 REM
870 REM
880 REM
890 REM CONTINUE TO LOOP FOR ALL
     THERMOCOUPLES
900 REM
910 IF L1<79 THEN GOTO 760
920 IF L1=79 THEN L1=L1+20
930 IF L1<>139 THEN GOTO 760
940 GOSUB 2410
950 BEEP 10,10
960 A(0)=U
970 PRINT "AMBIENT T(C):",A(0)
980 PRINT
990 REM TRANSFORM TO SI UNITS
1000 A=A*3385.82
1010 C=C*248.7
1020 T1=C1(109)+273.15
1030 R1=A/(287*T1)
1040 U1=(2*C/R1)^.5
1050 IF Z1=1 THEN GOSUB 2940
1060 REM
1070 REM
1080 REM
1090 REM PRINT OUT DATA
1100 REM
1110 PRINT "DENSITY (KG/M3)"
1120 PRINT R1
1130 PRINT "VELOCITY (M/S)"
```

```
1140 PRINT U1
1150 PRINT "PAMB (N/M2)"
1160 PRINT A
1170 PRINT "FS TEMP (K)"
1180 PRINT T1
1190 PRINT "THERMOMETER AMB(C)"
1200 PRINT A1
1210 REM
1220 REM AVG PLATE TEMP
1230 REM
1240 REM
1250 REM
1260 T9=0
1270 FOR I=1 TO 79
1280 T9=T9+C1(I)
1290 NEXT I
1300 FOR I=100 TO 108
1310 T9=T9+C1(I)
1320 NEXT I
1330 T9=T9/88
1340 PRINT "AVG PLATE TEMP(C)"
1350 PRINT T9
1360 REM
1370 REM
1380 REM ENERGY BALANCE
1390 REM
1400 D1=T9-U
1410 Q1=.093+1.45*D1-.051*D1^2+.
     00058*D1^3
1420 K9=T9+273.15
1430 U9=U+273.15
1440 Q2= 00000002169*(K9^4-U9^4)
1450 Q3=I1*V
1460 Q=Q3-Q1-Q2
1470 REM
1480 REM
1490 PRINT "T PLATE-T AMB (C)"
1500 PRINT D1
1510 PRINT "POWER IN (WT)"
1520 PRINT Q3
1530 PRINT "COND LOSS (WT)"
1540 PRINT Q1
1550 PRINT "RAD LOSS (WT)"
1560 PRINT Q2
1570 PRINT "CONV LOSS (WT)"
1580 PRINT Q
1590 PRINT "CURRENT (AMPS)"
1600 PRINT I1
1610 PRINT "VOLTAGE (VOLTS)"
1620 PRINT V
1630 REM
1640 REM
1650 REM
1660 C9=1005
1670 REM
1680 REM WALL TEMP. CORRECTIONS
1690 REM
1700 Z=.016
1710 D5=Q*Z
1720 Q=Q/.4897
```

```
1730 REM
1740 PRINT
1750 PRINT "No         H         S
     T/ST0"
1760 REM CALCULATE HEAT TRANSFER
     COEFFICIENTS AND STANTON NU
     MBERS
1770 ! OPEN FILE TO RETRIEVE BAS
     ELINE ST VALUES
1780 ASSIGN# 1 TO "HDATA"
1790 FOR J=1 TO 2
1800 IF J=1 THEN GOTO 1820
1810 GOTO 1860
1820 M=1
1830 M1=79
1840 M2=0
1850 GOTO 1890
1860 M=100
1870 M1=108
1880 M2=20
1890 FOR I=M TO M1
1900 C1(I)=C1(I)-05
1910 H(I)=Q/(C1(I)-C1(109))
1920 READ# 1 ; S0(I)
1930 S(I)=H(I)/(R1*U1*C9)
1950 S0(I)=S(I)/S0(I)
1960 J1=I-M2
1970 PRINT USING 1980 ; J1,H(I),
     S0(I)
1980 IMAGE 2D,2X,SD.DDDE,2X,DDD.
     DDD
1990 NEXT I
2000 NEXT J
2010 PRINT# 2 ; N9
2020 ASSIGN# 1 TO *
2030 ASSIGN# 2 TO *
2040 REM
2050 REM CALCULATE LOCAL REYNOLD
     S NUMBER
2060 REM
2070 PRINT
2080 REM
2090 N1=.0000156
2100 F=U1/N1
2110 X1(1)=1.11329
2120 X1(2)=1.20269
2130 X1(3)=1.30429
2140 X1(4)=1.45669
2150 X1(5)=1.60909
2160 X1(6)=1.76149
2170 X1(7)=1.91389
2180 X1(8)=2.06629
2190 PRINT "ROW #      RE"
2200 FOR I=1 TO 8
2210 R2(I)=X1(I)*F
2220 PRINT USING 2230 ; I,R2(I)
2230 IMAGE DD,3X,D.4DE
2240 NEXT I
2250 !
2260 ! CALCULATE AVG STANTON NO
```

```
2270 GOSUB 2550
2280 END
2290 !
2300 ! SUBROUTINE
2310 !
2320 !
2330 ! VOLTAGE TO TEMPERATURE
2340 ! CONVERSION
2350 !
2360 ! V(MV) TO T(C)
2370 !
2380 E=X*1000
2390 T=26.573*E-1.936879*E*E+.99
     785*E*E*E-.261277*E*E*E*E
2400 RETURN
2410 !
2420 ! FIND THE AMBIENT TEMPERAT
     URE
2430 !
2440 OUTPUT 709 ;"AI";C1(0);"VT1
     "
2450 ENTER 709 ; X
2460 GOSUB 2300
2470 U=T
2480 OUTPUT 709 ;"AI";C1(0);"VT1
     "
2490 ! U = AMBIENT TEMP.
2500 !
2510 RETURN
2520 REM   U=AMBIENT TEMP.
2530 REM
2540 RETURN
2550 !
2560 ! SUBROUTINE TO FIND AVG ST
     ANTON NO
2570 !
2580 FOR I=1 TO 7
2590 H1(I)=0
2600 M=I*11-10
2610 FOR J=M TO I*11
2620 H1(I)=H1(I)+H(J)
2630 NEXT J
2640 H1(I)=H1(I)/11
2650 S1(I)=H1(I)/(R1*U1*C9)
2660 NEXT I
2670 H1(8)=0
2680 FOR I=78 TO 79
2690 H1(8)=H1(8)+H(I)
2700 NEXT I
2710 FOR I=100 TO 108
2720 H1(8)=H1(8)+H(I)
2730 NEXT I
2740 H1(8)=H1(8)/11
2750 S1(8)=H1(8)/(R1*U1*C9)
2760 !
2770 ! PRINT AVG STANTON NO
2780 PRINT
2790 PRINT "ROW #  AVG ST NO"
2800 FOR I=1 TO 8
2810 PRINT USING 2820 ; I,S1(I)
```

```
2820 IMAGE DD,3X,D.4DE
2830 NEXT I
2840 RETURN
2850 !
2860 ! SUBROUTINE FOR FC DATA
2870 DISP "ENTER FLOW VALUE (%)"
2880 INPUT F1
2890 DISP "ENTER PLEN DEL P (IN
     H20)"
2900 INPUT P1
2910 P1=P1*248.7
2920 F1=F1*.000093456
2930 RETURN
2940 !
2950 ! SUBROUTINE FOR CD CALCULT
     IONS
2960 T5=(C1(110)+C1(111)+C1(112)
     )/3
2970 ! CONVERT PLEN TEMP TO INJE
     CT TEMP
2980 T6=1.45463*T5^.868162
2990 T7=T6+273.15
3000 U2=F1/.000921468
3010 T8=T7-U2*U2/(2*1005)
3020 R2=A/(T8*287)
3030 D2=R2*U2
3040 R3=A/(T7*287)
3050 U3=(P1*2/R3)^.5
3060 D3=R3*U3
3070 D4=D2/D3
3080 F2=U2*.009525/.0000156
3090 ! PRINT RESULTS
3100 PRINT "INJECTION TEMP(C)"
3110 PRINT T6
3120 PRINT "PLENUM TEMP(C)"
3130 PRINT T5
3140 PRINT "PLENUM DEL P (N/M^2)
     "
3150 PRINT P1
3160 PRINT "RHOC (KG/M^2)"
3170 PRINT R2
3180 PRINT "VELOCITY,UC (M/S)"
3190 PRINT U2
3200 PRINT "MASS FLUX(KG/M^2*S)"
3210 PRINT D2
3220 PRINT "REYNOLDS NO. (DIA)"
3230 PRINT F2
3240 PRINT "DISCHARGE COEFFICIEN
     T"
3250 PRINT D4
3260 PRINT "BLOWING RATIO"
3270 PRINT D2/(R1*U1)
3280 PRINT "DENSITY RATIO"
3290 PRINT R2/R1
3300 PRINT "VELOCITY RATIO"
3310 PRINT U2/U1
3320 PRINT "MOMENTUM FLUX RATIO"
3330 PRINT R2*U2*U2/(R1*U1*U1)
3360 RETURN
```

```
 10 REM PROGRAM TPROF
 20 REM
 30 REM THIS PROGRAM
 40 REM ACQUIRES TEMPERATURE
 50 REM PROFILE DATA USING
 60 REM A THERMOCOUPLE
 70 REM  ME 2410
 80 REM
 90 REM LIGRANI, NOV 1986
100 REM
110 CLEAR
120 DIM C1(140),Y(50),T(50)
130 DIM A(50),B(50),C(50)
140 DIM D(50),E(50),G(50)
150 DIM Z(50)
160 REM
170 REM
180 CLEAR
190 REM
200 REM CHANNEL 130 FOR TC
210 REM
220 REM CU-CONSTANTAN TC

230 REM
240 REM
250 DISP "ENTER RUN NO (MMDDYY.H
    HMM)"
260 INPUT N9
270 DISP "X LOCATION (M)"
280 INPUT X1
290 DISP "Z LOCATION (M)"
300 INPUT Z1
310 DISP "UINF (M/SEC)"
320 INPUT U1
330 DISP "CF/2"
340 INPUT C2
350 DISP "Q CONV"
360 INPUT Q1
370 DISP "TWALL (C)"
380 INPUT T1
390 DISP "DENSITY (KG/M3)"
400 INPUT D1
410 DISP "CP (WT SEC/KG K)"
420 INPUT C1
430 DISP "WALL DSPLMNT (MM)"
440 INPUT Y3
450 Q2=Q1/.4897
460 U2=U1*C2^.5
470 T3=Q2/(D1*C1*U2)
480 V1=.0000156
490 REM
500 REM
510 REM
520 REM
530 C1(130)=130
540 L1=130
550 REM
560 REM
570 PRINT "TEMP PROFILE STUDY NO
    V 1986"
```

```
580 PRINT
590 PRINT "**********************
    ****"
600 REM
610 REM
620 D5=50.9
630 REM
640 REM
650 REM ENTER MAIN LOOP
660 REM
670 FOR I=1 TO 50
680 REM
690 DISP "I= ";I
700 DISP "ENTER ROTATIONS"
710 INPUT R1
720 DISP "ENTER DEGREES"
730 INPUT R2
740 Y1=R1*25.4/18
750 Y2=Y1+R2*25.4/(360*18)
760 IF I=1 THEN Y(I)=Y2
770 IF I=1 THEN GOTO 790
780 Y(I)=Y2+Y(I-1)
790 REM
800 DISP "HIT CONT. FOR D.A."
810 PAUSE
820 CLEAR
830 DISP "CHANNEL #";C1(L1)
840 W=0
850 FOR K=1 TO 20
860 OUTPUT 709 ;"AI";C1(L1);"VT1
    "
870 ENTER 709 ; X
880 W=W+X
890 NEXT K
900 X=W/20
910 PRINT "E(";I;")=";
920 PRINT USING "D.6D" ; X
930 GOSUB 2320
940 BEEP 10,10
950 !
960 CLEAR
970 REM
1050 REM
1060 REM
1070 T(I)=T
1080 REM
1090 PRINT "POSITION DATA";
1100 PRINT
1110 PRINT "ROTATIONS";R1;
1120 PRINT " DEGREES";R2;
1130 PRINT
1140 PRINT "Y=";Y(I);" MM";
1150 PRINT
1160 PRINT "T=";T(I);" C";
1170 PRINT
1180 PRINT "**********************
     ******"
1190 PRINT
1200 REM
1210 BEEP 10,10
```

```
1220 REM
1230 REM
1240 DISP "LAST POINT?"
1250 DISP "1 IF YES"
1260 INPUT J
1270 IF J=1 THEN GOTO 1310
1280 REM
1290 NEXT I
1300 REM
1310 REM
1320 I7=I
1330 Y5=Y(I)
1340 T2=(T(1)+T(2))/2
1350 REM
1360 REM
1370 GOSUB 2440
1380 REM
1390 REM
1400 REM
1410 REM
1420 PRINT "TEMP PROFILE STUDY N
     OV 1986"
1430 PRINT "**********************
     *******"
1440 PRINT "RUN NUMBER"
1450 PRINT N9
1460 PRINT "X LOCATION (M)"
1470 PRINT X1
1480 PRINT "Z LOCATION (M)"
1490 PRINT Z1
1500 PRINT "UINF (M/SEC)"
1510 PRINT U1
1520 PRINT "CF/2"
1530 PRINT C2
1540 PRINT "Q CONV (WATTS/M2)"
1550 PRINT Q2
1560 PRINT "DENSITY (KG/M3)"
1570 PRINT D1
1580 PRINT "CP (WT SEC/KG K)"
1590 PRINT C1
1600 PRINT "WALL DSPLCMNT (MM)"
1610 PRINT Y3
1620 PRINT "WALL TEMP (C)"
1630 PRINT T1
1640 PRINT "FS TEMP (C)"
1650 PRINT T2
1660 PRINT "FRICTION TEMP (K)"
1670 PRINT T3
1680 PRINT "THERMAL DEL (MM)"
1690 PRINT D5
1700 REM
1710 REM
1720 REM
1730 REM
1740 FOR I=1 TO I7
1750 Y(I)=Y5-Y(I)+Y3
1760 A(I)=(T1-T(I))/(T1-T2)
1770 B(I)=(T1-T(I))/T3
1780 C(I)=Y(I)*U2/(V1*1000)
1790 D(I)=Y(I)/D5
```

```
1800 Z(I)=T(I)-T2
1810 NEXT I
1820 REM
1830 PRINT "**********************
     ***********"
1840 PRINT "  I     Y(MM)       T(
     C)"
1850 FOR I=1 TO I7
1860 PRINT USING 1870 ; I,Y(I),T
     (I)
1870 IMAGE DD,3X,DDD.1DE,2X,DD.2
     DE
1880 NEXT I
1890 PRINT
1900 REM
1910 REM
1920 PRINT
1930 PRINT "  I     Y/DEL    (TW-T
     )/(TW-TINF)"
1940 FOR I=1 TO I7
1950 PRINT USING 1960 ; I,D(I),A
     (I)
1960 IMAGE DD,3X,D.3DE,2X,DD.3DE
1970 NEXT I
1980 PRINT
1990 REM
2000 REM
2010 PRINT "  I      Y/DEL      T-
     TINF(C)"
2020 FOR I=1 TO I7
2030 PRINT USING 2040 ; I,D(I),Z
     (I)
2040 IMAGE DD,3X,D.3DE,2X,DD.3DE
2050 NEXT I
2060 PRINT
2070 REM
2080 REM
2090 REM
2100 REM
2110 REM
2120 REM
2130 PRINT "  I       Y+         T+
     "
2140 FOR I=1 TO I7
2150 PRINT USING 2160 ; I,C(I),B
     (I)
2160 IMAGE DD,3X,DDD.1DE,2X,DDD.
     1DE
2170 NEXT I
2180 PRINT
2190 REM
2200 REM
2210 REM
2220 REM
2230 REM
2240 PRINT
2250 DISP "RUN COMPLETE"
2260 PRINT "RUN COMPLETE"
2270 PRINT
2280 REM
```

```
2290 END
2300 !
2310 !
2320 ! SUBROUTINE
2330 !
2340 !
2350 ! VOLTAGE TO TEMPERATURE
2360 ! CONVERSION
2370 !
2380 ! V(MV) TO T(C)
2390 !
2400 E=X*1000
2410 T=26.573*E-1.936879*E*E+.99
     785*E*E*E-.261277*E*E*E*E
2420 RETURN
2430 REM
2440 REM SUBROUTINE FOR
2450 REM CALCULATING THERMAL
2460 REM BOUNDARY LAYER
2470 REM THICKNESS
2480 REM
2490 REM
2500 REM
2510 REM
2520 Z=.99
2530 FOR K=1 TO 17
2540 E(18-K)=(T1-T(K))/(T1-T2)
2550 G(18-K)=Y5+Y3-Y(K)
2560 NEXT K
2570 FOR K=1 TO 17
2580 IF E(K)>Z THEN GOTO 2600
2590 NEXT K
2600 REM
2610 F4=G(K-2)^2*G(K-1)+G(K)^2*G
     (K-2)+G(K-1)^2*G(K)-G(K)^2*
     G(K-1)-G(K-1)^2*G(K-2)-G(K-
     2)^2*G(K)
2620 REM
2630 REM
2640 F1=((E(K-1)-E(K-2))*(G(K)-G
     (K-2))-(E(K)-E(K-2))*(G(K-1
     )-G(K-2)))/F4
2650 REM
2660 F2=((E(K)-E(K-2))*(G(K-1)^2
     -G(K-2)^2)-(E(K-1)-E(K-2))*
     (G(K)^2-G(K-2)^2))/F4
2670 REM
2680 F3=G(K-2)^2*G(K-1)*E(K)+G(K
     )^2*G(K-2)*E(K-1)
2690 F3=F3+G(K-1)^2*G(K)*E(K-2)-
     G(K)^2*G(K-1)*E(K-2)
2700 F3=F3-G(K-1)^2*G(K-2)*E(K)-
     G(K-2)^2*G(K)*E(K-1)
2710 F3=F3/F4
2720 REM
2730 D5=G(K-1)
2740 FOR K1=1 TO 10
2750 D5=D5+(Z-F1*D5^2-F2*D5-F3)/
     (2*F1*D5+F2)
2760 Z7=(Z-F1*D5^2-F2*D5-F3)/(2*
     F1*D5+F2)
```

```
2770 IF Z7<.001 THEN GOTO 2790
2780 NEXT K1
2790 REM
2800 RETURN
2810 REM
2820 REM
2830 REM
2840 REM
2850 REM
2860 REM
     2660 REM
```

APPENDIX E

BASELINE DATA

NOMENCLATURE

H	-	h, h_o
No.	-	thermocouple position
RE	-	Re_x
ST	-	St
ST/ST0	-	St/St_o
ST/STF	-	St/St_f

RUN NUMBER	DESCRIPTION
111786.1304	10 m/s
112086.1630	10 m/s
112186.1201	10 m/s
111886.1337	15 m/s
111586.1141	20 m/s
112186.1255	temp. profile, 10 m/s, Z=-0.038 m, X=1.85 m
112186.1225	temp. profile, 10 m/s, Z=0.038 m, X=1.85 m
112186.1201	temp. profile, 10 m/s, Z=0 m, X=1.85 m
112886.1401	temp. profile, 10 m/s, Z=0 m, X=1.443 m

STANTON NO RESULTS

RUN #
111786.1304

AMBIENT T(C):
19.1287302628

DENSITY (KG/M3)
1.23157722692
VELOCITY (M/S)
9.98781621315
PAMB (N/M2)
103142.23466
FS TEMP (K)
291.80517528
THERMOMETER AMB(C)
19.2
AVG PLATE TEMP(C)
40.7496077948
T PLATE-T AMB (C)
21.620877532
POWER IN (WT)
335.748
COND LOSS (WT)
14.4754161734
RAD LOSS (WT)
52.2945291806
CONV LOSS (WT)
268.978054646
CURRENT (AMPS)
5.71
VOLTAGE (VOLTS)
58.8

No	ST	H
1	+5.277E-003	+6.523E+001
2	+4.337E-003	+5.362E+001
3	+3.997E-003	+4.941E+001
4	+5.483E-003	+6.778E+001
5	+6.028E-003	+7.452E+001
6	+4.934E-003	+6.100E+001
7	+5.434E-003	+6.718E+001
8	+5.307E-003	+6.561E+001
9	+5.413E-003	+6.698E+001
10	+4.337E-003	+5.362E+001
11	+5.533E-003	+6.840E+001
12	+2.629E-003	+3.250E+001
13	+2.944E-003	+3.640E+001
14	+2.728E-003	+3.373E+001
15	+2.629E-003	+3.250E+001
16	+2.651E-003	+3.277E+001
17	+2.819E-003	+3.485E+001
18	+2.880E-003	+3.561E+001
19	+2.894E-003	+3.577E+001
20	+2.824E-003	+3.491E+001
21	+3.061E-003	+3.784E+001
22	+2.921E-003	+3.611E+001
23	+2.773E-003	+3.428E+001
24	+2.550E-003	+3.152E+001
25	+2.293E-003	+2.833E+001
26	+2.440E-003	+3.017E+001
27	+2.560E-003	+3.165E+001
28	+2.610E-003	+3.227E+001
29	+2.499E-003	+3.089E+001
30	+2.595E-003	+3.196E+001
31	+2.629E-003	+3.250E+001
32	+2.303E-003	+2.847E+001
33	+2.720E-003	+3.363E+001
34	+2.370E-003	+2.930E+001
35	+2.492E-003	+3.081E+001
36	+2.238E-003	+2.767E+001
37	+2.450E-003	+3.029E+001
38	+2.358E-003	+2.915E+001
39	+2.519E-003	+3.114E+001
40	+2.276E-003	+2.813E+001
41	+2.235E-003	+2.763E+001
42	+2.425E-003	+2.997E+001
43	+2.456E-003	+3.037E+001
44	+2.492E-003	+3.081E+001
45	+2.335E-003	+2.886E+001
46	+2.312E-003	+2.858E+001
47	+2.278E-003	+2.816E+001
48	+2.295E-003	+2.837E+001
49	+2.135E-003	+2.639E+001
50	+2.332E-003	+2.882E+001
51	+2.123E-003	+2.624E+001

52	+2.176E-003	+2.690E+001
53	+2.397E-003	+2.963E+001
54	+2.086E-003	+2.578E+001
55	+2.496E-003	+3.085E+001
56	+2.284E-003	+2.823E+001
57	+2.213E-003	+2.734E+001
58	+2.333E-003	+2.882E+001
59	+2.262E-003	+2.796E+001
60	+1.906E-003	+2.356E+001
61	+2.128E-003	+2.630E+001
62	+2.050E-003	+2.534E+001
63	+2.352E-003	+2.908E+001
64	+2.425E-003	+2.997E+001
65	+2.391E-003	+2.956E+001
66	+2.422E-003	+2.994E+001
67	+2.189E-003	+2.706E+001
68	+2.233E-003	+2.760E+001
69	+2.207E-003	+2.728E+001
70	+2.176E-003	+2.690E+001
71	+2.083E-003	+2.576E+001
72	+1.889E-003	+2.335E+001
73	+2.057E-003	+2.542E+001
74	+2.289E-003	+2.830E+001
75	+2.355E-003	+2.911E+001
76	+2.306E-003	+2.851E+001
77	+2.284E-003	+2.823E+001
78	+2.057E-003	+2.542E+001
79	+2.035E-003	+2.515E+001
80	+2.121E-003	+2.621E+001
81	+2.079E-003	+2.570E+001
82	+1.857E-003	+2.295E+001
83	+1.797E-003	+2.221E+001
84	+2.070E-003	+2.559E+001
85	+2.063E-003	+2.551E+001
86	+2.128E-003	+2.630E+001
87	+2.254E-003	+2.786E+001
88	+2.189E-003	+2.706E+001

ROW #	RE
1	7.1278E+005
2	7.7002E+005
3	8.3506E+005
4	9.3264E+005
5	1.0302E+006
6	1.1278E+006
7	1.2254E+006
8	1.3229E+006

ROW #	AVG ST NO
1	5.0986E-003
2	2.8163E-003
3	2.5420E-003
4	2.3919E-003
5	2.2694E-003
6	2.2511E-003
7	2.1880E-003
8	2.0589E-003

```
RUN #
 112006.163

AMBIENT T(C)
 18.4556573107

DENSITY (KG/M3)
 1.21886241354
VELOCITY (M/S)
 10.0397760335
PAMB (N/M2)
 102251.764
FS TEMP (K)
 292.303642633
THERMOMETER AMB(C)
 17.8
AVG PLATE TEMP(C)
 39.6379162992
T PLATE-T AMB (C)
 21.1822589885
POWER IN (WT)
 339.216
COND LOSS (WT)
 14.3870573116
RAD LOSS (WT)
 50.7802063011
CONV LOSS (WT)
 274.048736387
CURRENT (AMPS)
 5.73
VOLTAGE (VOLTS)
 59.2
```

No	ST	H
1	+6.823E-003	+8.391E+001
2	+5.324E-003	+6.548E+001
3	+4.817E-003	+5.924E+001
4	+7.137E-003	+8.777E+001
5	+7.996E-003	+9.833E+001
6	+6.148E-003	+7.561E+001
7	+7.029E-003	+8.644E+001
8	+6.823E-003	+8.391E+001
9	+7.003E-003	+8.612E+001
10	+5.309E-003	+6.529E+001
11	+7.164E-003	+8.811E+001
12	+2.960E-003	+3.641E+001
13	+3.346E-003	+4.115E+001
14	+3.085E-003	+3.794E+001
15	+2.960E-003	+3.641E+001
16	+3.036E-003	+3.734E+001
17	+3.194E-003	+3.928E+001
18	+3.265E-003	+4.016E+001
19	+3.294E-003	+4.050E+001
20	+3.237E-003	+3.981E+001
21	+3.546E-003	+4.361E+001
22	+3.358E-003	+4.129E+001
23	+3.157E-003	+3.882E+001
24	+2.876E-003	+3.537E+001
25	+2.544E-003	+3.129E+001
26	+2.736E-003	+3.365E+001
27	+2.884E-003	+3.547E+001
28	+2.924E-003	+3.596E+001
29	+2.796E-003	+3.438E+001
30	+2.915E-003	+3.585E+001
31	+2.588E-003	+3.675E+001
32	+2.583E-003	+3.175E+001
33	+3.115E-003	+3.831E+001
34	+2.653E-003	+3.262E+001
35	+2.800E-003	+3.443E+001
36	+2.495E-003	+3.068E+001
37	+2.764E-003	+3.399E+001
38	+2.642E-003	+3.249E+001
39	+2.837E-003	+3.489E+001
40	+2.537E-003	+3.120E+001
41	+2.491E-003	+3.064E+001
42	+2.760E-003	+3.394E+001
43	+2.788E-003	+3.428E+001
44	+2.854E-003	+3.510E+001
45	+2.613E-003	+3.214E+001
46	+2.617E-003	+3.218E+001
47	+2.564E-003	+3.154E+001
48	+2.595E-003	+3.192E+001
49	+2.369E-003	+2.914E+001
50	+2.627E-003	+3.231E+001
51	+2.355E-003	+2.896E+001

52	+2.432E-003	+2.991E+001
53	+2.713E-003	+3.336E+001
54	+2.327E-003	+2.862E+001
55	+2.850E-003	+3.505E+001
56	+2.575E-003	+3.166E+001
57	+2.495E-003	+3.068E+001
58	+2.627E-003	+3.231E+001
59	+2.541E-003	+3.125E+001
60	+2.097E-003	+2.579E+001
61	+2.364E-003	+2.907E+001
62	+2.294E-003	+2.821E+001
63	+2.653E-003	+3.262E+001
64	+2.768E-003	+3.404E+001
65	+2.717E-003	+3.341E+001
66	+2.764E-003	+3.399E+001
67	+2.473E-003	+3.041E+001
68	+2.524E-003	+3.104E+001
69	+2.466E-003	+3.033E+001
70	+2.447E-003	+3.010E+001
71	+2.319E-003	+2.851E+001
72	+2.069E-003	+2.544E+001
73	+2.287E-003	+2.808E+001
74	+2.582E-003	+3.175E+001
75	+2.664E-003	+3.276E+001
76	+2.599E-003	+3.196E+001
77	+2.585E-003	+3.179E+001
78	+2.302E-003	+2.831E+001
79	+2.273E-003	+2.795E+001
80	+2.369E-003	+2.914E+001
81	+2.330E-003	+2.865E+001
82	+2.026E-003	+2.495E+001
83	+1.962E-003	+2.413E+001
84	+2.291E-003	+2.818E+001
85	+2.294E-003	+2.821E+001
86	+2.399E-003	+2.950E+001
87	+2.534E-003	+3.116E+001
88	+2.466E-003	+3.033E+001

ROW #	RE
1	7.1649E+005
2	7.7402E+005
3	8.3941E+005
4	9.3749E+005
5	1.0356E+006
6	1.1337E+006
7	1.2317E+006
8	1.3298E+006

ROW #	AVG ST NO
1	6.5056E-003
2	3.2074E-003
3	2.8651E-003
4	2.6927E-003
5	2.5513E-003
6	2.5357E-003
7	2.4554E-003
8	2.2953E-003

```
 RUN #
  112186.1201

 AMBIENT T(C):
  19.5271910997

 DENSITY (KG/M3)
  1.21048100595
 VELOCITY (M/S)
  10.155721006S
 PAMB (N/M2).
  101574.6
 FS TEMP (K)
  292.37837286
 THERMOMETER AMB(C)
  19.3
 AVG PLATE TEMP(C)
  40.5979528222
 T PLATE-T AMB (C)
  21.0707617225
 POWER IN (WT)
  340.4
 COND LOSS (WT)
  14.364132346
 RAD LOSS (WT)
  51.0229293139
 CONV LOSS (WT)
  275.01293834
 CURRENT (AMPS)
  5.75
 VOLTAGE (VOLTS)
  59.2
```

No	ST	H
1	+6.016E-003	+7.433E+001
2	+4 833E-003	+5.971E+001
3	+4 423E-003	+5.464E+001
4	+6.301E-003	+7.785E+001
5	+7.067E-003	+8.731E+001
6	+5 567E-003	+6.878E+001
7	+6.253E-003	+7.733E+001
8	+6 115E-003	+7.555E+001
9	+6.217E-003	+7.681E+001
10	+4.871E-003	+6.018E+001
11	+6.366E-003	+7.865E+001
12	+2 809E-003	+3.459E+001
13	+3.142E-003	+3.881E+001
14	+2.507E-003	+3.591E+001
15	+2.795E-003	+3.454E+001
16	+2 808E-003	+3.470E+001
17	+3 017E-003	+3.728E+001
18	+3.096E-003	+3.825E+001
19	+3 111E-003	+3.843E+001
20	+3.051E-003	+3.769E+001
21	+3.323E-003	+4.106E+001
22	+3 147E-003	+3.888E+001
23	+2.956E-003	+3.652E+001
24	+2.705E-003	+3.342E+001
25	+2.426E-003	+2.997E+001
26	+2.599E-003	+3.211E+001
27	+2.736E-003	+3.380E+001
28	+2.788E-003	+3.444E+001
29	+2.671E-003	+3.300E+001
30	+2 769E-003	+3.419E+001
31	+2.825E-003	+3.490E+001
32	+2 460E-003	+3.039E+001
33	+2.933E-003	+3.624E+001
34	+2 514E-003	+3.106E+001
35	+2.649E-003	+3.273E+001
36	+2.378E-003	+2.938E+001
37	+2.620E-003	+3.237E+001
38	+2.524E-003	+3.118E+001
39	+2.709E-003	+3.347E+001
40	+2.426E-003	+2.997E+001
41	+2.384E-003	+2.945E+001
42	+2 610E-003	+3.224E+001
43	+2.642E-003	+3.264E+001
44	+2.698E-003	+3.333E+001
45	+2.475E-003	+3.058E+001
46	+2.479E-003	+3.062E+001
47	+2.435E-003	+3.008E+001
48	+2.457E-003	+3.035E+001
49	+2.272E-003	+2.808E+001
50	+2.511E-003	+3.102E+001
51	+2.262E-003	+2.794E+001

52	+2.327E-003	+2.875E+001
53	+2.571E-003	+3.177E+001
54	+2.226E-003	+2.750E+001
55	+2.694E-003	+3.328E+001
56	+2.435E-003	+3.008E+001
57	+2.366E-003	+2.924E+001
58	+2.498E-003	+3.086E+001
59	+2.420E-003	+2.989E+001
60	+2.018E-003	+2.493E+001
61	+2.267E-003	+2.801E+001
62	+2.201E-003	+2.719E+001
63	+2.517E-003	+3.110E+001
64	+2.617E-003	+3.233E+001
65	+2.568E-003	+3.172E+001
66	+2.603E-003	+3.215E+001
67	+2.332E-003	+2.882E+001
68	+2.390E-003	+2.953E+001
69	+2.358E-003	+2.913E+001
70	+2.327E-003	+2.875E+001
71	+2.223E-003	+2.747E+001
72	+2.003E-003	+2.475E+001
73	+2.191E-003	+2.707E+001
74	+2.450E-003	+3.027E+001
75	+2.517E-003	+3.110E+001
76	+2.472E-003	+3.054E+001
77	+2.450E-003	+3.027E+001
78	+2.196E-003	+2.701E+001
79	+2.167E-003	+2.677E+001
80	+2.262E-003	+2.794E+001
81	+2.213E-003	+2.734E+001
82	+1.962E-003	+2.424E+001
83	+1.902E-003	+2.350E+001
84	+2.203E-003	+2.722E+001
85	+2.196E-003	+2.713E+001
86	+2.278E-003	+2.814E+001
87	+2.414E-003	+2.982E+001
88	+2.346E-003	+2.899E+001

ROW #	RE
1	7.2476E+005
2	7.8296E+005
3	8.4910E+005
4	9.4832E+005
5	1.0475E+006
6	1.1467E+006
7	1.2460E+006
8	1.3452E+006

ROW #	AVG ST NO
1	5.8213E-003
2	3.0179E-003
3	2.7152E-003
4	2.5594E-003
5	2.4280E-003
6	2.4099E-003
7	2.3377E-003
8	2.1934E-003

```
RUN #
 111886.1337

AMBIENT T(C):
 19.999988065

DENSITY (KG/M3)
 1.23401441571
VELOCITY (M/S)
 14.8486317603
PAMB (N/M2)
 103487.5883
FS TEMP (K)
 292.203986248
THERMOMETER AMB(C)
 20
AVG PLATE TEMP(C)
 43.2990753813
T PLATE-T AMB (C)
 23.2990873163
POWER IN (WT)
 451.559
COND LOSS (WT)
 14.7919940566
RAD LOSS (WT)
 57.323842071
CONV LOSS (WT)
 379.443163872
CURRENT (AMPS)
 6.67
VOLTAGE (VOLTS)
 67.7
```

No	ST	H
1	+4.638E-003	+8.541E+001
2	+3.718E-003	+6.847E+001
3	+3.414E-003	+6.287E+001
4	+4.984E-003	+9.178E+001
5	+5.688E-003	+1.047E+002
6	+4.494E-003	+8.276E+001
7	+5.086E-003	+9.367E+001
8	+4.872E-003	+8.972E+001
9	+4.984E-003	+9.178E+001
10	+3.858E-003	+7.104E+001
11	+5.240E-003	+9.650E+001
12	+2.303E-003	+4.240E+001
13	+2.635E-003	+4.852E+001
14	+2.424E-003	+4.464E+001
15	+2.326E-003	+4.284E+001
16	+2.357E-003	+4.340E+001
17	+2.574E-003	+4.740E+001
18	+2.647E-003	+4.874E+001
19	+2.639E-003	+4.859E+001
20	+2.552E-003	+4.699E+001
21	+2.814E-003	+5.183E+001
22	+2.658E-003	+4.896E+001
23	+2.574E-003	+4.740E+001
24	+2.345E-003	+4.318E+001
25	+2.052E-003	+3.779E+001
26	+2.226E-003	+4.099E+001
27	+2.376E-003	+4.375E+001
28	+2.434E-003	+4.482E+001
29	+2.312E-003	+4.257E+001
30	+2.398E-003	+4.416E+001
31	+2.457E-003	+4.525E+001
32	+2.085E-003	+3.840E+001
33	+2.567E-003	+4.726E+001
34	+2.178E-003	+4.010E+001
35	+2.342E-003	+4.312E+001
36	+2.050E-003	+3.775E+001
37	+2.297E-003	+4.230E+001
38	+2.191E-003	+4.034E+001
39	+2.392E-003	+4.404E+001
40	+2.102E-003	+3.871E+001
41	+2.052E-003	+3.779E+001
42	+2.285E-003	+4.208E+001
43	+2.300E-003	+4.235E+001
44	+2.357E-003	+4.340E+001
45	+2.175E-003	+4.005E+001
46	+2.194E-003	+4.039E+001
47	+2.122E-003	+3.907E+001
48	+2.144E-003	+3.949E+001
49	+1.952E-003	+3.594E+001
50	+2.218E-003	+4.084E+001
51	+1.954E-003	+3.598E+001

52	+2.014E-003	+3.709E+001
53	+2.265E-003	+4.171E+001
54	+1.909E-003	+3.516E+001
55	+2.401E-003	+4.422E+001
56	+2.162E-003	+3.982E+001
57	+2.092E-003	+3.853E+001
58	+2.194E-003	+4.039E+001
59	+2.109E-003	+3.884E+001
60	+1.706E-003	+3.142E+001
61	+1.975E-003	+3.637E+001
62	+1.925E-003	+3.545E+001
63	+2.226E-003	+4.099E+001
64	+2.323E-003	+4.279E+001
65	+2.282E-003	+4.203E+001
66	+2.329E-003	+4.290E+001
67	+2.071E-003	+3.814E+001
68	+2.137E-003	+3.935E+001
69	+2.055E-003	+3.784E+001
70	+2.027E-003	+3.733E+001
71	+1.929E-003	+3.553E+001
72	+1.725E-003	+3.177E+001
73	+1.903E-003	+3.505E+001
74	+2.180E-003	+4.015E+001
75	+2.262E-003	+4.166E+001
76	+2.207E-003	+4.064E+001
77	+2.175E-003	+4.005E+001
78	+1.935E-003	+3.564E+001
79	+1.909E-003	+3.516E+001
80	+1.954E-003	+3.598E+001
81	+1.925E-003	+3.545E+001
82	+1.672E-003	+3.078E+001
83	+1.634E-003	+3.010E+001
84	+1.933E-003	+3.560E+001
85	+1.915E-003	+3.527E+001
86	+1.990E-003	+3.664E+001
87	+2.142E-003	+3.944E+001
88	+2.069E-003	+3.809E+001

ROW #	RE
1	1.0597E+006
2	1.1448E+006
3	1.2415E+006
4	1.3865E+006
5	1.5316E+006
6	1.6766E+006
7	1.8217E+006
8	1.9668E+006

ROW #	AVG ST NO
1	4.6342E-003
2	2.5390E-003
3	2.3477E-003
4	2.2313E-003
5	2.1224E-003
6	2.1204E-003
7	2.0611E-003
8	1.9162E-003

```
RUN #
 111586.114

AMBIENT T(C)
 18.0813557669

DENSITY (KG/M3)
 1.22950311245
VELOCITY (M/S)
 20.073252308
PAMB (N/M2)
 102519.24378
FS TEMP (K)
 290.531937104
THERMOMETER AMB(C)
 18
AVG PLATE TEMP(C)
 46.1115215113
T PLATE-T AMB (C)
 28.0301657444
POWER IN (WT)
 642.27
COND LOSS (WT)
 15.642198436
RAD LOSS (WT)
 69.3125052448
CONV LOSS (WT)
 557.315296319
CURRENT (AMPS)
 7.9
VOLTAGE (VOLTS)
 81.3
```

No	ST	H
1	+4.714E-003	+1.169E+002
2	+3.618E-003	+8.974E+001
3	+3.285E-003	+8.148E+001
4	+5.321E-003	+1.320E+002
5	+6.420E-003	+1.592E+002
6	+4.714E-003	+1.169E+002
7	+5.554E-003	+1.378E+002
8	+5.161E-003	+1.280E+002
9	+5.396E-003	+1.338E+002
10	+3.827E-003	+9.492E+001
11	+5.863E-003	+1.454E+002
12	+2.211E-003	+5.484E+001
13	+2.644E-003	+6.557E+001
14	+2.374E-003	+5.888E+001
15	+2.266E-003	+5.621E+001
16	+2.308E-003	+5.725E+001
17	+2.571E-003	+6.377E+001
18	+2.654E-003	+6.584E+001
19	+2.633E-003	+6.531E+001
20	+2.506E-003	+6.215E+001
21	+2.856E-003	+7.083E+001
22	+2.640E-003	+6.548E+001
23	+2.633E-003	+6.531E+001
24	+2.357E-003	+5.846E+001
25	+1.994E-003	+4.945E+001
26	+2.201E-003	+5.460E+001
27	+2.391E-003	+5.931E+001
28	+2.462E-003	+6.107E+001
29	+2.305E-003	+5.718E+001
30	+2.403E-003	+5.959E+001
31	+2.487E-003	+6.169E+001
32	+2.023E-003	+5.019E+001
33	+2.647E-003	+6.566E+001
34	+2.145E-003	+5.321E+001
35	+2.414E-003	+5.988E+001
36	+2.023E-003	+5.019E+001
37	+2.321E-003	+5.758E+001
38	+2.189E-003	+5.431E+001
39	+2.456E-003	+6.092E+001
40	+2.096E-003	+5.200E+001
41	+2.009E-003	+4.984E+001
42	+2.284E-003	+5.666E+001
43	+2.324E-003	+5.765E+001
44	+2.388E-003	+5.923E+001
45	+2.192E-003	+5.437E+001
46	+2.209E-003	+5.478E+001
47	+2.127E-003	+5.276E+001
48	+2.145E-003	+5.321E+001
49	+1.910E-003	+4.738E+001
50	+2.251E-003	+5.583E+001
51	+1.916E-003	+4.752E+001

52	+1.975E-003	+4.897E+001
53	+2.308E-003	+5.725E+001
54	+1.852E-003	+4.594E+001
55	+2.519E-003	+6.247E+001
56	+2.192E-003	+5.437E+001
57	+2.088E-003	+5.178E+001
58	+2.218E-003	+5.503E+001
59	+2.098E-003	+5.205E+001
60	+1.633E-003	+4.050E+001
61	+1.959E-003	+4.860E+001
62	+1.852E-003	+4.594E+001
63	+2.266E-003	+5.621E+001
64	+2.394E-003	+5.938E+001
65	+2.360E-003	+5.853E+001
66	+2.438E-003	+6.047E+001
67	+2.092E-003	+5.189E+001
68	+2.168E-003	+5.378E+001
69	+2.048E-003	+5.079E+001
70	+2.017E-003	+5.004E+001
71	+1.905E-003	+4.725E+001
72	+1.668E-003	+4.138E+001
73	+1.869E-003	+4.636E+001
74	+2.209E-003	+5.478E+001
75	+2.311E-003	+5.731E+001
76	+2.327E-003	+5.771E+001
77	+2.223E-003	+5.515E+001
78	+1.941E-003	+4.814E+001
79	+1.883E-003	+4.669E+001
80	+1.930E-003	+4.787E+001
81	+1.902E-003	+4.717E+001
82	+1.605E-003	+3.981E+001
83	+1.574E-003	+3.904E+001
84	+1.916E-003	+4.752E+001
85	+1.883E-003	+4.669E+001
86	+1.990E-003	+4.936E+001
87	+2.182E-003	+5.413E+001
88	+2.086E-003	+5.173E+001

ROW #	RE
1	1.4325E+006
2	1.5476E+006
3	1.6783E+006
4	1.8744E+006
5	2.0705E+006
6	2.2666E+006
7	2.4627E+006
8	2.6588E+006

ROW #	AVG ST NO
1	4.8976E-003
2	2.5148E-003
3	2.3549E-003
4	2.2411E-003
5	2.1276E-003
6	2.1363E-003
7	2.0761E-003
8	1.8991E-003

```
**************************

TEMP PROFILE STUDY NOV 1986
**************************
RUN NUMBER
 112186.1255
X LOCATION (M)
 1.849
Z LOCATION (M)
-.036
UINF (M/SEC)
 10.16
CF/2
 .00165
Q CONV (WATTS/M2)
 561.588727793
DENSITY (KG/M3)
 1.21
CP (WT SEC/KG K)
 1005
WALL DSPLCMNT (MM)
 .17
WALL TEMP (C)
 38.43
FS TEMP (C)
 19.2794318977
FRICTION TEMP (K)
 1.11900394913
THERMAL DEL (MM)
 23.653987144
```

I	Y(MM)	T(C)
1	427 0E-001	19.31E+000
2	356.4E-001	19.25E+000
3	285.9E-001	19.32E+000
4	243.5E-001	19.44E+000
5	201 2E-001	19.67E+000
6	158.9E-001	20.01E+000
7	116 5E-001	20.56E+000
8	883 3E-002	21.07E+000
9	742 2E-002	21.39E+000
10	601.0E-002	21.67E+000
11	530 5E-002	21.97E+000
12	459.3E-002	22.11E+000
13	389.4E-002	22.44E+000
14	318.8E-002	22.75E+000
15	283 5E-002	23.00E+000
16	248 3E-002	23.09E+000
17	213 0E-002	23.42E+000
18	177.7E-002	23.65E+000
19	142 4E-002	24.17E+000
20	107.2E-002	24.61E+000
21	895.2E-003	24.86E+000
22	797.2E-003	25.15E+000
23	718.8E-003	25.38E+000
24	542.4E-003	26.10E+000
25	366 0E-003	27.41E+000
26	248.4E-003	27.89E+000
27	170.0E-003	28.42E+000

I	Y/DEL	(TW-T)/(TW-TINF)
1	1.805E+000	99.857E-002
2	1.507E+000	10.014E-001
3	1.209E+000	99.785E-002
4	1.030E+000	99.155E-002
5	8.507E-001	97.965E-002
6	6.717E-001	96.166E-002
7	4.927E-001	93.323E-002
8	3.734E-001	90.625E-002
9	3.138E-001	88.999E-002
10	2.541E-001	87.535E-002
11	2.243E-001	85.962E-002
12	1.944E-001	85.205E-002
13	1.646E-001	83.478E-002
14	1.348E-001	81.861E-002
15	1.199E-001	80.562E-002
16	1.050E-001	80.084E-002
17	9.004E-002	78.373E-002
18	7.513E-002	77.172E-002
19	6.021E-002	74.437E-002
20	4.530E-002	72.188E-002
21	3.784E-002	70.873E-002
22	3.370E-002	69.322E-002
23	3.039E-002	68.157E-002
24	2.293E-002	64.407E-002
25	1.547E-002	57.544E-002
26	1.050E-002	55.057E-002
27	7.187E-003	52.290E-002

I	Y+	T+
1	113.0E+001	170.9E-001
2	943.0E+000	171.4E-001
3	756.3E+000	170.8E-001
4	644.3E+000	169.7E-001
5	532.3E+000	167.7E-001
6	420.3E+000	164.6E-001
7	308.3E+000	159.7E-001
8	233.7E+000	155.1E-001
9	196.3E+000	152.3E-001
10	159.0E+000	149.8E-001
11	140.3E+000	147.1E-001
12	121.7E+000	145.8E-001
13	103.0E+000	142.9E-001
14	843.4E-001	140.1E-001
15	750.1E-001	137.9E-001
16	656.8E-001	137.1E-001
17	563.5E-001	134.1E-001
18	470.1E-001	132.1E-001
19	376.8E-001	127.4E-001
20	283.5E-001	123.5E-001
21	236.8E-001	121.3E-001
22	210.9E-001	118.6E-001
23	190.2E-001	116.6E-001
24	143.5E-001	110.2E-001
25	968.2E-002	984.8E-002
26	657.1E-002	942.2E-002
27	449.7E-002	894.9E-002

```
**************************

TEMP PROFILE STUDY NOV 1986
**************************
RUN NUMBER
 112186 1225
X LOCATION (M)
 1.849
Z LOCATION (M)
 .036
UINF (M/SEC)
 10.16
CF/2
 .00165
Q CONV (WATTS/M2)
 561.586727793
DENSITY (KG/M3)
 1.21
CP (WT SEC/KG K)
 1005
WALL DSPLCMNT (MM)
 .17
WALL TEMP (C)
 38.43
FS TEMP (C)
 19.346674665
FRICTION TEMP (K)
 1.11900304913
THERMAL DEL (MM)
 21.9948585652
```

```
**********************************
  I      Y(MM)          T(C)
  1    421.1E-001   19.35E+000
  2    350.6E-001   19.35E+000
  3    280 0E-001   19.37E+000
  4    237 7E-001   19.48E+000
  5    195 3E-001   19.67E+000
  6    153 0E-001   20.05E+000
  7    119 7E-001   20.59E+000
  8    824.5E-002   21.18E+000
  9    683.4E-002   21.52E+000
 10    542.2E-002   21.95E+000
 11    471.7E-002   22.09E+000
 12    401.1E-002   22.41E+000
 13    330 6E-002   22.69E+000
 14    260.0E-002   23.01E+000
 15    224 7E-002   23.35E+000
 16    189.5E-002   23.61E+000
 17    154.2E-002   23.91E+000
 18    118.9E-002   24.33E+000
 19    836 4E-003   25.31E+000
 20    483.6E-003   26.70E+000
 21    307.2E-003   27.90E+000
 22    209.2E-003   28.02E+000
 23    170.0E-003   28.17E+000
```

I	Y/DEL	(TW-T)/(TW-TINF)
1	1.915E+000	99.993E-002
2	1.594E+000	10.001E-001
3	1.273E+000	99.863E-002
4	1.081E+000	99.322E-002
5	8.881E-001	98.284E-002
6	6.956E-001	96.322E-002
7	5.032E-001	93.483E-002
8	3.748E-001	90.392E-002
9	3.107E-001	88.636E-002
10	2.465E-001	86.356E-002
11	2.145E-001	85.648E-002
12	1.624E-001	83.934E-002
13	1.503E-001	82.500E-002
14	1.182E-001	80.794E-002
15	1.022E-001	79.025E-002
16	8.614E-002	77.671E-002
17	7.010E-002	76.065E-002
18	5.406E-002	73.871E-002
19	3.803E-002	68.739E-002
20	2.199E-002	61.456E-002
21	1.397E-002	55.187E-002
22	9.511E-003	54.563E-002
23	7.729E-003	53.779E-002

I	Y+	T+
1	111.4E+001	170.5E-001
2	927.4E+000	170.5E-001
3	740.8E+000	170.3E-001
4	628.8E+000	169.4E-001
5	516.8E+000	167.6E-001
6	404.8E+000	164.3E-001
7	292.8E+000	159.4E-001
8	218.1E+000	154.2E-001
9	180.8E+000	151.2E-001
10	143.5E+000	147.3E-001
11	124.8E+000	146.1E-001
12	106.1E+000	143.1E-001
13	874.6E-001	140.7E-001
14	687.9E-001	137.8E-001
15	594.6E-001	134.8E-001
16	501.2E-001	132.5E-001
17	407.9E-001	129.7E-001
18	314.6E-001	126.0E-001
19	221.3E-001	117.2E-001
20	127.9E-001	104.8E-001
21	812.7E-002	941.1E-002
22	553.4E-002	930.5E-002
23	449.7E-002	917.1E-002

```
**************************

 TEMP PROFILE STUDY NOV 1986
**************************
RUN NUMBER
 112186.1201
X LOCATION (M)
 1.849
Z LOCATION (M)
 0
UINF (M/SEC)
 10.16
CF/2
 .00165
Q CONV (WATTS/M2)
 561.588727793
DENSITY (KG/M3)
 1.21
CP (WT SEC/KG K)
 1005
WALL DSPLCMNT (MM)
 .17
WALL TEMP (C)
 38.43
FS TEMP (C)
 19.4917147995
FRICTION TEMP (K)
 1.11900304913
THERMAL DEL (MM)
 22.5281306192
```

I	Y(MM)	T(C)
1	422.7E-001	19.51E+000
2	352.1E-001	19.48E+000
3	281.6E-001	19.56E+000
4	239.2E-001	19.64E+000
5	196.9E-001	19.82E+000
6	154.6E-001	20.16E+000
7	112.2E-001	20.78E+000
8	840.1E-002	21.39E+000
9	699.0E-002	21.66E+000
10	557.9E-002	22.03E+000
11	487.4E-002	22.30E+000
12	416.8E-002	22.58E+000
13	346.3E-002	22.87E+000
14	275.7E-002	23.24E+000
15	240.4E-002	23.53E+000
16	205.1E-002	23.71E+000
17	169.9E-002	23.93E+000
18	134.6E-002	24.42E+000
19	993.1E-003	24.95E+000
20	640.4E-003	25.58E+000
21	464.0E-003	26.29E+000
22	366.0E-003	26.71E+000
23	287.6E-003	27.20E+000
24	170.0E-003	28.10E+000

I	Y/DEL	(TW-T)/(TW-TINF)
1	1.875E+000	99.924E-002
2	1.563E+000	10.008E-001
3	1.250E+000	99.635E-002
4	1.062E+000	99.221E-002
5	8.740E-001	98.269E-002
6	6.861E-001	96.476E-002
7	4.982E-001	93.221E-002
8	3.729E-001	89.983E-002
9	3.103E-001	88.549E-002
10	2.477E-001	86.592E-002
11	2.163E-001	85.185E-002
12	1.850E-001	83.688E-002
13	1.537E-001	82.139E-002
14	1.224E-001	80.205E-002
15	1.067E-001	78.671E-002
16	9.106E-002	77.711E-002
17	7.540E-002	76.543E-002
18	5.974E-002	73.981E-002
19	4.408E-002	71.192E-002
20	2.843E-002	67.860E-002
21	2.060E-002	64.096E-002
22	1.625E-002	61.894E-002
23	1.277E-002	59.298E-002
24	7.546E-003	54.528E-002

I	Y+	T+
1	111.8E+001	169.1E-001
2	931.6E+000	169.4E-001
3	744.9E+000	168.6E-001
4	632.9E+000	167.9E-001
5	520.9E+000	166.3E-001
6	408.9E+000	163.3E-001
7	296.9E+000	157.8E-001
8	222.3E+000	152.3E-001
9	184.9E+000	149.9E-001
10	147.6E+000	146.5E-001
11	128.9E+000	144.2E-001
12	110.3E+000	141.6E-001
13	916.0E-001	139.0E-001
14	729.4E-001	135.7E-001
15	636.1E-001	133.1E-001
16	542.7E-001	131.5E-001
17	449.4E-001	129.5E-001
18	356.1E-001	125.2E-001
19	262.7E-001	120.5E-001
20	169.4E-001	114.8E-001
21	122.7E-001	108.5E-001
22	968.2E-002	104.8E-001
23	760.8E-002	100.4E-001
24	449.7E-002	922.8E-002

```
**************************

TEMP PROFILE STUDY NOV 1986
**************************
RUN NUMBER
 112886.1401
X LOCATION (M)
 1.443
Z LOCATION (M)
 0
UINF (M/SEC)
 10.07
CF/2
 .00173
Q CONV (WATTS/M2)
 559.607923218
DENSITY (KG/M3)
 1.221
CP (WT SEC/KG K)
 1005.1
WALL DSPLCMNT (MM)
 .17
WALL TEMP (C)
 35.17
FS TEMP (C)
 17.6080982557
FRICTION TEMP (K)
 1.08869541969
THERMAL DEL (MM)
 34.7663533983
```

****

I	Y(MM)	T(C)
1	690.8E-001	17.62E+000
2	620.2E-001	17.60E+000
3	549.7E-001	17.52E+000
4	479.1E-001	17.63E+000
5	408.6E-001	17.74E+000
6	338.0E-001	17.73E+000
7	267.5E-001	17.81E+000
8	225.1E-001	17.81E+000
9	182.8E-001	17.85E+000
10	140.5E-001	17.92E+000
11	981.3E-002	18.17E+000
12	699.0E-002	18.49E+000
13	416.8E-002	19.20E+000
14	134.6E-002	20.48E+000
15	640.4E-003	21.42E+000
16	287.6E-003	22.49E+000
17	228.8E-003	22.75E+000
18	209.2E-003	22.87E+000
19	170.0E-003	23.08E+000

I	Y/DEL	(TW-T)/(TW-TINF)
1	1.987E+000	99.950E-002
2	1.784E+000	10.005E-001
3	1.581E+000	10.050E-001
4	1.378E+000	99.858E-002
5	1.175E+000	99.232E-002
6	9.722E-001	99.303E-002
7	7.693E-001	98.834E-002
8	6.475E-001	98.862E-002
9	5.258E-001	98.635E-002
10	4.040E-001	98.201E-002
11	2.822E-001	96.822E-002
12	2.011E-001	94.982E-002
13	1.199E-001	90.916E-002
14	3.871E-002	83.634E-002
15	1.842E-002	78.303E-002
16	8.272E-003	72.219E-002
17	6.581E-003	70.697E-002
18	6.017E-003	70.055E-002
19	4.890E-003	68.822E-002

I	Y/DEL	T-TINF(C)
1	1.987E+000	87.450E-004
2	1.734E+000	-8.745E-003
3	1.581E+000	-8.745E-002
4	1.378E+000	24.985E-003
5	1.175E+000	13.490E-002
6	9.722E-001	12.241E-002
7	7.693E-001	20.484E-002
8	6.475E-001	19.985E-002
9	5.258E-001	23.981E-002
10	4.040E-001	31.597E-002
11	2.822E-001	55.812E-002
12	2.011E-001	88.123E-002
13	1.199E-001	15.954E-001
14	3.871E-002	28.742E-001
15	1.842E-002	38.104E-001
16	8.272E-003	48.788E-001
17	6.581E-003	51.462E-001
18	6.017E-003	52.589E-001
19	4.890E-003	54.754E-001

I	Y+	T+
1	185.5E+001	161.2E-001
2	166.5E+001	161.4E-001
3	147.6E+001	162.1E-001
4	128.6E+001	161.1E-001
5	109.7E+001	160.1E-001
6	907.5E+000	160.2E-001
7	718.1E+000	159.4E-001
8	604.4E+000	159.5E-001
9	490.8E+000	159.1E-001
10	377.1E+000	158.4E-001
11	263.5E+000	156.2E-001
12	187.7E+000	153.2E-001
13	111.9E+000	146.7E-001
14	361.4E-001	134.9E-001
15	171.9E-001	126.3E-001
16	772.2E-002	116.5E-001
17	614.3E-002	114.0E-001
18	561.7E-002	113.0E-001
19	456.4E-002	111.0E-001

APPENDIX F

FILM COOLING DATA

NOMENCLATURE - refer to Appendix E

RUN NUMBER	DESCRIPTION
112186.1444	10 m/s, m=0.682
112286.1908	10 m/s, m=0.547
112286.2010	10 m/s, m=0.409
112586.1233	temp. profile, 10 m/s, Z=0, X=1.443 m
112586.1253	temp. profile, 10 m/s, Z=0.038 m, X=1.443 m
112586.1201	temp. profile, 10 m/s, Z=-0.038 m, X=1.443 m

```
RUN #
 112186 1444

AMBIENT T(C):
 18.779835764

INJECTION TEMP(C)
 51.4888587754
PLENUM TEMP(C)
 60.839266926
PLENUM DEL P (N/M^2)
 105.6973
RHOC (KG/M^2)
 1.09755258605
VELOCITY,UC (M/S)
 7.606552231
MASS FLUX(KG/M^2*S)
 8.34862808361
REYNOLDS NO. (DIA)
 4644.38891989
DISCHARGE COEFFICIENT
 .548117356253
BLOWING RATIO
 .682193839216
DENSITY RATIO
 .904002723967
VELOCITY RATIO
 .754636928773
MOMENTUM FLUX RATIO
 .514806663655

DENSITY (KG/M3)
 1.21410760936
VELOCITY (M/S)
 10.0797588098
PAMB (N/M2)
 102251.754
FS TEMP (K)
 293.448390075
THERMOMETER AMB(C)
 19
AVG PLATE TEMP(C)
 44.7010952581
T PLATE-T AMB (C)
 25.9212594941
POWER IN (WT)
 340.4
COND LOSS (WT)
 15.2547520969
RAD LOSS (WT)
 63.8544614896
CONV LOSS (WT)
 261.290786413
CURRENT (AMPS)
 5.75
VOLTAGE (VOLTS)
 59.2
```

No	H	ST/ST0
1	+4.338E+001	.668
2	+3.799E+001	.712
3	+3.442E+001	.700
4	+3.911E+001	.580
5	+3.981E+001	.537
6	+3.988E+001	.657
7	+4.398E+001	.658
8	+4.618E+001	.707
9	+4.697E+001	.705
10	+3.981E+001	.746
11	+4.638E+001	.681
12	+2.600E+001	.804
13	+2.824E+001	.780
14	+2.648E+001	.789
15	+2.488E+001	.770
16	+2.504E+001	.768
17	+2.756E+001	.795
18	+2.831E+001	.799
19	+2.877E+001	.808
20	+2.881E+001	.830
21	+3.080E+001	.818
22	+2.918E+001	.812
23	+2.800E+001	.821
24	+2.562E+001	.817
25	+2.364E+001	.839
26	+2.423E+001	.807
27	+2.523E+001	.801
28	+2.635E+001	.821
29	+2.574E+001	.837
30	+2.682E+001	.843
31	+2.726E+001	.843
32	+2 439E+001	.861
33	+2.796E+001	.836
34	+2.501E+001	.858
35	+2.591E+001	.845
36	+2.369E+001	.861
37	+2.509E+001	.833
38	+2.433E+001	.839
39	+2.626E+001	.848
40	+2.405E+001	.859
41	+2.403E+001	.874
42	+2.606E+001	.874
43	+2.609E+001	.863
44	+2.657E+001	.867
45	+2.523E+001	.879
46	+2.534E+001	.891
47	+2.477E+001	.884
48	+2.467E+001	.874
49	+2.301E+001	.876
50	+2.531E+001	.883
51	+2.322E+001	.889

52	+2.391E+001	.893
53	+2.614E+001	.887
54	+2.310E+001	.901
55	+2.713E+001	.884
56	+2.537E+001	.903
57	+2.480E+001	.912
58	+2 576E+001	.898
59	+2 482E+001	.892
60	+2.127E+001	.908
61	+2.364E+001	.903
62	+2.261E+001	.897
63	+2.588E+001	.895
64	+2.644E+001	.887
65	+2 641E+001	.898
66	+2.707E+001	.909
67	+2.490E+001	.925
68	+2.531E+001	.922
69	+2.507E+001	.924
70	+2.467E+001	.922
71	+2.336E+001	.911
72	+2.156E+001	.928
73	+2.315E+001	.915
74	+2.559E+001	.909
75	+2.657E+001	.917
76	+2.591E+001	.914
77	+2.576E+001	.917
78	+2.347E+001	.928
79	+2 329E+001	.931
80	+2.418E+001	.927
81	+2.374E+001	.928
82	+2.114E+001	.926
83	+2.087E+001	.944
84	+2.345E+001	.921
85	+2.352E+001	.927
86	+2.451E+001	.937
87	+2.548E+001	.919
88	+2.490E+001	.925

ROW #	RE
1	7.1934E+005
2	7.7710E+005
3	8.4275E+005
4	9.4122E+005
5	1.0397E+006
6	1.1382E+006
7	1 2366E+006
8	1.3351E+006

ROW #	AVG ST NO
1	3.3846E-003
2	2.2474E-003
3	2.1082E-003
4	2.0481E-003
5	2.0093E-003
6	2.0260E-003
7	2.0094E-003
8	1.9111E-003

```
RUN #
 112286.1908

AMBIENT T(C):
 19.1287302628

INJECTION TEMP(C)
 51.4092387347
PLENUM TEMP(C)
 60.7309138333
PLENUM DEL P (N/M^2)
 67.6464
RHOC (KG/M^2)
 1.10506094272
VELOCITY,UC (M/S)
 6.0852465848
MASS FLUX(KG/M^2*S)
 6.72456832768
REYNOLDS NO. (DIA)
 3715.51113591
DISCHARGE COEFFICIENT
 .549979218862
BLOWING RATIO
 .547002458499
DENSITY RATIO
 .901972769131
VELOCITY RATIO
 .606451189238
MOMENTUM FLUX RATIO
 .331730291472

DENSITY (KG/M3)
 1.22515998325
VELOCITY (M/S)
 10.0341302082
PAMB (N/M2)
 102928.328
FS TEMP (K)
 292.726378267
THERMOMETER AMB(C)
 18.5
AVG PLATE TEMP(C)
 45.2593791694
T PLATE-T AMB (C)
 26.1306489066
POWER IN (WT)
 341.55
COND LOSS (WT)
 15.2918464199
RAD LOSS (WT)
 64.6595324841
CONV LOSS (WT)
 261.598621096
CURRENT (AMPS)
 5.75
VOLTAGE (VOLTS)
 59.4
```

No	H	ST/ST0
1	+3.665E+001	.562
2	+3.275E+001	.611
3	+2.989E+001	.605
4	+3.308E+001	.488
5	+3.318E+001	.446
6	+3.398E+001	.557
7	+3.708E+001	.552
8	+3.910E+001	.596
9	+3.994E+001	.597
10	+3 456E+001	.645
11	+3.903E+001	.571
12	+2.366E+001	.729
13	+2.554E+001	.702
14	+2.410E+001	.715
15	+2.283E+001	.703
16	+2.285E+001	.698
17	+2.504E+001	.719
18	+2.571E+001	.722
19	+2.639E+001	.738
20	+2.597E+001	.745
21	+2.770E+001	.732
22	+2.639E+001	.731
23	+2.580E+001	.753
24	+2.383E+001	.756
25	+2.187E+001	.772
26	+2.254E+001	.748
27	+2.340E+001	.740
28	+2.430E+001	.754
29	+2.376E+001	.770
30	+2.464E+001	.772
31	+2.504E+001	.771
32	+2 256E+001	.793
33	+2.583E+001	.768
34	+2.383E+001	.814
35	+2.448E+001	.795
36	+2.241E+001	.811
37	+2.385E+001	.788
38	+2.319E+001	.796
39	+2.488E+001	.799
40	+2.314E+001	.823
41	+2.278E+001	.825
42	+2.454E+001	.819
43	+2.469E+001	.814
44	+2.520E+001	.819
45	+2.428E+001	.842
46	+2.428E+001	.850
47	+2.368E+001	.841
48	+2.368E+001	.835
49	+2.220E+001	.842
50	+2.430E+001	.844
51	+2.233E+001	.851

52	+2.289E+001	.851
53	+2.504E+001	.846
54	+2.216E+001	.860
55	+2.606E+001	.845
56	+2.456E+001	.870
57	+2.385E+001	.873
58	+2.477E+001	.860
59	+2.395E+001	.857
60	+2.062E+001	.876
61	+2.287E+001	.870
62	+2.204E+001	.870
63	+2.501E+001	.861
64	+2.597E+001	.867
65	+2.560E+001	.867
66	+2.606E+001	.871
67	+2.405E+001	.889
68	+2.441E+001	.885
69	+2.403E+001	.881
70	+2.361E+001	.878
71	+2.273E+001	.885
72	+2.094E+001	.897
73	+2.252E+001	.886
74	+2.491E+001	.881
75	+2.577E+001	.886
76	+2.512E+001	.882
77	+2.510E+001	.889
78	+2.296E+001	.904
79	+2.269E+001	.903
80	+2.345E+001	.895
81	+2.263E+001	.881
82	+2.067E+001	.901
83	+2.024E+001	.912
84	+2.292E+001	.896
85	+2.287E+001	.897
86	+2.383E+001	.907
87	+2.483E+001	.892
88	+2.436E+001	.901

ROW #	RE
1	7.1609E+005
2	7.7359E+005
3	8.3894E+005
4	9.3697E+005
5	1.0350E+006
6	1.1330E+006
7	1.2310E+006
8	1.3291E+006

ROW #	AVG ST NO
1	2.8640E-003
2	2.0322E-003
3	1.9394E-003
4	1.9353E-003
5	1.9198E-003
6	1.9522E-003
7	1.9369E-003
8	1.8501E-003

```
RUN #
 112286.201

AMBIENT T(C):
 19.4027033901

INJECTION TEMP(C)
 51.4662288729
PLENUM TEMP(C)
 60.8084678193
PLENUM DEL P (N/M^2)
 39.2946
RHOC (KG/M^2)
 1.10483949129
VELOCITY,UC (M/S)
 4.5639349386
MASS FLUX(KG/M^2*S)
 5.04241555584
REYNOLDS NO. (DIA)
 2796.63335194
DISCHARGE COEFFICIENT
 .54114610590l
BLOWING RATIO
 .409484356216
DENSITY RATIO
 .90240538659
VELOCITY RATIO
 .453769849229
MOMENTUM FLUX RATIO
 .185811654581

DENSITY (KG/M3)
 1.22432723442
VELOCITY (M/S)
 10.0575l884
PAMB (N/M2)
 102928.928
FS TEMP (K)
 292.926081939
THERMOMETER AMB(C)
 18.7
AVG PLATE TEMP(C)
 45.5392584755
T PLATE-T AMB (C)
 26.1365550854
POWER IN (WT)
 346.84
COND LOSS (WT)
 15.2928954843
RAD LOSS (WT)
 64.8501107068
CONV LOSS (WT)
 266.696993809
CURRENT (AMPS)
 5.8
VOLTAGE (VOLTS)
 59.8
```

No	H	ST/ST0
1	+3.338E+001	.511
2	+3.019E+001	.562
3	+2.764E+001	.559
4	+3.063E+001	.451
5	+3.104E+001	.416
6	+3.108E+001	.509
7	+3.397E+001	.505
8	+3 623E+001	.552
9	+3.723E+001	.555
10	+3.257E+001	.607
11	+3.550E+001	.518
12	+2.339E+001	.719
13	+2.523E+001	.692
14	+2.381E+001	.705
15	+2.243E+001	.690
16	+2.275E+001	.693
17	+2.473E+001	.709
18	+2.548E+001	.715
19	+2.610E+001	.729
20	+2.573E+001	.736
21	+2.743E+001	.725
22	+2.624E+001	.726
23	+2.627E+001	.766
24	+2.430E+001	.770
25	+2.227E+001	.785
26	+2.319E+001	.768
27	+2.415E+001	.762
28	+2.491E+001	.771
29	+2.430E+001	.786
30	+2.521E+001	.788
31	+2.562E+001	.787
32	+2.310E+001	.810
33	+2.672E+001	.794
34	+2.460E+001	.839
35	+2.526E+001	.819
36	+2.314E+001	.836
37	+2.489E+001	.821
38	+2.423E+001	.830
39	+2.627E+001	.843
40	+2.346E+001	.833
41	+2.355E+001	.852
42	+2.562E+001	.854
43	+2.567E+001	.844
44	+2.619E+001	.849
45	+2.510E+001	.869
46	+2.494E+001	.872
47	+2.453E+001	.870
48	+2.479E+001	.873
49	+2.314E+001	.876
50	+2.512E+001	.871
51	+2.317E+001	.882
52	+2.377E+001	.882

53	+2.598E+001	.876
54	+2.297E+001	.890
55	+2.719E+001	.880
56	+2.537E+001	.898
57	+2.440E+001	.891
58	+2.567E+001	.890
59	+2.494E+001	.891
60	+2.142E+001	.908
61	+2.374E+001	.902
62	+2.319E+001	.914
63	+2.604E+001	.895
64	+2.691E+001	.897
65	+2.681E+001	.906
66	+2.787E+001	.930
67	+2.481E+001	.916
68	+2.526E+001	.914
69	+2.521E+001	.923
70	+2.476E+001	.919
71	+2.367E+001	.918
72	+2.165E+001	.926
73	+2.339E+001	.919
74	+2.590E+001	.914
75	+2.675E+001	.918
76	+2.630E+001	.922
77	+2.616E+001	.925
78	+2.377E+001	.934
79	+2.355E+001	.935
80	+2.433E+001	.927
81	+2.389E+001	.928
82	+2.144E+001	.933
83	+2.091E+001	.940
84	+2.321E+001	.930
85	+2.377E+001	.931
86	+2.460E+001	.934
87	+2.590E+001	.928
88	+2.534E+001	.935

ROW #	RE
1	7.1777E+005
2	7.7541E+005
3	8.4092E+005
4	9.3917E+005
5	1.0374E+006
6	1.1357E+006
7	1.2339E+006
8	1.3322E+006

ROW #	AVG ST NO
1	2.6404E-003
2	2.0082E-003
3	1.9836E-003
4	2.0045E-003
5	1.9884E-003
6	2.0301E-003
7	2.0117E-003
8	1.9194E-003

```
**************************

TEMP PROFILE STUDY NOV 1986
**************************
RUN NUMBER
 112586.1233
X LOCATION (M)
 1.443
Z LOCATION (M)
 0
UINF (M/SEC)
 10.15
CF/2
 .00173
Q CONV (WATTS/M2)
 533.081478456
DENSITY (KG/M3)
 1.218
CP (WT SEC/KG K)
 1005
WALL DSPLCMNT (MM)
 .17
WALL TEMP (C)
 42.3
FS TEMP (C)
 18.9742478495
FRICTION TEMP (K)
 1.03155205758
THERMAL DEL (MM)
 31.8228206416
```

****

I	Y(MM)	T(C)
1	562.7E-001	18.97E+000
2	492.2E-001	18.98E+000
3	421.6E-001	18.96E+000
4	351.1E-001	19.01E+000
5	280.5E-001	19.72E+000
6	238.2E-001	20.67E+000
7	195.8E-001	21.90E+000
8	153.5E-001	23.03E+000
9	111.2E-001	24.16E+000
10	829.6E-002	24.84E+000
11	688.5E-002	25.21E+000
12	547.3E-002	25.50E+000
13	406.2E-002	26.04E+000
14	335.7E-002	26.27E+000
15	265.1E-002	26.63E+000
16	194.6E-002	27.15E+000
17	124.0E-002	27.82E+000
18	534.5E-003	30.07E+000
19	179.0E-003	32.94E+000

I	Y/DEL	(TW-T)/(TW-TINF)
1	1.768E+000	10.001E-001
2	1.547E+000	99.989E-002
3	1.325E+000	10.006E-001
4	1.103E+000	99.840E-002
5	8.815E-001	96.792E-002
6	7.485E-001	92.730E-002
7	6.154E-001	87.443E-002
8	4.824E-001	82.601E-002
9	3.494E-001	77.789E-002
10	2.607E-001	74.842E-002
11	2.163E-001	73.256E-002
12	1.720E-001	72.036E-002
13	1.277E-001	69.691E-002
14	1.055E-001	68.715E-002
15	8.331E-002	67.175E-002
16	6.114E-002	64.941E-002
17	3.897E-002	62.098E-002
18	1.680E-002	52.438E-002
19	5.342E-003	40.123E-002

I	Y/DEL	T-TINF(C)
1	1.768E+000	-2.492E-003
2	1.547E+000	24.920E-004
3	1.325E+000	-1.370E-002
4	1.103E+000	37.379E-003
5	8.815E-001	74.833E-002
6	7.485E-001	16.957E-001
7	6.154E-001	29.291E-001
8	4.824E-001	40.585E-001
9	3.494E-001	51.808E-001
10	2.607E-001	58.683E-001
11	2.163E-001	62.382E-001
12	1.720E-001	65.229E-001
13	1.277E-001	70.697E-001
14	1.055E-001	72.974E-001
15	8.331E-002	76.566E-001
16	6.114E-002	81.778E-001
17	3.897E-002	88.409E-001
18	1.680E-002	11.094E+000
19	5.342E-003	13.967E+000

I	Y+	T+
1	152.3E+001	226.1E-001
2	133.2E+001	226.1E-001
3	114.1E+001	226.3E-001
4	950.1E+000	225.8E-001
5	759.1E+000	218.9E-001
6	644.6E+000	209.7E-001
7	530.0E+000	197.7E-001
8	415.4E+000	186.8E-001
9	300.9E+000	175.9E-001
10	224.5E+000	169.2E-001
11	186.3E+000	165.6E-001
12	148.1E+000	162.9E-001
13	109.9E+000	157.6E-001
14	903.4E-001	155.4E-001
15	717.5E-001	151.9E-001
16	526.5E-001	146.8E-001
17	335.6E-001	140.4E-001
18	144.7E-001	118.6E-001
19	460.1E-002	907.3E-002

```
**************************

TEMP PROFILE STUDY NOV 1986
**************************
RUN NUMBER
 112586.1253
X LOCATION (M)
 1.443
Z LOCATION (M)
 .038
UINF (M/SEC)
 10.15
CF/2
 .00173
Q CONV (WATTS/M2)
 533.081478456
DENSITY (KG/M3)
 1.218
CP (WT SEC/KG K)
 1005
WALL DSPLCMNT (MM)
 .17
WALL TEMP (C)
 42.3
FS TEMP (C)
 19.0845079726
FRICTION TEMP (K)
 1.03155205758
THERMAL DEL (MM)
 30.9434996435
```

****

I	Y(MM)	T(C)
1	557.6E-001	19.08E+000
2	487.0E-001	19.09E+000
3	416.4E-001	19.13E+000
4	345.9E-001	19.17E+000
5	275.3E-001	19.70E+000
6	233.0E-001	20.51E+000
7	190.7E-001	21.71E+000
8	148.3E-001	22.91E+000
9	106.0E-001	24.26E+000
10	777.8E-002	24.90E+000
11	636.7E-002	25.30E+000
12	495.6E-002	25.91E+000
13	354.5E-002	26.20E+000
14	283.9E-002	26.59E+000
15	213.4E-002	26.95E+000
16	142.8E-002	27.52E+000
17	722.7E-003	28.44E+000
18	542.4E-003	29.01E+000
19	228.8E-003	30.51E+000
20	170.9E-003	31.03E+000

I	Y/DEL	(TW-T)/(TW-TINF)
1	1.802E+000	10.000E-001
2	1.574E+000	99.997E-002
3	1.346E+000	99.788E-002
4	1.118E+000	99.622E-002
5	8.898E-001	97.353E-002
6	7.530E-001	93.877E-002
7	6.162E-001	88.670E-002
8	4.794E-001	83.515E-002
9	3.426E-001	77.717E-002
10	2.514E-001	74.937E-002
11	2.058E-001	73.211E-002
12	1.602E-001	70.590E-002
13	1.146E-001	69.370E-002
14	9.176E-002	67.690E-002
15	6.896E-002	66.112E-002
16	4.616E-002	63.662E-002
17	2.335E-002	59.694E-002
18	1.753E-002	57.255E-002
19	7.394E-003	50.783E-002
20	5.494E-003	48.543E-002

I	Y/DEL	T-TINF(C)
1	1.802E+000	-6.228E-004
2	1.574E+000	62.287E-005
3	1.346E+000	49.205E-003
4	1.118E+000	87.818E-003
5	8.898E-001	61.443E-002
6	7.530E-001	14.214E-001
7	6.162E-001	26.304E-001
8	4.794E-001	38.270E-001
9	3.426E-001	51.731E-001
10	2.514E-001	58.185E-001
11	2.058E-001	62.192E-001
12	1.602E-001	68.277E-001
13	1.146E-001	71.108E-001
14	9.176E-002	75.008E-001
15	6.896E-002	78.672E-001
16	4.616E-002	84.360E-001
17	2.335E-002	93.573E-001
18	1.753E-002	99.233E-001
19	7.394E-003	11.426E+000
20	5.494E-003	11.946E+000

I	Y+	T+
1	150.9E+001	225.1E-001
2	131.8E+001	225.0E-001
3	112.7E+001	224.6E-001
4	936.1E+000	224.2E-001
5	745.1E+000	219.1E-001
6	630.6E+000	211.3E-001
7	516.0E+000	199.6E-001
8	401.4E+000	188.0E-001
9	286.9E+000	174.9E-001
10	210.5E+000	168.6E-001
11	172.3E+000	164.8E-001
12	134.1E+000	158.9E-001
13	959.3E-001	156.1E-001
14	768.4E-001	152.3E-001
15	577.5E-001	148.8E-001
16	386.5E-001	143.3E-001
17	195.6E-001	134.3E-001
18	146.8E-001	128.9E-001
19	619.2E-002	114.3E-001
20	469.1E-002	109.2E-001

```
**************************

TEMP PROFILE STUDY NOV 1986
**************************
RUN NUMBER
 112586.1201
X LOCATION (M)
 1.443
Z LOCATION (M)
-.038
UINF (M/SEC)
 10.15
CF/2
 .00173
Q CONV (WATTS/M2)
 533.081478456
DENSITY (KG/M3)
 1.218
CP (WT SEC/KG K)
 1005
WALL DSPLCMNT (MM)
 .17
WALL TEMP (C)
 42.35
FS TEMP (C)
 19.094473795
FRICTION TEMP (K)
 1.03155205758
THERMAL DEL (MM)
 27.9995032939
```

****

I	Y(MM)	T(C)
1	425.3E-001	19.10E+000
2	354.8E-001	19.09E+000
3	284.2E-001	19.29E+000
4	241.9E-001	19.84E+000
5	199.6E-001	20.76E+000
6	157.2E-001	21.69E+000
7	114.9E-001	22.79E+000
8	866.8E-002	23.47E+000
9	725.7E-002	23.74E+000
10	584.5E-002	24.15E+000
11	443.5E-002	24.52E+000
12	372.9E-002	24.79E+000
13	302.4E-002	25.24E+000
14	220.0E-002	25.57E+000
15	161.2E-002	25.97E+000
16	906.9E-003	26.92E+000
17	319.0E-003	29.42E+000
18	170.0E-003	30.68E+000

I	Y/DEL	(TW-T)/(TW-TINF)
1	1.519E+000	99.960E-002
2	1.267E+000	10.004E-001
3	1.015E+000	99.167E-002
4	8.640E-001	96.791E-002
5	7.128E-001	92.846E-002
6	5.616E-001	88.828E-002
7	4.104E-001	84.113E-002
8	3.096E-001	81.199E-002
9	2.592E-001	80.029E-002
10	2.088E-001	78.244E-002
11	1.584E-001	76.662E-002
12	1.332E-001	75.527E-002
13	1.080E-001	73.570E-002
14	7.959E-002	72.140E-002
15	5.759E-002	70.434E-002
16	3.239E-002	66.330E-002
17	1.139E-002	55.588E-002
18	6.072E-003	50.202E-002

I	Y/DEL	T-TINF(C)
1	1.519E+000	93.429E-004
2	1.267E+000	-9.342E-003
3	1.015E+000	19.368E-002
4	8.640E-001	74.630E-002
5	7.128E-001	16.636E-001
6	5.616E-001	25.981E-001
7	4.104E-001	36.945E-001
8	3.096E-001	43.724E-001
9	2.592E-001	46.443E-001
10	2.088E-001	50.594E-001
11	1.584E-001	54.273E-001
12	1.332E-001	56.913E-001
13	1.080E-001	61.463E-001
14	7.859E-002	64.791E-001
15	5.759E-002	68.756E-001
16	3.239E-002	78.302E-001
17	1.139E-002	10.328E+000
18	6.072E-003	11.581E+000

I	Y+	T+
1	115.1E+001	225.4E-001
2	960.1E+000	225.5E-001
3	769.2E+000	223.6E-001
4	654.6E+000	218.2E-001
5	540.1E+000	209.3E-001
6	425.5E+000	200.3E-001
7	311.0E+000	189.6E-001
8	234.6E+000	183.1E-001
9	196.4E+000	180.4E-001
10	158.2E+000	176.4E-001
11	120.0E+000	172.8E-001
12	100.9E+000	170.3E-001
13	818.2E-001	165.9E-001
14	595.5E-001	162.6E-001
15	436.4E-001	158.8E-001
16	245.4E-001	149.5E-001
17	863.2E-002	125.3E-001
18	460.1E-002	113.2E-001

APPENDIX G

SINGLE VORTEX DATA

NOMENCLATURE - refer to Appendix E

RUN NUMBER	DESCRIPTION
111786.1703	Vortex #1, 10 m/s, Z=-4.29 cm
111786.1812	Vortex #2, 10 m/s, Z=-4.79 cm
111786.2030	Vortex #3, 10 m/s, Z=-8.08 cm
111786.2139	Vortex #4, 10 m/s, Z=-9.096 cm

```
RUN #
 111786.1703

AMBIENT T(C):
 19.0539662482

DENSITY (KG/M3)
 1.22937223829
VELOCITY (M/S)
 10.0974441573
PAMB (N/M2)
 103142.33466
FS TEMP (K)
 292.328553856
THERMOMETER AMB(C)
 18.7
AVG PLATE TEMP(C)
 40.8281072544
T PLATE-T AMB (C)
 21.7741210062
POWER IN (WT)
 346.84
COND LOSS (WT)
 14.5056439506
RAD LOSS (WT)
 52.6671098813
CONV LOSS (WT)
 279.667246168
CURRENT (AMPS)
 5.8
VOLTAGE (VOLTS)
 59.8
```

No	H	ST/ST0
1	+7.232E+001	1.099
2	+5.832E+001	1.078
3	+5.367E+001	1.076
4	+7.708E+001	1.127
5	+8.912E+001	1.185
6	+7.415E+001	1.205
7	+7.467E+001	1.104
8	+7.016E+001	1.060
9	+7.323E+001	1.083
10	+5.789E+001	1.070
11	+7.608E+001	1.102
12	+3.413E+001	1.041
13	+3.852E+001	1.049
14	+3.581E+001	1.052
15	+3.493E+001	1.065
16	+3.635E+001	1.099
17	+4.096E+001	1.165
18	+3.791E+001	1.055
19	+3.669E+001	1.016
20	+3.646E+001	1.035
21	+4.007E+001	1.049
22	+3.815E+001	1.047
23	+3.624E+001	1.048
24	+3.319E+001	1.044
25	+3.003E+001	1.050
26	+3.257E+001	1.070
27	+3.555E+001	1.113
28	+3.827E+001	1.175
29	+3.375E+001	1.083
30	+3.244E+001	1.006
31	+3.389E+001	1.034
32	+2.988E+001	1.040
33	+3.560E+001	1.049
34	+3.091E+001	1.045
35	+3.270E+001	1.052
36	+2.955E+001	1.059
37	+3.297E+001	1.079
38	+3.274E+001	1.113
39	+3.738E+001	1.189
40	+3.102E+001	1.093
41	+2.774E+001	.995
42	+3.106E+001	1.027
43	+3.192E+001	1.042
44	+3.261E+001	1.049
45	+3.059E+001	1.050
46	+3.044E+001	1.056
47	+3.029E+001	1.066
48	+3.091E+001	1.080
49	+2.948E+001	1.107
50	+3.458E+001	1.189
51	+2.970E+001	1.121

52	+2.687E+001	.990
53	+3.063E+001	1.024
54	+2.687E+001	1.032
55	+3.257E+001	1.046
56	+2.992E+001	1.050
57	+2.913E+001	1.056
58	+3.114E+001	1.071
59	+3.052E+001	1.081
60	+2.602E+001	1.094
61	+3.118E+001	1.175
62	+2.889E+001	1.130
63	+2.863E+001	.975
64	+3.098E+001	1.024
65	+3.094E+001	1.037
66	+3.163E+001	1.047
67	+2.872E+001	1.052
68	+2.948E+001	1.059
69	+2.945E+001	1.070
70	+2.941E+001	1.083
71	+2.896E+001	1.110
72	+2.740E+001	1.163
73	+2.899E+001	1.130
74	+2.778E+001	.973
75	+3.003E+001	1.022
76	+2.973E+001	1.034
77	+2.573E+001	1.044
78	+2.687E+001	1.047
79	+2.678E+001	1.055
80	+2.816E+001	1.064
81	+2.800E+001	1.079
82	+2.533E+001	1.093
83	+2.572E+001	1.147
84	+2.966E+001	1.149
85	+2.548E+001	.990
86	+2.684E+001	1.011
87	+2.892E+001	1.029
88	+2.842E+001	1.041

ROW #	RE
1	7.2060E+005
2	7.7847E+005
3	8.4423E+005
4	9.4287E+005
5	1.0415E+006
6	1.1402E+006
7	1.2388E+006
8	1.3375E+006

ROW #	AVG ST NO
1	5.6612E-003
2	2.9876E-003
3	2.7065E-003
4	2.5549E-003
5	2.4259E-003
6	2.3972E-003
7	2.3288E-003
8	2.1873E-003

```
RUN #
 111786.1812

AMBIENT T(C):
 18.7299750855

DENSITY (KG/M3)
 1.23157732692
VELOCITY (M/S)
 10.0281711895
PAMB (N/M2)
 103142.23466
FS TEMP (K)
 291.80517528
THERMOMETER AMB(C)
 18.5
AVG PLATE TEMP(C)
 40.3863787572
T PLATE-T AMB (C)
 21.6564036717
POWER IN (WT)
 345.68
COND LOSS (WT)
 14.4824521125
RAD LOSS (WT)
 52.1835588731
CONV LOSS (WT)
 279.013989015
CURRENT (AMPS)
 5.8
VOLTAGE (VOLTS)
 59.6
```

No	H	ST/ST0
1	+7.044E+001	1.075
2	+5.719E+001	1.062
3	+5.294E+001	1.067
4	+7.544E+001	1.109
5	+8.763E+001	1.171
6	+7.285E+001	1.190
7	+7.770E+001	1.152
8	+6.643E+001	1.008
9	+6.873E+001	1.023
10	+5.583E+001	1.037
11	+7.285E+001	1.061
12	+3.365E+001	1.031
13	+3.810E+001	1.043
14	+3.555E+001	1.050
15	+3.467E+001	1.063
16	+3.619E+001	1.100
17	+4.085E+001	1.167
18	+4.057E+001	1.135
19	+3.518E+001	.979
20	+3.477E+001	.992
21	+3.841E+001	1.011
22	+3.698E+001	1.020
23	+3.571E+001	1.037
24	+3.282E+001	1.037
25	+2.992E+001	1.048
26	+3.234E+001	1.068
27	+3.544E+001	1.115
28	+3.816E+001	1.178
29	+3.647E+001	1.176
30	+3.191E+001	.994
31	+3.203E+001	.982
32	+2.873E+001	1.005
33	+3.437E+001	1.018
34	+3.053E+001	1.038
35	+3.234E+001	1.045
36	+2.932E+001	1.055
37	+3.273E+001	1.076
38	+3.255E+001	1.112
39	+3.721E+001	1.190
40	+3.351E+001	1.186
41	+2.897E+001	1.044
42	+2.932E+001	.974
43	+3.046E+001	.999
44	+3.141E+001	1.015
45	+3.023E+001	1.043
46	+3.015E+001	1.051
47	+3.008E+001	1.064
48	+3.069E+001	1.077
49	+2.928E+001	1.105
50	+3.423E+001	1.183
51	+3.153E+001	1.197

52	+2.921E+001	1.081
53	+2.842E+001	.955
54	+2.568E+001	.992
55	+3.116E+001	1.006
56	+2.960E+001	1.044
57	+2.879E+001	1.049
58	+3.089E+001	1.067
59	+3.019E+001	1.075
60	+2.582E+001	1.091
61	+3.081E+001	1.167
62	+3.061E+001	1.203
63	+3.273E+001	1.121
64	+2.856E+001	.949
65	+2.893E+001	.975
66	+3.015E+001	1.003
67	+2.839E+001	1.045
68	+2.921E+001	1.054
69	+2.921E+001	1.066
70	+2.910E+001	1.077
71	+2.859E+001	1.106
72	+2.716E+001	1.158
73	+3.085E+001	1.208
74	+3.273E+001	1.152
75	+2.806E+001	.960
76	+2.794E+001	.976
77	+2.829E+001	.998
78	+2.666E+001	1.042
79	+2.657E+001	1.052
80	+2.787E+001	1.059
81	+2.768E+001	1.073
82	+2.508E+001	1.088
83	+2.550E+001	1.143
84	+3.093E+001	1.204
85	+2.978E+001	1.163
86	+2.584E+001	.979
87	+2.692E+001	.962
88	+2.695E+001	.992

ROW #	RE
1	7.1566E+005
2	7.7313E+005
3	8.3844E+005
4	9.3641E+005
5	1.0344E+006
6	1.1323E+006
7	1.2303E+006
8	1.3283E+006

ROW #	AVG ST NO
1	5.5524E-003
2	2.9657E-003
3	2.6938E-003
4	2.5513E-003
5	2.4219E-003
6	2.3956E-003
7	2.3403E-003
8	2.1952E-003

```
RUN #
 111786.203

AMBIENT T(C):
 18.8047543499

DENSITY (KG/M3)
 1.23178775171
VELOCITY (M/S)
 10.0273141957
PAMB (N/M2)
 103142.23466
FS TEMP (K)
 291.755302869
THERMOMETER AMB(C)
 18.5
AVG PLATE TEMP(C)
 39.9557594711
T PLATE-T AMB (C)
 21.1509951212
POWER IN (WT)
 345.084
COND LOSS (WT)
 14.3806489237
RAD LOSS (WT)
 50.8729818
CONV LOSS (WT)
 279.830369276
CURRENT (AMPS)
 5.79
VOLTAGE (VOLTS)
 59.6
```

No	H	ST/ST0
1	+7.228E+001	1.103
2	+5.901E+001	1.096
3	+5.514E+001	1.111
4	+8.075E+001	1.186
5	+9.334E+001	1.247
6	+7.075E+001	1.155
7	+7.053E+001	1.046
8	+6.928E+001	1.052
9	+6.888E+001	1.024
10	+5.633E+001	1.046
11	+7.364E+001	1.072
12	+3.450E+001	1.057
13	+3.938E+001	1.077
14	+3.752E+001	1.108
15	+3.694E+001	1.132
16	+3.874E+001	1.177
17	+4.072E+001	1.164
18	+3.610E+001	1.010
19	+3.683E+001	1.025
20	+3.474E+001	.991
21	+3.861E+001	1.016
22	+3.717E+001	1.025
23	+3.705E+001	1.076
24	+3.430E+001	1.084
25	+3.164E+001	1.112
26	+3.495E+001	1.154
27	+3.867E+001	1.217
28	+3.899E+001	1.203
29	+3.245E+001	1.046
30	+3.206E+001	.999
31	+3.215E+001	.985
32	+2.879E+001	1.007
33	+3.450E+001	1.021
34	+3.168E+001	1.077
35	+3.410E+001	1.102
36	+3.127E+001	1.126
37	+3.557E+001	1.170
38	+3.562E+001	1.217
39	+3.925E+001	1.255
40	+3.119E+001	1.104
41	+2.689E+001	.969
42	+3.003E+001	.998
43	+3.049E+001	1.000
44	+3.131E+001	1.012
45	+3.144E+001	1.085
46	+3.177E+001	1.107
47	+3.223E+001	1.140
48	+3.326E+001	1.167
49	+3.185E+001	1.202
50	+3.688E+001	1.274
51	+3.095E+001	1.175

52	+2.649E+001	.981
53	+2.956E+001	.993
54	+2.577E+001	.995
55	+3.103E+001	1.002
56	+3.084E+001	1.088
57	+3.037E+001	1.106
58	+3.316E+001	1.146
59	+3.276E+001	1.167
60	+2.778E+001	1.174
61	+3.339E+001	1.264
62	+3.076E+001	1.209
63	+2.952E+001	1.011
64	+2.945E+001	.979
65	+2.963E+001	.998
66	+3.011E+001	1.002
67	+2.963E+001	1.091
68	+3.091E+001	1.115
69	+3.123E+001	1.140
70	+3.156E+001	1.168
71	+3.123E+001	1.208
72	+2.913E+001	1.242
73	+3.156E+001	1.236
74	+3.041E+001	1.070
75	+2.781E+001	.951
76	+2.819E+001	.985
77	+2.826E+001	.997
78	+2.771E+001	1.086
79	+2.790E+001	1.105
80	+2.970E+001	1.128
81	+2.992E+001	1.160
82	+2.698E+001	1.171
83	+2.737E+001	1.227
84	+3.232E+001	1.258
85	+2.886E+001	1.127
86	+2.512E+001	.951
87	+2.722E+001	.973
88	+2.698E+001	.993

ROW #	RE
1	7.1560E+005
2	7.7306E+005
3	8.3837E+005
4	9.3633E+005
5	1.0343E+006
6	1.1322E+006
7	1.2302E+006
8	1.3282E+006

ROW #	AVG ST NO
1	5.6385E-003
2	3.0118E-003
3	2.7504E-003
4	2.6176E-003
5	2.4990E-003
6	2.4737E-003
7	2.4163E-003
8	2.2710E-003

```
RUN #
 111786.2139

AMBIENT T(C):
 18.3059690222

DENSITY (KG/M3)
 1.2313667939
VELOCITY (M/S)
 9.96843911785
PAMB (N/M2)
 103142.33466
FS TEMP (K)
 291.85504299
THERMOMETER AMB(C)
 18
AVG PLATE TEMP(C)
 39.1591437759
T PLATE-T AMB (C)
 20.8531747537
POWER IN (WT)
 340.4
COND LOSS (WT)
 14.3188151431
RAD LOSS (WT)
 49.8337477321
CONV LOSS (WT)
 276.247437125
CURRENT (AMPS)
 5.75
VOLTAGE (VOLTS)
 59.2
```

No	H	ST/ST0
1	+7.883E+001	1.211
2	+6.382E+001	1.193
3	+5.941E+001	1.205
4	+8.851E+001	1.308
5	+9.668E+001	1.300
6	+7.107E+001	1.168
7	+7.427E+001	1.108
8	+7.403E+001	1.131
9	+7.151E+001	1.070
10	+5.851E+001	1.094
11	+7.777E+001	1.139
12	+3.634E+001	1.121
13	+4.221E+001	1.162
14	+4.039E+001	1.200
15	+3.899E+001	1.202
16	+3.899E+001	1.192
17	+3.848E+001	1.106
18	+3.685E+001	1.037
19	+3.905E+001	1.094
20	+3.536E+001	1.015
21	+3.918E+001	1.038
22	+3.792E+001	1.052
23	+3.964E+001	1.159
24	+3.691E+001	1.173
25	+3.404E+001	1.204
26	+3.762E+001	1.250
27	+3.971E+001	1.257
28	+3.691E+001	1.146
29	+3.103E+001	1.006
30	+3.515E+001	1.102
31	+3.380E+001	1.042
32	+2.896E+001	1.019
33	+3.484E+001	1.038
34	+3.375E+001	1.155
35	+3.703E+001	1.204
36	+3.385E+001	1.226
37	+3.873E+001	1.281
38	+3.756E+001	1.291
39	+3.823E+001	1.230
40	+2.862E+001	1.020
41	+2.903E+001	1.053
42	+3.282E+001	1.097
43	+3.043E+001	1.004
44	+3.152E+001	1.025
45	+3.361E+001	1.167
46	+3.439E+001	1.206
47	+3.515E+001	1.251
48	+3.629E+001	1.282
49	+3.375E+001	1.282
50	+3.714E+001	1.291
51	+2.872E+001	1.097

52	+2.714E+001	1.011
53	+3.277E+001	1.108
54	+2.576E+001	1.001
55	+3.103E+001	1.008
56	+3.309E+001	1.175
57	+3.282E+001	1.203
58	+3.623E+001	1.260
59	+3.574E+001	1.281
60	+2.950E+001	1.255
61	+3.424E+001	1.305
62	+2.928E+001	1.158
63	+2.842E+001	.979
64	+3.300E+001	1.103
65	+3.005E+001	1.019
66	+3.013E+001	1.009
67	+3.181E+001	1.178
68	+3.356E+001	1.219
69	+3.404E+001	1.251
70	+3.454E+001	1.287
71	+3.366E+001	1.309
72	+3 005E+001	1.289
73	+3.055E+001	1.204
74	+2.822E+001	.999
75	+3.075E+001	1.058
76	+2.910E+001	1.023
77	+2.828E+001	1.004
78	+2.957E+001	1.165
79	+2.986E+001	1.190
80	+3.220E+001	1.231
81	+3.237E+001	1.262
82	+2.889E+001	1.262
83	+2.832E+001	1.278
84	+3.211E+001	1.258
85	+2.708E+001	1.064
86	+2.657E+001	1.012
87	+2.862E+001	1.029
88	+2.693E+001	.997

ROW #	RE
1	7.1139E+005
2	7.6852E+005
3	8.3344E+005
4	9.3083E+005
5	1.0282E+006
6	1.1256E+006
7	1.2230E+006
8	1.3204E+006

ROW #	AVG ST NO
1	6.0017E-003
2	3.1228E-003
3	2.8639E-003
4	2.7382E-003
5	2.6216E-003
6	2.5977E-003
7	2.5392E-003
8	2.3768E-003

APPENDIX H

SINGLE VORTEX WITH FILM COOLING

NOMENCLATURE - refer Appendix E

RUN NUMBER	DESCRIPTION
112286.1516	Vortex #2, 10 m/s, m=0.68, Z=-4.79 cm
112286.1734	Vortex #2, 10 m/s, m=0.68 Z=-3.52 cm
112286.1623	Vortex #2, 10 m/s, m=0.68 Z=-6.06 cm

RUN #
112286.1516

AMBIENT T(C):
18.9044670372

INJECTION TEMP(C)
52.2181368201
PLENUM TEMP(C)
61.8329045493
PLENUM DEL P (N/M^2)
100.7235
RHOC (KG/M^2)
1.10234860558
VELOCITY,UC (M/S)
7.606558231
MASS FLUX(KG/M^2*S)
8.38507885921
REYNOLDS NO. (DIA)
4644.38891989
DISCHARGE COEFFICIENT
.562712396907
BLOWING RATIO
.680645927065
DENSITY RATIO
.899605273994
VELOCITY RATIO
.7566045829
MOMENTUM FLUX RATIO
.514979827752

DENSITY (KG/M3)
1.22536839459
VELOCITY (M/S)
10.0535450127
PAMB (N/M2)
102928.928
FS TEMP (K)
292.6771911
THERMOMETER AMB(C)
18.7
AVG PLATE TEMP(C)
43.9110611253
T PLATE-T AMB (C)
25.0065940881
POWER IN (WT)
338.052
COND LOSS (WT)
15.0941539656
RAD LOSS (WT)
61.3923799143
CONV LOSS (WT)
261.56545612
CURRENT (AMPS)
5.72
VOLTAGE (VOLTS)
59.1

No	H	ST
1	+4.021E+001	+3.248E-003
2	+3.582E+001	+2.893E-003
3	+3.222E+001	+2.602E-003
4	+3.589E+001	+2.898E-003
5	+3.377E+001	+2.728E-003
6	+3.808E+001	+3.076E-003
7	+4.165E+001	+3.364E-003
8	+4.212E+001	+3.402E-003
9	+4.361E+001	+3.522E-003
10	+3.795E+001	+3.065E-003
11	+4.344E+001	+3.509E-003
12	+2.522E+001	+2.037E-003
13	+2.779E+001	+2.245E-003
14	+2.575E+001	+2.081E-003
15	+2.455E+001	+1.983E-003
16	+2.567E+001	+2.074E-003
17	+3.241E+001	+2.617E-003
18	+2.525E+001	+2.040E-003
19	+2.663E+001	+2.151E-003
20	+2.700E+001	+2.181E-003
21	+2.903E+001	+2.345E-003
22	+2.796E+001	+2.259E-003
23	+2.726E+001	+2.202E-003
24	+2.548E+001	+2.058E-003
25	+2.330E+001	+1.882E-003
26	+2.430E+001	+1.962E-003
27	+2.736E+001	+2.210E-003
28	+2.984E+001	+2.410E-003
29	+3.128E+001	+2.527E-003
30	+2.440E+001	+1.971E-003
31	+2.506E+001	+2.024E-003
32	+2.298E+001	+1.856E-003
33	+2.647E+001	+2.138E-003
34	+2.455E+001	+1.983E-003
35	+2.548E+001	+2.058E-003
36	+2.344E+001	+1.893E-003
37	+2.545E+001	+2.055E-003
38	+2.704E+001	+2.184E-003
39	+2.824E+001	+2.281E-003
40	+3.133E+001	+2.530E-003
41	+2.490E+001	+2.011E-003
42	+2.351E+001	+1.899E-003
43	+2.419E+001	+1.954E-003
44	+2.495E+001	+2.015E-003

45	+2.479E+001	+2.002E-003
46	+2.517E+001	+2.033E-003
47	+2.463E+001	+1.990E-003
48	+2.506E+001	+2.024E-003
49	+2.531E+001	+2.044E-003
50	+2.678E+001	+2.163E-003
51	+2.681E+001	+2.166E-003
52	+2.608E+001	+2.107E-003
53	+2.370E+001	+1.914E-003
54	+2.145E+001	+1.732E-003
55	+2.525E+001	+2.040E-003
56	+2.503E+001	+2.022E-003
57	+2.466E+001	+1.992E-003
58	+2.567E+001	+2.074E-003
59	+2.539E+001	+2.051E-003
60	+2.300E+001	+1.858E-003
61	+2.536E+001	+2.097E-003
62	+2.582E+001	+2.085E-003
63	+2.856E+001	+2.307E-003
64	+2.455E+001	+1.983E-003
65	+2.417E+001	+1.952E-003
66	+2.490E+001	+2.011E-003
67	+2.458E+001	+1.985E-003
68	+2.528E+001	+2.042E-003
69	+2.495E+001	+2.015E-003
70	+2.509E+001	+2.026E-003
71	+2.579E+001	+2.083E-003
72	+2.404E+001	+1.942E-003
73	+2.638E+001	+2.131E-003
74	+2.821E+001	+2.278E-003
75	+2.422E+001	+1.956E-003
76	+2.349E+001	+1.897E-003
77	+2.387E+001	+1.928E-003
78	+2.334E+001	+1.886E-003
79	+2.337E+001	+1.887E-003
80	+2.432E+001	+1.964E-003
81	+2.445E+001	+1.975E-003
82	+2.307E+001	+1.863E-003
83	+2.351E+001	+1.899E-003
84	+2.766E+001	+2.234E-003
85	+2.626E+001	+2.121E-003
86	+2.282E+001	+1.843E-003
87	+2.307E+001	+1.863E-003
88	+2.309E+001	+1.865E-003

NO	ST/ST0	ST/STF
1	.616	.921
2	.667	.937
3	.651	.930
4	.529	.911
5	.452	.843
6	.623	.949
7	.619	.941
8	.641	.906
9	.650	.922
10	.707	.947
11	.634	.930
12	.775	.964
13	.762	.978
14	.763	.967
15	.754	.980
16	.782	1.019
17	.928	1.168
18	.708	.886
19	.743	.919
20	.772	.931
21	.766	.936
22	.773	.952
23	.794	.967
24	.807	.988
25	.821	.979
26	.804	.996
27	.863	1.077
28	.923	1.125
29	1.011	1.207
30	.762	.904
31	.770	.913
32	.806	.936
33	.786	.941
34	.837	.975
35	.826	.977
36	.846	.983
37	.839	1.007
38	.926	1.104
39	.906	1.068
40	1.112	1.294
41	.900	1.029
42	.783	.896
43	.796	.921
44	.809	.933
45	.858	.976
46	.879	.987
47	.873	.988
48	.882	1.009
49	.958	1.092
50	.928	1.051
51	1.020	1.147

52	.968	1.084
53	.799	.901
54	.831	.922
55	.817	.925
56	.885	.980
57	.900	.988
58	.889	.990
59	.907	1.016
60	.975	1.074
61	.986	1.091
62	1.017	1.134
63	.981	1.096
64	.818	.922
65	.817	.909
66	.830	.914
67	.907	.980
68	.915	.992
69	.913	.989
70	.931	1.010
71	1.000	1.097
72	1.028	1.108
73	1.036	1.132
74	.995	1.095
75	.831	.906
76	.823	.900
77	.844	.920
78	.917	.988
79	.928	.997
80	.926	.999
81	.950	1.023
82	1.004	1.084
83	1.057	1.119
84	1.079	1.172
85	1.028	1.109
86	.866	.925
87	.827	.899
88	.852	.921

ROW #	RE
1	7.1747E+005
2	7.7508E+005
3	8.4056E+005
4	9.3878E+005
5	1.0370E+006
6	1.1352E+006
7	1.2334E+006
8	1.3316E+006

ROW #	AVG ST NO
1	3.1188E-003
2	2.1829E-003
3	2.1126E-003
4	2.0785E-003
5	2.0195E-003
6	2.0392E-003
7	2.0258E-003
8	1.9455E-003

RUN #
112286.1734

AMBIENT T(C):
18.8296917689

INJECTION TEMP(C)
52.1334367727
PLENUM TEMP(C)
61.7173924063
PLENUM DEL P (N/M^2)
101.2209
RHOC (KG/M^2)
1.10263566982
VELOCITY,UC (M/S)
7.606558231
MASS FLUX(KG/M^2*S)
8.38726243006
REYNOLDS NO. (DIA)
4644.38291989
DISCHARGE COEFFICIENT
.561401198327
BLOWING RATIO
.680475532114
DENSITY RATIO
.898921420816
VELOCITY RATIO
.756991118861
MOMENTUM FLUX RATIO
.51511393441

DENSITY (KG/M3)
1.2266207527
VELOCITY (M/S)
10.0484114562
PAMB (N/M2)
102928.928
FS TEMP (K)
292.37837286
THERMOMETER AMB(C)
18.2
AVG PLATE TEMP(C)
44.5232471386
T PLATE-T AMB (C)
25.6935553697
POWER IN (WT)
344.488
COND LOSS (WT)
15.2145990468
RAD LOSS (WT)
63.2517389428
CONV LOSS (WT)
266.02166201
CURRENT (AMPS)
5.78
VOLTAGE (VOLTS)
59.6

No	H	ST
1	+3.930E+001	+3.173E-003
2	+3 495E+001	+2.821E-003
3	+3.153E+001	+2.545E-003
4	+3.583E+001	+2.892E-003
5	+3 463E+001	+2.796E-003
6	+3.484E+001	+2.813E-003
7	+4.493E+001	+3.627E-003
8	+3.937E+001	+3.178E-003
9	+4 224E+001	+3.410E-003
10	+3.646E+001	+2.943E-003
11	+4.216E+001	+3.404E-003
12	+2 451E+001	+1.978E-003
13	+2.678E+001	+2.162E-003
14	+2.503E+001	+2.021E-003
15	+2.386E+001	+1.926E-003
16	+2.448E+001	+1.976E-003
17	+2.895E+001	+2.337E-003
18	+2.586E+001	+2.087E-003
19	+2.681E+001	+2.164E-003
20	+2.626E+001	+2.120E-003
21	+2.807E+001	+2.266E-003
22	+2.703E+001	+2.182E-003
23	+2.641E+001	+2.132E-003
24	+2.453E+001	+1.981E-003
25	+2.253E+001	+1.819E-003
26	+2.344E+001	+1.892E-003
27	+2.552E+001	+2.060E-003
28	+2.691E+001	+2.334E-003
29	+2 418E+001	+1.952E-003
30	+2.632E+001	+2.125E-003
31	+2.473E+001	+1.968E-003
32	+2.236E+001	+1.805E-003
33	+2.569E+001	+2.074E-003
34	+2.384E+001	+1.925E-003
35	+2 466E+001	+1.991E-003
36	+2.272E+001	+1.834E-003
37	+2.448E+001	+1.976E-003
38	+2.527E+001	+2.040E-003
39	+2.950E+001	+2.382E-003
40	+2 895E+001	+2.337E-003
41	+2.326E+001	+1.877E-003
42	+2.256E+001	+1.854E-003
43	+2.339E+001	+1.888E-003
44	+2.411E+001	+1.946E-003

45	+2.406E+001	+1.942E-003
46	+2.436E+001	+1.966E-003
47	+2.386E+001	+1.926E-003
48	+2 406E+001	+1.942E-003
49	+2.386E+001	+1.926E-003
50	+2.764E+001	+2.231E-003
51	+2.784E+001	+2.247E-003
52	+2.650E+001	+2.140E-003
53	+2.323E+001	+1.876E-003
54	+2.066E+001	+1.668E-003
55	+2.433E+001	+1.964E-003
56	+2.428E+001	+1.960E-003
57	+2.384E+001	+1.925E-003
58	+2.484E+001	+2.006E-003
59	+2.433E+001	+1.964E-003
60	+2.201E+001	+1.777E-003
61	+2.541E+001	+2.051E-003
62	+2.741E+001	+2.213E-003
63	+3.110E+001	+2.511E-003
64	+2.519E+001	+2.034E-003
65	+2.305E+001	+1.861E-003
66	+2.398E+001	+1.936E-003
67	+2.382E+001	+1.923E-003
68	+2.446E+001	+1.974E-003
69	+2.421E+001	+1.954E-003
70	+2.406E+001	+1.942E-003
71	+2.451E+001	+1.978E-003
72	+2.301E+001	+1.857E-003
73	+2.767E+001	+2.234E-003
74	+3.153E+001	+2.545E-003
75	+2 644E+001	+2.135E-003
76	+2.247E+001	+1 814E-003
77	+2.296E+001	+1.854E-003
78	+2.264E+001	+1.827E-003
79	+2.274E+001	+1.836E-003
80	+2.346E+001	+1.894E-003
81	+2.337E+001	+1.887E-003
82	+2.211E+001	+1.785E-003
83	+2.195E+001	+1.772E-003
84	+2.754E+001	+2.223E-003
85	+2.835E+001	+2.288E-003
86	+2.519E+001	+2.034E-003
87	+2.213E+001	+1.787E-003
88	+2.220E+001	+1.792E-003

NO	ST/ST0	ST/STF
1	.601	.900
2	.651	.914
3	.637	.909
4	.527	.910
5	.464	.864
6	.570	.867
7	.668	1.014
8	.599	.846
9	.629	.893
10	.679	.909
11	.615	.903
12	.753	.936
13	.734	.942
14	.741	.939
15	.733	.952
16	.746	.971
17	.829	1.043
18	.725	.907
19	.748	.925
20	.751	.905
21	.740	.905
22	.747	.920
23	.769	.937
24	.777	.951
25	.794	.946
26	.775	.961
27	.805	1.004
28	.894	1.089
29	.781	.933
30	.822	.975
31	.749	.888
32	.784	.911
33	.762	.912
34	.812	.946
35	.799	.945
36	.820	.952
37	.807	.969
38	.865	1.031
39	.946	1.115
40	1.027	1.195
41	.840	.961
42	.765	.875
43	.769	.890
44	.781	.901
45	.832	.947
46	.851	.954
47	.846	.957
48	.846	.968
49	.902	1.030
50	.957	1.084
51	1.059	1.190

52	.983	1.101
53	.782	.882
54	.800	.888
55	.787	.890
56	.858	.950
57	.870	.955
58	.860	.957
59	.868	.973
60	.932	1.027
61	.964	1.067
62	1.079	1.203
63	1.067	1.193
64	.839	.946
65	.778	.867
66	.800	.880
67	.878	.949
68	.884	.959
69	.886	.959
70	.892	.968
71	.950	1.042
72	.983	1.059
73	1.086	1.187
74	1.112	1.223
75	.906	.988
76	.786	.861
77	.812	.885
78	.889	.957
79	.902	.970
80	.893	.963
81	.907	.978
82	.962	1.038
83	.986	1.045
84	1.074	1.166
85	1.109	1.197
86	.956	1.020
87	.793	.862
88	.819	.885

ROW #	RE
1	7.1710E+005
2	7.7469E+005
3	8.4013E+005
4	9.3830E+005
5	1.0355E+006
6	1.1346E+006
7	1.2328E+006
8	1.3310E+006

ROW #	AVG ST NO
1	3.0547E-003
2	2.1110E-003
3	2.0129E-003
4	2.0046E-003
5	1.9844E-003
6	2.0215E-003
7	2.0191E-003
8	1.9205E-003

```
RUN #
 112286.1623

AMBIENT T(C)
 19.2781872864

INJECTION TEMP(C)
 51.8837128122
PLENUM TEMP(C)
 61.376990131
PLENUM DEL P (N/M^2)
 100.9722
RHOC (KG/M^2)
 1.10348290174
VELOCITY,UC (M/S)
 7.806558231
MASS FLUX(KG/M^2*S)
 8.393706949
REYNOLDS NO. (DIA)
 4644.38891989
DISCHARGE COEFFICIENT
 .562308078869
BLOWING RATIO
 .681693842293
DENSITY RATIO
 .901450477899
VELOCITY RATIO
 .756218848408
MOMENTUM FLUX RATIO
 .515509732388

DENSITY (KG/M3)
 1.22411927088
VELOCITY (M/S)
 10.0586731566
PAMB (N/M2)
 102928.328
FS TEMP (K)
 292.975846653
THERMOMETER AMB(C)
 18.7
AVG PLATE TEMP(C)
 44.0996988858
T PLATE-T AMB (C)
 24.8215115994
POWER IN (WT)
 336.336
COND LOSS (WT)
 15.0617606632
RAD LOSS (WT)
 61.1052269545
CONV LOSS (WT)
 260.169012383
CURRENT (AMPS)
 5.72
VOLTAGE (VOLTS)
 58.8
```

No	H	ST
1	+4.077E+001	+3.295E-003
2	+3.613E+001	+2.919E-003
3	+3.226E+001	+2.607E-003
4	+3.561E+001	+2.877E-003
5	+3.347E+001	+2.705E-003
6	+4.233E+001	+3.421E-003
7	+4.308E+001	+3.481E-003
8	+4.325E+001	+3.495E-003
9	+4.385E+001	+3.543E-003
10	+3.811E+001	+3.080E-003
11	+4.385E+001	+3.543E-003
12	+2.506E+001	+2.025E-003
13	+2.798E+001	+2.261E-003
14	+2.565E+001	+2.073E-003
15	+2.432E+001	+1.965E-003
16	+2.645E+001	+2.137E-003
17	+2.955E+001	+2.388E-003
18	+2.815E+001	+2.275E-003
19	+2.781E+001	+2.247E-003
20	+2.701E+001	+2.183E-003
21	+2.906E+001	+2.348E-003
22	+2.784E+001	+2.250E-003
23	+2.711E+001	+2.191E-003
24	+2.525E+001	+2.041E-003
25	+2.320E+001	+1.875E-003
26	+2.450E+001	+1.980E-003
27	+2.894E+001	+2.339E-003
28	+2.539E+001	+2.052E-003
29	+2.861E+001	+2.312E-003
30	+2.492E+001	+2.014E-003
31	+2.525E+001	+2.041E-003
32	+2.299E+001	+1.858E-003
33	+2.648E+001	+2.140E-003
34	+2.445E+001	+1.976E-003
35	+2.539E+001	+2.052E-003
36	+2.350E+001	+1.899E-003
37	+2.597E+001	+2.099E-003
38	+2.833E+001	+2.289E-003
39	+2.887E+001	+2.333E-003
40	+2.422E+001	+1.957E-003
41	+2.242E+001	+1.812E-003
42	+2.370E+001	+1.915E-003
43	+2.432E+001	+1.965E-003
44	+2.487E+001	+2.010E-003

45	+2.471E+001	+1.997E-003
46	+2.498E+001	+2.019E-003
47	+2.479E+001	+2.003E-003
48	+2.551E+001	+2.061E-003
49	+2.609E+001	+2.108E-003
50	+3.072E+001	+2.482E-003
51	+2.534E+001	+2.048E-003
52	+2.229E+001	+1.801E-003
53	+2.358E+001	+1.905E-003
54	+2.149E+001	+1.737E-003
55	+2.534E+001	+2.048E-003
56	+2.492E+001	+2.014E-003
57	+2.492E+001	+2.014E-003
58	+2.585E+001	+2.089E-003
59	+2.606E+001	+2.106E-003
60	+2.318E+001	+1.873E-003
61	+2.921E+001	+2.360E-003
62	+2.673E+001	+2.160E-003
63	+2.466E+001	+1.993E-003
64	+2.424E+001	+1.959E-003
65	+2.440E+001	+1.971E-003
66	+2.559E+001	+2.068E-003
67	+2.437E+001	+1.969E-003
68	+2.528E+001	+2.043E-003
69	+2.503E+001	+2.023E-003
70	+2.551E+001	+2.061E-003
71	+2.591E+001	+2.094E-003
72	+2.606E+001	+2.106E-003
73	+2.889E+001	+2.327E-003
74	+2.645E+001	+2.137E-003
75	+2.367E+001	+1.913E-003
76	+2.257E+001	+1.824E-003
77	+2.402E+001	+1.941E-003
78	+2.329E+001	+1.882E-003
79	+2.297E+001	+1.856E-003
80	+2.437E+001	+1.969E-003
81	+2.517E+001	+2.034E-003
82	+2.290E+001	+1.851E-003
83	+2.437E+001	+1.969E-003
84	+2.982E+001	+2.410E-003
85	+2.591E+001	+2.094E-003
86	+2.183E+001	+1.764E-003
87	+2.327E+001	+1.880E-003
88	+2.322E+001	+1.877E-003

NO	ST/ST0	ST/STF
1	.624	.934
2	.673	.945
3	.652	.932
4	525	.905
5	.449	.836
6	.693	1.055
7	.641	.973
8	.658	.931
9	.654	.928
10	.710	.951
11	640	.940
12	770	.958
13	.768	.985
14	760	.963
15	.748	.972
16	.806	1.050
17	.847	1.066
18	.790	.988
19	.777	.961
20	.773	.932
21	.767	.938
22	.770	.948
23	790	.963
24	.800	.980
25	.818	.975
26	.811	1.005
27	.914	1.140
28	.786	.958
29	.925	1.105
30	.779	.924
31	.776	.921
32	.807	.937
33	787	.941
34	834	.971
35	.823	.974
36	.849	.986
37	.857	1.029
38	.971	1.157
39	.926	1.093
40	.860	1.001
41	.810	.927
42	.790	.904
43	800	.927
44	.806	.930
45	.855	.973
46	.873	.980
47	879	.995
48	.898	1.028
49	988	1.127
50	1.065	1.206
51	.964	1.085

52	.828	.927
53	.795	.896
54	.833	.925
55	.820	.928
56	.882	.977
57	.911	.999
58	.896	.997
59	.931	1.043
60	.983	1.083
61	1.109	1.228
62	1.054	1.175
63	.847	.947
64	.808	.911
65	.825	.918
66	.854	.940
67	.900	.973
68	.915	.993
69	.917	.993
70	.947	1.028
71	1.005	1.103
72	1.115	1.201
73	1.132	1.236
74	.934	1.027
75	.812	.886
76	.791	.866
77	.850	.926
78	.915	.986
79	.912	.980
80	.929	1.002
81	.978	1.054
82	.997	1.077
83	1.096	1.161
84	1.164	1.264
85	1.015	1.095
86	.829	.885
87	.834	.908
88	.857	.927

ROW #	RE
1	7.1783E+005
2	7.7548E+005
3	8.4099E+005
4	9.3925E+005
5	1.0375E+006
6	1.1358E+006
7	1.2341E+006
8	1.3323E+006

ROW #	AVG ST NO
1	3.1788E-003
2	2.1957E-003
3	2.0766E-003
4	2.0279E-003
5	2.0190E-003
6	2.0552E-003
7	2.0398E-003
8	1.9625E-003

LIST OF REFERENCES

1. Goldstein, R. J. and Chen, H. P., "Film Cooling on a Gas Turbine Near the End Wall," Journal for Gas Turbines and Power, v. 107, pp. 117-122, Jaunuary 1985.

2. Öngören, A., Heat Transfer on the Endwalls of a Turbine Cascade with Film Cooling, Project Report 1981-19, Von Karmen Institute for Fluid Dynamics, Rhode Saint Genese, Belgium, June 1981.

3. Gas Turbine Division of the American Society of Mechanical Engineers, Paper No. 84-GT-78, Recent Progress in the Understanding of Basic Aspects of Secondary Flows in Turbine Blade Passages, by C. H. Sieverding, pp. 1-10, 5 January 1984.

4. Ligrani, P. M. and Camci, C., "Adiabatic Film Cooling Effectiveness From Heat Transfer Measurements in Compressible, Variable-Property Flow," Journal of Heat Transfer, v. 107, pp. 313-320, May 1985.

5. Gaugler, R. E. and Russell, L. M., "Comparison of Visualized Turbine Endwall Secondary Flows and Measured Heat Transfer Patterns," Journal of Engineering for Gas Turbines and Power, v. 106, pp. 168-172, January 1984.

6. Heat Transfer Division of the American Society of Mechanical Engineers, Paper No. 84-HT-22, Vortex Generating Flow Passage Design for Increased Film Cooling Effectiveness and Surface Coverage, by S. S. Papell, pp. 1-11, November 1984.

7. Makki, Y. H. and Jakubowski, G. S., An Experimental Study of Film Cooling from Diffused Trapezoidal Shaped Holes, paper presented at the AIAA/ASME 4th Joint Thermophysics and Heat Transfer Conference, Boston, Massachusetts, June 1986.

8. Film Cooling and Turbine Blade Heat Transfer, Editor P. M. Ligrani., Lecture Series 1982-02, Von Karmen Institute for Fluid Dynamics, Rhode Saint Genese, Belgium, February 1982.

9. Eibeck, P. A. and Eaton, J. K., An Experimental Investigation of the Heat - Transfer Effects of a Longitudinal Vortex Embedded in a Turbulent Boundary Layer, Report MD-48, Department of Mechanical Engineering, Stanford University, November 1985.

10. Shabaka, I. M. M. A., Melta, D. D., and Bradshaw, P., "Logitudinal Vortices Imbedded in Turbulent Boundary Layers. Part 1. Single Vortex," Journal of Fluid Mechanics, v. 155, pp. 37-57, 1985.

11. Cutler, A. D. and Bradshaw, P., The Interaction Between a Strong Longitudinal Vortex and a Turbulent Boundary Layer, paper presesented at AIAA/ASME 4th Fluid Mechanics, Plasma Dynamics and Lasers Conference, Atlanta, Georgia, May 1986.

12. Goldstein, R. J. and Yoshida, T., "The Influence of a Laminar Boundary Layer and Laminar Injection on Film Cooling Performance," Journal of Heat Transfer, v. 104, pp. 355-362, May 1982.

13. Wang, T., An Experimental Investigation of Curvature and Freestream Turbulence Effects on Heat Transfer and Fluid Mechanics in Transitional Boundary Layer Flows, Ph.D. Thesis, Mechanical Engineering Department, University of Minnesota, December 1984.

14. Gas Turbine Division of the American Society of Mechanical Engineers, Paper No. 85-GT-113, Heat Transfer and Fluid Mechanics, Measurements in Transitional Boundary Layer Flows, by T. Wang, T. W. Simon, and J. Buddhavarapin, pp. 1-9, 1985.

15. Incropera, F. P. and DeWitt, D. P., Fundamentals of Heat and Mass Transfer, 2d ed., pp. 624-661, John Wiley & Sons, Inc., 1985.

16. Aerolab, Operating Instructions for Aerolab 8" x 24" Laminar/Turbulent Shear Layer Research Facility with Variable Height Test Section For US Naval Postgraduate School, November 1985.

17. Ligrani, P. M., "Qualification and Performance of NPS Shear Layer Research Facility," NPS Report, Department of Mechanical Engineering, Naval Postgraduate School, Monterey, California, in preparation to appear in 1987.

18. Kays, W. M. and Crawford, M. E., Convective Heat and Mass Transfer, 2d ed., pp. 213-217, McGraw-Hill, Inc., 1980.

19. Telephone conversation between R. V. Westphal, NASA-AMES Research Center and P. M. Ligrani, code 69Li, Naval Postgraduate School, October 1986.

20. Kline, S. J. and McClintock, F. A., "Describing Uncertainties in Single - Sample Experiments," Mechanical Engineering, pp. 3-8, January 1953.

INITIAL DISTRIBUTION LIST

		No. of Copies
1.	Defense Technical Information Center Cameron Station Alexandria, Virginia 22304-6145	2
2.	Library, Code 0142 Naval Postgraduate School Monterey, California, 93943-5002	2
3.	Department Chairman, Code 69 Department of Mechanical Engineering Naval Postgraduate School Monterey, California, 93943-5000	1
4.	Professor Phillip M. Ligrani, Code 69Li Department of Mechanical Engineering Naval Postgraduate School Monterey, California, 93943-5000	10
5.	Dr. Charles MacArthur Project Engineer Components Branch Turbine Engine Division Aero Propulsion Laboratory Department of the Air Force Air Force Wright Aeronautical Laboratories Wright-Patterson Air Force Base, Ohio, 45433	10
6.	LT. Stephen L. Joseph, USN 15 Brewster Road Milford, Connecticut, 06460	4